University of California
Santa Barbara

Quantum Representations of MCGs and Their Applications to Quantum Computing

A dissertation submitted in partial satisfaction
of the requirements for the degree

Doctor of Philosophy
in
Mathematics

by

Wade Bloomquist

Committee in charge:

Professor Zhenghan Wang, Chair
Professor Stephen Bigelow
Professor Darren Long

June 2019

The Dissertation of Wade Bloomquist is approved.

Professor Stephen Bigelow

Professor Darren Long

Professor Zhenghan Wang, Committee Chair

April 2019

Quantum Representations of MCGs and Their Applications to Quantum Computing

Wade Bloomquist

Acknowledgements

I would like to start by thanking my advisor Zhenghan Wang. His guidance has been invaluable as I transition from a student to a working mathematician. This is not limited to the volume of mathematics that he has shared with me, but also includes providing an entry point to the world of professional mathematics.

Next I would like to thank the department of Mathematics at the University of California Santa Barbara. The faculty, the staff, and my fellow graduate students have all created an atmosphere of support that I would recommend to any prospective student.

Finally, I would like to thank my friends and family. I would not have been able to succeed without their willingness to commiserate in the worst of times and celebrate in the best.

Curriculum Vitæ
Wade Bloomquist

Education

2019	Ph.D. in Mathematics (Expected), University of California, Santa Barbara.
2016	M.A. in Mathematics, University of California, Santa Barbara.
2014	B.S. in Mathematics, University of Iowa

Professional Employment

2014-2019	Teaching Assistant, Department of Mathematics- University of California Santa Barbara

Publications

1	*Comparing Skein and Quantum Group Representations and Their Applications to Asymptotic Faithfulness*, with Zhenghan Wang, Pure and Applied Mathematics Quarterly, Vol. 12, No. 4 (2016), pp. 473-492
2	*On Topological Quantum Computing with Mapping Class Group Representations*, with Zhenghan Wang, Accepted for Publication Journal of Physics A.
3	*Asymptotic Faithfulness of Quantum* SP(4) *Mapping Class Group Representations*, Submitted.
4	*Admissibility and the C_2 Spider* with Andres Mejia, Submitted.

Fields of Study

Quantum Topology - Zhenghan Wang

Abstract

Quantum Representations of MCGs and Their Applications to Quantum Computing

by

Wade Bloomquist

We explore how skein theoretic techniques can be applied to the study of quantum representations of mapping class groups. Of particular interest will be looking into the asymptotic faithfulness property of quantum representations coming from unimodal versions of representation categories of quantum groups. We then introduce a combinatorial property on the graphical calculus of these representation categories which implies asymptotic faithfulness. We proceed to show that this property is satisfied in some specific cases, in short we provide support for the conjecture that these quantum representations will always be asymptotically faithful. This will lead into a discussion of other applications within low dimensional topology. Finally applications to topological quantum computing will be given, introducing a potential encoding of qudits making use of these quantum representations.

Contents

Chapter 1

Introduction

In its relatively short lifespan quantum topology has emerged as a rich and exciting corner of mathematics. This raises an opening question: what is quantum topology? This question is not particularly well formulated. What one mathematician views as an acceptable answer may fall short in the eyes of another. Rather than attempting to resolve this debate we will instead provide a start to the story. Then we will take quantum topology to be any mathematics that can be linked with this core originating work.

The rediscovery of the Temperley-Lieb algebras by Jones [22], and in turn the introduction of the Jones polynomial, [24, 25] will be what we consider the birth of quantum topology. This concept was reformulated into a diagrammatic language by Kauffman [26], which is in many ways the path the work discussed here will follow. From a seemingly different direction the introduction of "quantum groups" or $1-$parameter families of deformations of semisimple complex Lie algebras by Drinfeld and Jimbo could be seen as an alternative starting point [21, 16]. An observation due to Witten saw how this newly introduced knot polynomial of Jones sat inside of a much more intricate and deep mathematical structure, namely a topological quantum field theory [50]. This framework,

brought more rigorously into the mathematical world by Atiyah [3], in many ways opens the door to seeing is how these two starting points are intimately related.

We proceed with an analogy. Utilizing the work of Kirby it is possible to view framed link invariants and oriented closed 3−manifold invariants as one in the same. This connection arises from link invariants which are invariant under the famous Kirby moves on the corresponding diagrams and performing surgery on the link in question sitting inside of S^3 [29]. The power of Kirby's work is in finding the moves on a link diagram which correspond to changing the link in a way that is not seen by the surgery. Coloring framed links by a weighted sum of algebraic data is one way to force the necessary invariance under Kirby moves. In summary (omitting some adjectives):

$$\text{Framed Link Invariants} \rightarrow 3-\text{Manifold Invariants.}$$

This was only the start, or first half, of our analogy. From here we make the shift from framed link invariants to colored ribbon graph invariants. In fact, this analogy can be thought of a generalization or extension as a framed link is simply a ribbon graph with no vertices. We avoid any technical details here, but by a coloring of a ribbon graph we mean a certain assignment of algebraic data to a ribbon graph. The required algebraic data happens to be equivalent to an algebraic object called a ribbon tensor category [39, 40]. Then from a ribbon graph sitting inside of a 3−manifold we can construct operator valued invariants. Now that we have the appropriate generalization of framed link invariants, we can look at what 3−manifold invariants should generalize to. That answer is a $(2+1)$ TQFT. In particular, this analogy is a quick and rough description of the Reshetikhin Turaev construction associated to a modular tensor category [45]. In summary,

$$\text{Colored Ribbon Graph Invariant} \rightarrow (2+1)\text{TQFT.}$$

Now of particular interest to us will be one small aspect of a $(2+1)$ TQFT, and that is the afforded tower of mapping class group representations. In particular, this tells us that given a TQFT we have a mapping class group representation for any possible surface.

Sitting inside this tower of mapping class group representations are braid group representations on any number of strands. This family of braid group representations is the genesis of mathematically describing the physical theory of anyons. This amounts to describing exchange statistics. When two indistinguishable bosons are exchanged there is no change to the underlying vector, or state, describing the physical system. When two indistinguishable fermions are exchanged the underlying state is negated. In certain situations, here meaning confining to a $2-$dimensional system, quasi-particles can emerge which have the potential to exhibit exotic exchange statistics. For an abelian anyon this means picking up an overall phase, say $e^{i\theta}$. Of incredible interest are non-abelian anyons, these quasi-particles exhibit exchange statistics that not only change the state vector by a phase, but can act by a non-trivial unitary operator on the entire system. In particular, when indistinguishable non-abelian anyons are exchanged the state vector can be changed by some unitary representation of the braid group on the number of anyons in question. This remarkable property is at the center of the field of topological quantum computing [31, 20]. These unitary braid group representations are used to encode logic gates, and then a computation is performed through successive interchangings of non-abelian anyons. This is a very rough overview and further details can be found in [48].

We look to explore some mathematical properties of these mapping class group representations, not limited to braid group representations, as well as look into some possibilities of incorporating the entire mapping class group representation into topological quantum computing.

Chapter 2

Quantum Representations Preliminaries

Definition 2.0.1 *A* **quantum representation** *of a mapping class group will refer to the projective representation of a mapping class group afforded by a* $(2+1)$ *TQFT. In particular, these representations arise from the map induced on the state space via the mapping cylinder construction.*

2.1 $(2+1)$ TQFTs

We will now give a brief overview of axiomatic $(2+1)$ TQFTs, similar to that given in [48]. We will avoid a complete description of the list of all axioms here and instead refer to the reference above. We will often make an effort to mention implications on the quantum representations in a hope to increase understanding and provide grounding in the context we will be working in.

2.1.1 Framing Anomaly

There is an overall ambiguity that must be dealt with throughout the following construction. Reducing to the level of quantum representations this should be thought of as the driving force in quantum representations being projective rather than honest linear representations. We have a few potential routes to make sense of this ambiguity, each with various benefits and disadvantages. We will refer to a surface with any of the following additional structure as an extended surface, and will often pass between the various notions to what is most useful in context.

Parametrization

One method of incorporating the above ambiguity is by looking at not only surfaces, but surfaces equipped with a parametrization into $\mathbb{R}^3$ such that the surface bounds the standardly embedded handlebody. Then an extended $3-$manifold will be one with parametrized boundary. We refer readers to chapter IV of Turaev's book for additional details [45]. We will often uitilize this particular approach as it is very concrete and perhaps easier to think about. The disadvantage of this approach is this parametrization is a much stronger condition added to the surface than is actually needed.

Lagrangian Subspaces

Definition 2.1.1 *A* **Lagrangian subspace** *of a surface Σ is a maximal isotropic subspace of $H_1(\Sigma;\mathbb{R})$ with respect to the intersection pairing of $H_1(\Sigma;\mathbb{R})$.*

Then an extended surface will be a pair (Σ,λ) where λ is a Lagrangian subspace of $H_1(\Sigma;\mathbb{R})$. Similarly extended $3-$manifolds will be $3-$manifolds where the boundary is given a Lagrangian subspace. This approach has the advantage of being particularly concrete when describing the projective ambiguity in composing mapping classes, and so

we will adopt it in most contexts. We refer to the chapter VI of Turaev's book for an overview of how to reduce parametrizations to the weaker structure of just Lagrangian subspaces [45].

Other Options

Various weakenings can be applied to the extra structure given to 3−manifolds. A 2−framing, meaning a trivialization of the double of the tangent bundle, is one example. This structure is equivalent to choosing the signature of a bounding 4−manifold and is in particular very useful for descriptions of constructions requiring surgery. Often this will amount to just assuming the canonical 2−framing has been taken [4]. A p_1−structure, the first Pontryagin class, is another example, but this one will not be discussed here [8].

2.1.2 A Summary of Axiomatic TQFTs

A $(2+1)$ TQFT will be a modular functor from the category of extended cobordisms to the category of finite dimensional vector spaces. In particular this means we will assign to an extended surface (Σ, λ) a finite dimensional vector space. We will also assign an oriented 3−manifold with extended boundary to a linear map between the vector space associated to the extended boundary surfaces. In order to fix notation we will will say $V(\Sigma)$ is the vector space assigned to Σ and $Z(M)$ will be the vector in $V(\partial M)$ determined by viewing it as a linear map form $V(\emptyset) \cong \mathbb{C}$ to $V(\partial M)$.

2.2 Mapping Cylinder Construction

The axioms, which were omitted, in the above definition are enough to deduce the following construction. Let Σ be an extended surface, with $V(\Sigma)$ the associated vector space. We claim that $V(\Sigma)$ admits a (projective) action of $\mathrm{MCG}(\Sigma)$. Let $f \in \mathrm{MCG}(\Sigma)$

be an orientation preserving homeomorphism of Σ. Then we can construct the mapping cylinder

$$M_f := (([0,1] \times \Sigma))/\sim$$

where

$$(0,x) \sim f(x) \qquad x \in \Sigma.$$

We observe that M_f is a cobordism from Σ to Σ and thus induces a map $V(f) : V(\Sigma) \to V(\Sigma)$. Moreover if Σ is extended by the Lagrangian subspace λ, then using the TQFT axioms omitted above

$$V(f \circ g) = \kappa^{\mu(g_*(\lambda),\lambda,f_*^{-1}(\lambda))} V(f)V(g),$$

where μ is the Maslov index and $\kappa = e^{\pi i c/4}$ is called the anomaly with central charge c. In particular we note that not only is the projective ambiguity able to be described explicitly, but is also only projective up to particular roots of unity. This allows for linear representations to arise for central extensions of mapping class groups [35].

2.3 Modular Tensor Categories

This section will focus entirely on the algebraic formalism of modular tensor categories. The disinterested reader is welcome to skip to the next section where a more "hands on" approach where the focus is on ribbon graph invariants is taken. We only provide a brief overview of modular tensor categories, and direct the reader to find details in the following accounts [34, 45, 48, 17], our presentation will most closely follow that given in [17].

Definition 2.3.1 *A* **modular tensor category** *is an abelian $\mathbb{C}-$linear, which is bilin-*

ear on morphisms, semisimple rigid monoidal category with a simple unit object 1*, finite dimensional* Hom *spaces, finitely many isomorphism classes of simple objects, spherical structure, and a non-degenerate braiding which is compatible with the spherical structure.*

We look to individually make sense of each of these terms with a strong emphasis on the graphical calculus which is introduced by each level of additional structure.

2.3.1 Categorical Prerequisites

Definition 2.3.2 *An* **additive category**, $\mathcal{C}$, *is a category such that the set* $\mathrm{Hom}_{\mathcal{C}}(X,Y)$ *is an abelian group with composition being bi-additive for every pair of objects* X *and* Y*. There is also a distinguished object* 0 *such that* $\mathrm{Hom}(0,0) = 0$*. Finally for every pair of objects* X *and* Y *there exists an object* $X \oplus Y$ *and morphisms* $p_1 : X \oplus Y \to X$*,* $p_2 : X \oplus Y \to Y$*,* $i_1 : X \to X \oplus Y$*, and* $i_2 : Y \to X \oplus Y$ *such that* $p_1 \circ i_1 = id_X, p_2 \circ i_2 = id_Y$*, and* $i_1 p_1 + i_2 p_2 = id_{X \oplus Y}$*.*

Definition 2.3.3 *Let* $\mathbb{F}$ *be a field. An* **additive category**, $\mathcal{C}$*, is said to be* $\mathbb{F}-$*linear if for any objects* X *and* Y *of* $\mathcal{C}$ *we have that* $\mathrm{Hom}_{\mathcal{C}}(X,Y)$ *is equipped with the structure of a vector space over* $\mathbb{F}$*, such that composing morphisms is* $\mathbb{F}-$*linear.*

Definition 2.3.4 *An* $\mathbb{F}-$**algebroid** *is a small* $\mathbb{F}-$*linear category. Where small means that the collection of all objects forms a set rather than a class.*

We will rarely use this notation, but it serves a purpose in influencing how to think about linear categories. For every object X of $\mathcal{C}$ we have that

$$\mathrm{End}(X) := \mathrm{Hom}_{\mathcal{C}}(X,X)$$

is an $\mathbb{F}-$algebra. In addition we have that $\mathrm{Hom}(X,Y$ is an $\mathrm{End}(X) - \mathrm{End}(Y)$ bimodule.

Then an algebroid, and really a linear category in general, can be thought of as a family of parametrized algebras related to each other via parametrized bimodules.

Definition 2.3.5 *An* **abelian category** *is an additive category such that for every morphism* $f \in \mathrm{Hom}(X, Y)$ *there exists a sequence*

$$K \xrightarrow{k} X \xrightarrow{i} I \xrightarrow{j} Y \xrightarrow{c} C$$

such that $j \circ i = f$, $K = \mathrm{Ker}(f)$, $C = \mathrm{Coker}(f)$, $I = \mathrm{Coker}(k) = \mathrm{Ker}(c)$, *where the object* I *is called the image of* f, *denoted* $\mathrm{Im}(f)$.

Definition 2.3.6 *Let* $\mathcal{C}$ *be an abelian* $\mathbb{F}-$*linear category. A nonzero object* X *is* **simple** *if* $\mathrm{End}(X) = \mathbb{F}$. *Then* $\mathcal{C}$ *is* **semisimple** *if every object is a direct sum of simple objects.*

2.3.2 Monoidal Categories

Definition 2.3.7 *A* **monoidal category** *is a collection* $(\mathcal{C}, \otimes, a, 1, i)$ *where* $\mathcal{C}$ *is a category,* $\otimes : \mathcal{C} \times \mathcal{C} \to \mathcal{C}$ *is a bifunctor called the tensor product, for every collection of objects* X, Y *and* Z *of* $\mathcal{C}$ *we have the component of a natural isomorphism*

$$a_{X,Y,Z} : (X \otimes Y) \otimes Z \xrightarrow{\sim} X \otimes (Y \otimes Z),$$

called the associativity constraint or associator, 1 *is a distinguished object of* $\mathcal{C}$ *and* $i : 1 \otimes 1 \xrightarrow{\sim} 1$ *is an isomorphism. This collection must satisfy the following compatibility*

conditions: First we have

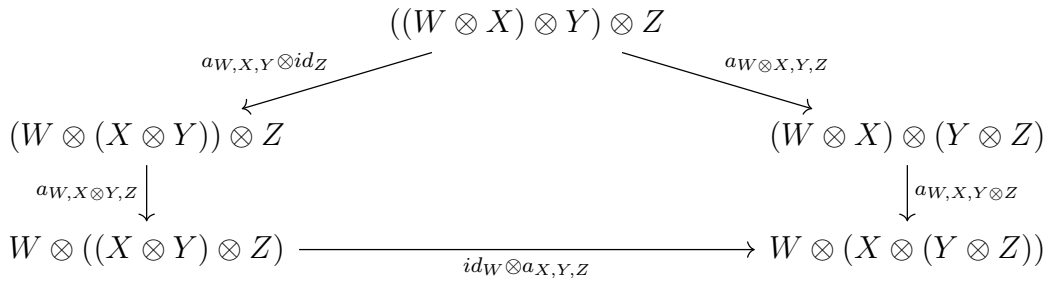

referred to as the pentagon axiom. Second the left and right "tensor by 1*" functors are autoequivalences of* $\mathcal{C}$*. Meaning*

$$L : X \to 1 \otimes X$$

and

$$R : X \to X \otimes 1$$

are both autoequivalences of $\mathcal{C}$*.*

Definition 2.3.8 *Let* $(\mathcal{C}, \otimes, 1, a, i)$ *be a monoidal category, which through an abuse of notational we will call* $\mathcal{C}$*. Then* $\mathcal{C}$ *is* **rigid** *if every object has both a left and right dual. An object* X^* *is said to be a left dual of* X *if there exist an evaluation morphism* $\mathrm{ev}_X \in \mathrm{Hom}(X^* \otimes X, 1)$ *and a coevaluation morphism* $\mathrm{coev}_X \in \mathrm{Hom}(1, X \otimes X^*)$ *such that*

$$X \xrightarrow{\mathrm{coev}_X \otimes id_x} (X \otimes X^*) \otimes X \xrightarrow{a_{X,X^*,X}} X \otimes (X^* \otimes X) \xrightarrow{id_X \otimes \mathrm{ev}_X} X$$

and

$$X^* \xrightarrow{id_{X^*} \otimes \mathrm{coev}_X} X^* \otimes (X \otimes X^* \xrightarrow{a^{-1}_{X^*,X,X^*}} (X^* \otimes X) \otimes X^* \xrightarrow{\mathrm{ev}_X \otimes id_{X^*}} X^*$$

are both the identity morphism. Similarly an object ${}^*X$ *is said to be a right dual of* X *if there exist an evaluation morphism* $\mathrm{ev}'_X \in \mathrm{Hom}(X \otimes {}^*X, 1)$ *and a coevaluation morphism*

$\text{coev}'_X \in \text{Hom}(1, {}^*X \otimes X)$ *such that*

$$X \xrightarrow{id_X \otimes \text{coev}'_X} X \otimes ({}^*X \otimes X) \xrightarrow{a^{-1}_{X,{}^*X,X}} (X \otimes {}^*X) \otimes X \xrightarrow{\text{ev}'_X \otimes id_X} X$$

and

$$({}^*X) \xrightarrow{\text{coev}'_X \otimes id_{{}^*X}} ({}^*X \otimes X) \otimes ({}^*X) \xrightarrow{a_{{}^*X,X,{}^*X}} ({}^*X) \otimes (X \otimes {}^*X) \xrightarrow{id_{{}^*X} \otimes \text{ev}'_X} ({}^*X)$$

are both the identity morphism.

Definition 2.3.9 *A* **fusion category** *is a* $\mathbb{C}-$*linear abelian rigid semisimple monoidal category with only finitely many simple objects where the monoidal unit must be simple, such that the tensor product is bilinear on morphisms.*

2.3.3 Quantum Traces

Definition 2.3.10 *Let* $\mathcal{C}$ *be a rigid monoidal category and* X *an object of* $\mathcal{C}$*, and* $a \in \text{Hom}(X, X^{**})$*, then the* left quantum trace *is defined as*

$$\text{Tr}^L(a) : 1 \xrightarrow{\text{coev}_X} X \otimes X^* \xrightarrow{a \otimes id_{X^*}} X^{**} \otimes X^* \xrightarrow{\text{ev}_{X^*}} 1.$$

Similarly the right quantum trace *can be defined for* $a \in \text{Hom}(X, {}^{**}V)$*, as*

$$\text{Tr}^R(a) : 1 \xrightarrow{\text{coev}_{{}^*X}} ({}^*X \otimes X) \xrightarrow{id_{{}^*X} \otimes a} ({}^*X \otimes {}^{**}X) \xrightarrow{\text{ev}_{{}^{**}X}} 1.$$

Definition 2.3.11 *A* **pivotal** *structure on a rigid monoidal category is a collection of isomorphisms*

$$\phi_X : X \xrightarrow{\sim} X^{**}$$

for all objects X, that is natural in X and

$$\phi_{X\otimes Y} = \phi_X \otimes \phi_Y$$

for all X and Y. A rigid monoidal category with pivotal structure is called pivotal.

Definition 2.3.12 *A rigid monoidal category with pivotal structure ϕ is called* **spherical** *if for all objects X*

$$\mathrm{Tr}^L(\phi_X) = \mathrm{Tr}^R(\phi_X^{-1}).$$

In this case the pivotal structure ϕ is called the spherical structure.

2.3.4 Ribbon Monoidal Categories

Definition 2.3.13 *A monoidal category $\mathcal{C}$ is* **braided** *if it is given a family of natural isomorphisms $c_{X,Y} : X \otimes Y \xrightarrow{\sim} Y \otimes X$ such that the following diagrams are commutative for all objects X, Y, and Z:*

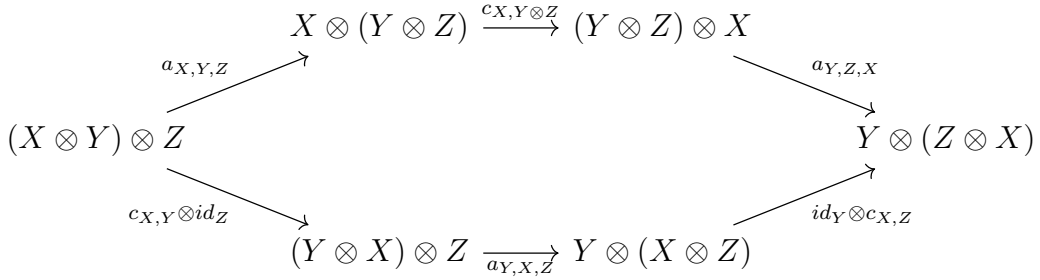

and

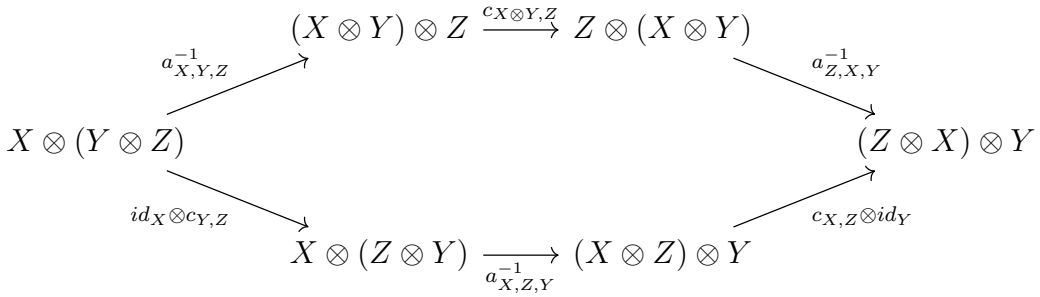

Definition 2.3.14 *A* **twist** *on a braided rigid monoidal category $\mathcal{C}$ is a natural transformation from the identity functor on $\mathcal{C}$ to itself. In terms of components this gives us a morphism $\theta_X \in \mathrm{Hom}(X, X)$ for all objects X. We also have the additional condition that*

$$\theta_{X\otimes Y} = (\theta_X \otimes \theta_Y) \circ c_{Y,X} \circ c_{X,Y}.$$

Definition 2.3.15 *A twist, θ, on a braided rigid monoidal category is called a* **ribbon structure** *if*

$$(\theta_X)^* = \theta_{X^*}.$$

This notion of ribbon structure is exactly the compatibility between the spherical structure and the braiding which was mentioned in the original definition of a modular tensor category.

Definition 2.3.16 *A* **ribbon fusion category** *is a braided fusion category with a ribbon structure structure.*

We note that a ribbon fusion category is often called a premodular category. A ribbon fusion category satisfies all of the definitions of a modular category aside from the final non-degeneracy condition.

2.3.5 Modularity

Definition 2.3.17 *Let $\mathcal{C}$ be a ribbon fusion category with spherical structure ϕ and finite set of isomorphism classes of simple objects $\mathcal{L}$. Let* Tr *be the quantum trace induced on morphisms using ϕ, noting that we do not need to specify R or L. Then $\mathcal{C}$ is* **modular** *if*

$$S = [s_{ij}]_{i,j\in\mathcal{L}}$$

where

$$s_{ij} = Tr(c_{j,i} \circ c_{i,j})$$

is non-degenerate.

2.4 Ribbon Graphs and Graphical Calculus

This section will repeat much of the above information given in the algebraic formality of the previous section. In particular we hope to ground ourselves in the graphical calculus of these categories while keeping an outlook toward developing ribbon graph invariants.

This jump to an entirely graphical interpretation is completely rigorous. In fact this stems from the category of framed tangles serving as a "universal ribbon category". In particular given any ribbon tensor category, $\mathcal{C}$, and any object, X, there is a uniquely determined monoidal functor from the category of framed tangles to $\mathcal{C}$ which sends the generating object of the framed tangles to X and preserves the ribbon structure coming from the double twist of a ribbon tangle [45].

Definition 2.4.1 *A* ***ribbon graph*** *is a graph equipped with a cyclic ordering on the half edges incident to each vertex.*

To each ribbon graph one can associate an oriented surface with boundary by replacing

edges by thin oriented rectangles (or ribbons), replacing vertices by disks, and pasting rectangles to disks according to the chosen cyclic orders at the vertices. Then we will extend the relationship of framed tangles to embedded ribbon graphs in a rectangle. Here the edges will be colored with objects of $\mathcal{C}$ and vertices will be colored by morphisms in $\mathrm{Hom}(\bigotimes_\alpha V_\alpha, 1)$ where V_α are the labels of the incident edges and the order of the tensor product is determined by the cyclic order of the ribbon graph.

For the rest of this section let $\mathcal{C}$ be a modular tensor category. We will explain the various structures of $\mathcal{C}$ in terms of the graphical calculus.

2.4.1 Graphical Calculus

This alternative description of modular tensor categories, based on on performing graphical calculus on basis elements of diagrams closely follows that of [45, 13] We will start with a finite label set L. This is coming from the finite set of isomorphism classes of simple objects of $\mathcal{C}$. This set L is equipped with an involution $\hat{}: L \to L$ called duality. This duality is coming exactly from the spherical structure on $\mathcal{C}$. In terms of the graphical calculus the elements of L will correspond to oriented edge labels of an oriented ribbon tangle, with $\hat{}$ giving a reversal of the orientation. We say that $(L, +, \otimes)$ is the underlying fusion algebra of $\mathcal{C}$ where

$$a \otimes b = \sum_{c \in L} N_{ab}^c c.$$

and

$$N_{ab}^c = \dim(\mathrm{Hom}(a \otimes b, c)).$$

In terms of the graphical calculus we have trivalent vertices corresponding to each of the N_{ab}^c basis vectors. In particular we have in figure 2.1:

Where the normalization factor is included so that we are consistent with an isotopy

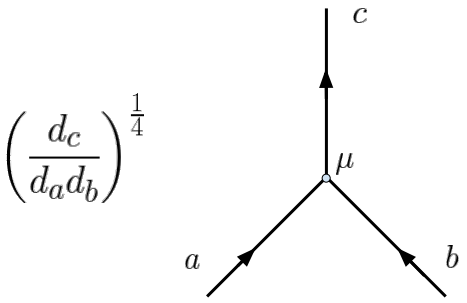

Figure 2.1: A basis element of $\mathrm{Hom}(a \otimes b, c)$

invariant convention and the values of d_a, d_b, and d_c will be explained below. From the associativity of the underlying fusion algebra we have

$$(a \otimes b) \otimes c = a \otimes (b \otimes c)$$

and this then gives rise to isomorphisms on the splitting spaces as seen in the language of the graphical calculus in figure 2.2.

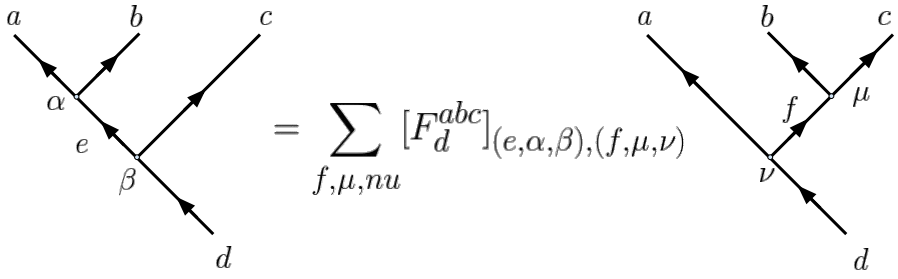

Figure 2.2: Associativy lifted to vector spaces

We call this diagrammatic equivalence an F-move. We note that this $F-$move is exactly the associativity constraint given in the definition of a monoidal category, definition 2.3.7. As such we have a diagrammatic version of the pentagon axiom commutative diagram as well, as seen in figure 2.3.

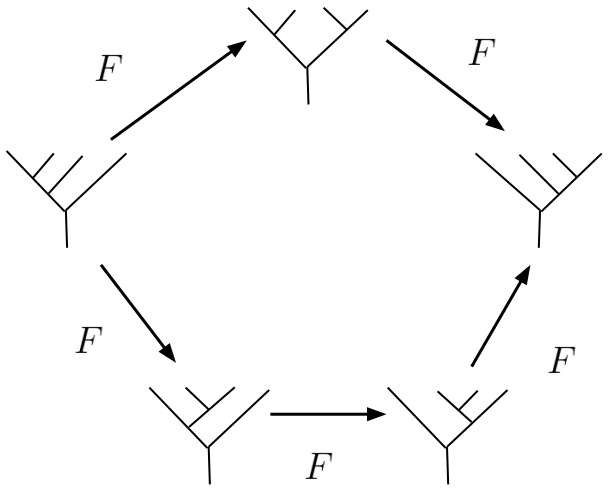

Figure 2.3: A diagrammatic version of the pentagon axiom

We can also utilize a notion of inner products on these vector spaces to introduce the move seen in figure 2.4. We will sometimes call this diagrammatic equivalence a

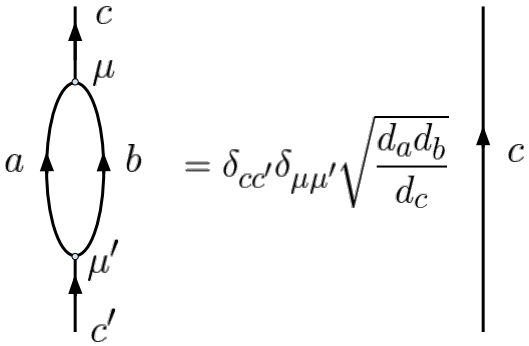

Figure 2.4: A diagrammatic interpretation of the inner product

Schur's Lemma-move, for obvious reasons. We note that this diagrammatic move is a direct consequence of the definition of a simple object, definition 2.3.6. Combining these two moves we are able to deduce the values used in our normalization, called quantum dimensions, seen in figure 2.5.

We see how this is exactly coming from the quantum trace of the identity morphisms

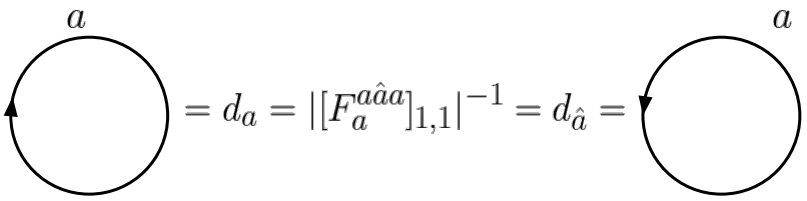

Figure 2.5: Quantum Dimension

in $\mathcal{C}$, referring to 2.3.3. From the above we also have the factorization of the identity on two element seen in figure 2.6.

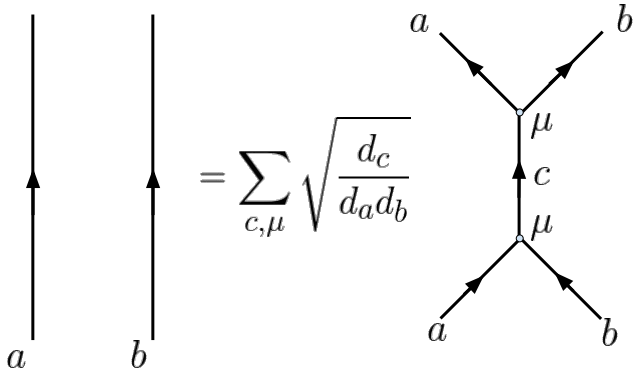

Figure 2.6: Factoring the identity

So far all of the graphical calculus discussed has been strictly planar, this changes as a braiding is introduced. The R-move as seen in figure 2.7 is our first and most powerful example. In particular this introduces invariance under the second and third Reidemeister moves to our graphical calculus coming from the definition of a braided monoidal category, this follows from the natural isomorphism requirement given to $c_{X,Y}$ in definition 2.3.13 . We also have a diagrammatic description of the hexagon axioms given the same definition of a braiding as seen in figure 2.8 for a positive crossing, noting again that the F moves correspond to the associativity constraints in $\mathcal{C}$.

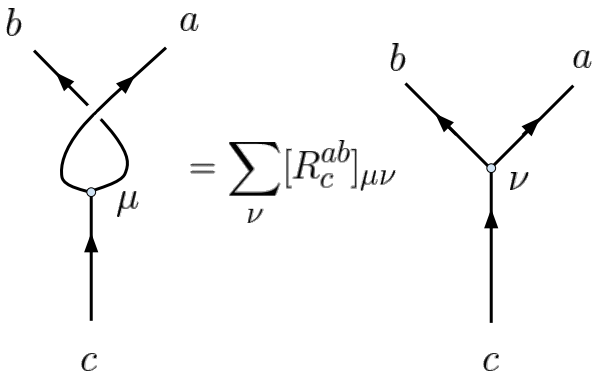

Figure 2.7: Introducing a braiding

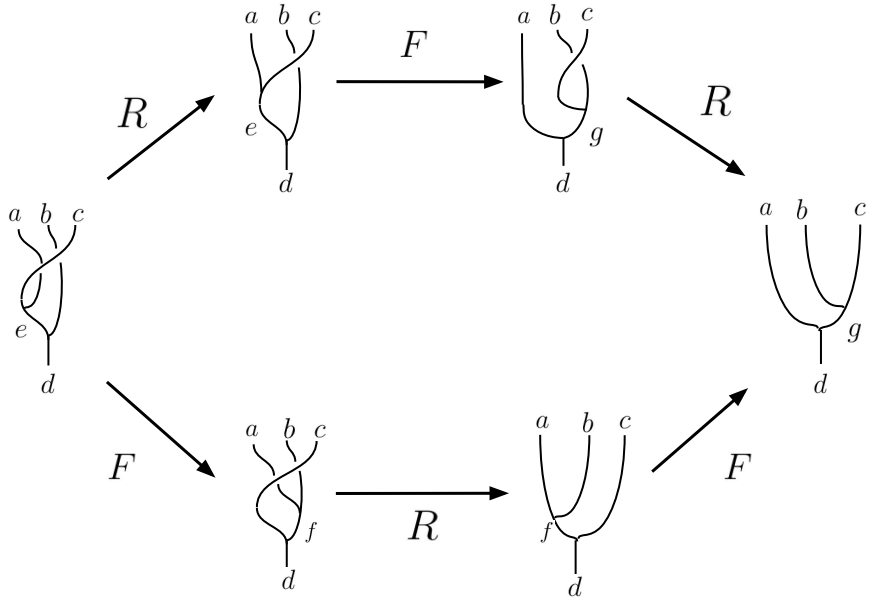

Figure 2.8: Compatibility of a braiding

This leads to looking at the first Reidemeister move. This is taken care of by the move seen in figure 2.9, which is exactly the twist in $\mathcal{C}$.

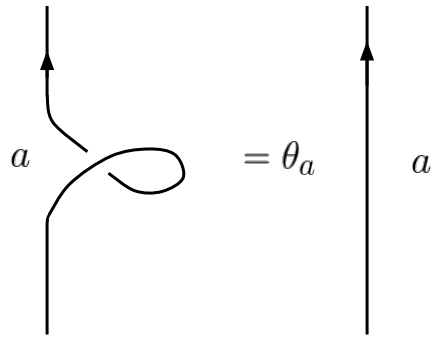

Figure 2.9: The twist

We also mention one consistency equation, as it will slightly simplify a future computation. We have that the R-moves and twists satisfy the following relation

$$\sum_{\lambda} [R_c^{ab}]_{\mu\lambda} [R_c^{ba}]_{\lambda\nu} = \frac{\theta_c}{\theta_a \theta_b} \delta_{\mu,\nu}.$$

Finally as describe the modularity condition. This is seen in the non-degeneracy of the matrix having entries defined in in figure 2.10, where $D^2 = \sum_{a \in L} d_a^2$

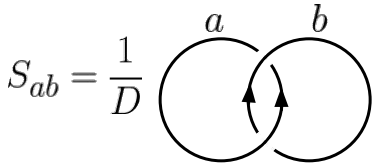

Figure 2.10: The $S-$matrix

We will refer to the full collection of these moves in the graphical calculus as evaluation moves.

2.4.2 Isotopy Invariance

We note that this section is based on and uses the majority of the conventions given in [13]. As we are looking to build a ribbon graph invariant, we hope to have ambient isotopy invariance built into our graphical calculus. As discussed above we need both R-moves and twists to account for all three Rediemiester moves. This leads us to explore further consistency between these two moves. The diagram seen in figure 2.11 brings this issue to light.

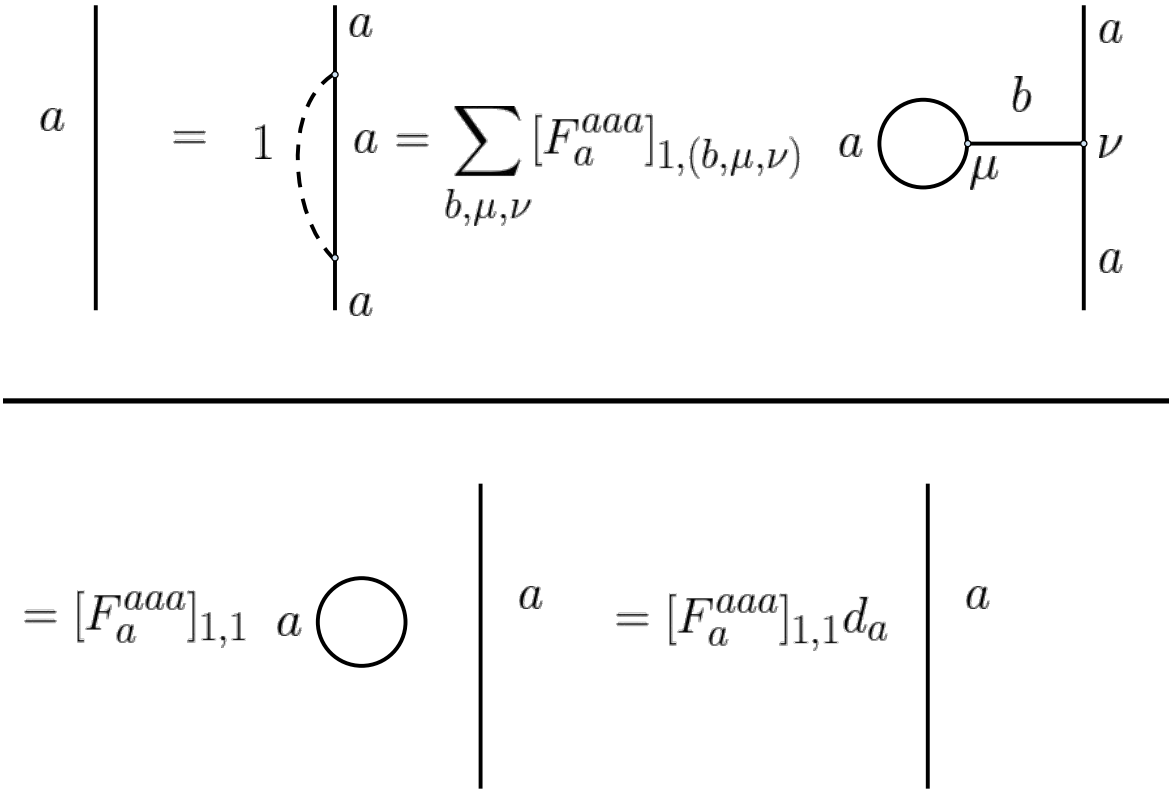

Figure 2.11: A potential issue with isotopy invariance

This then allow us to define

$$\nu_a := [F_a^{a\hat{a}a}]_{1,1} * d_a,$$

called the Frobenius-Schur indicator. We have that when a is not self-dual that $\nu_a = 1$, but when $a = \hat{a}$ we have that $\nu_a = \pm 1$. This leads to a potential inconsistency in isotopy invariance for edges labeled with a where $\nu_a = -1$.

This leads us to introduce the following convention. When removing a trivially labelled edge a right directed flag is introduced as seen in figure 2.12. Then cap-cup pairs

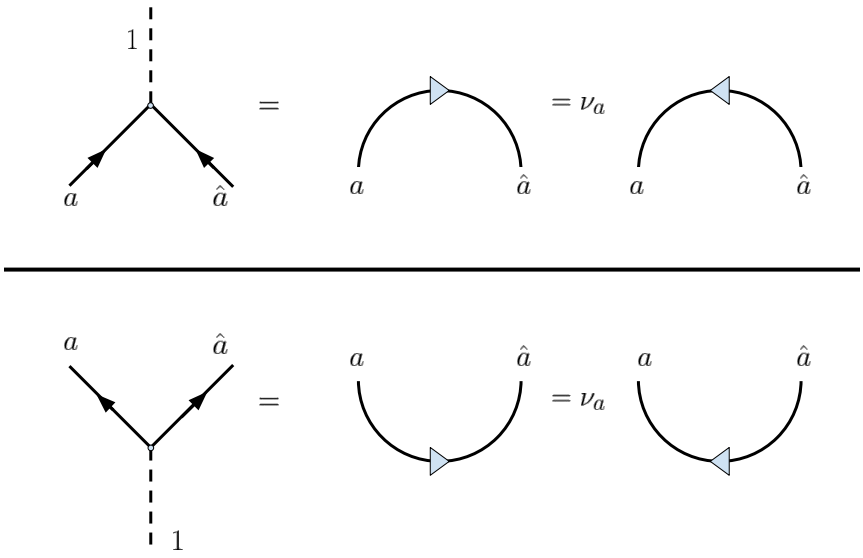

Figure 2.12: The addition of flags

with opposite flags cancel, as seen in figure 2.13. These flags will almost always be left implicit unless they are explicitly needed.

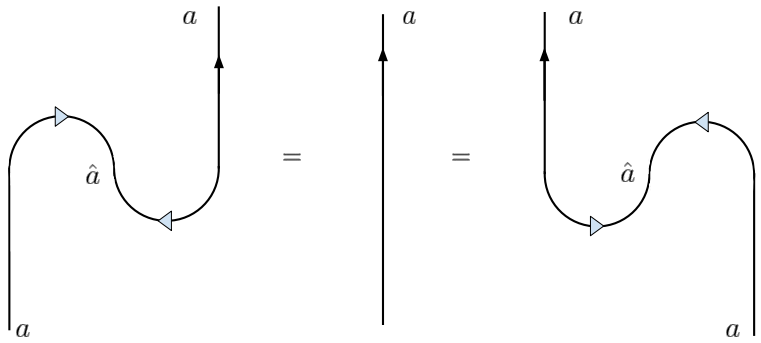

Figure 2.13: The canceling of flags

In particular, we have found our consistency between R-moves and twists in the relation

$$\theta_a = \nu_a [R_1^{\hat{a}a}]^{-1},$$

and so with this above convention we have isotopy invariance built into our graphical calculus. We note that this is essentially the flag convention originally used by Kirby and Melvin, [30], to compute the Jones polynomial and generalized in [18].

Now we can continue our discussion of how this isotopy convention manifests on the vertices of the ribbon graphs. In particular we are not able to freely rotate vertices as this would introduce flags. We have the following maps introduced when rotating one of the half incident edges to a vertex, seen in figure 2.14 and we have that

$$[A_c^{ab}]_{\mu,\nu} = \sqrt{\frac{d_a d_b}{d_c}} \frac{1}{\nu_a} [F_b^{\hat{a}ab}]^{-1}_{(c,\mu,\nu),1}$$

and

$$[B_c^{ab}]_{\mu,\nu} = \sqrt{\frac{d_a d_b}{d_c}} [F_b^{ab\hat{b}}]_{(c,\mu,\nu),1}$$

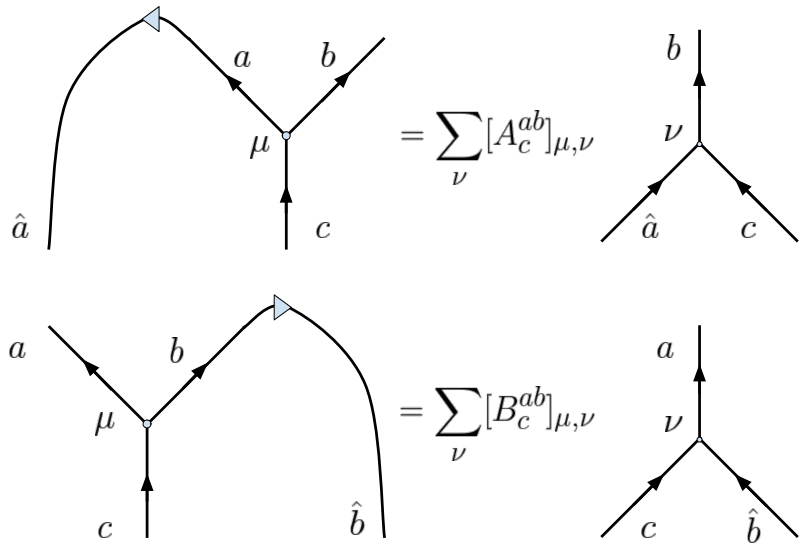

Figure 2.14: The bending map

Now the "$H = I$" form of the F-move can be written down. As can be seen in figure 2.15 this is simply an F-move with certain vertices rotated. where

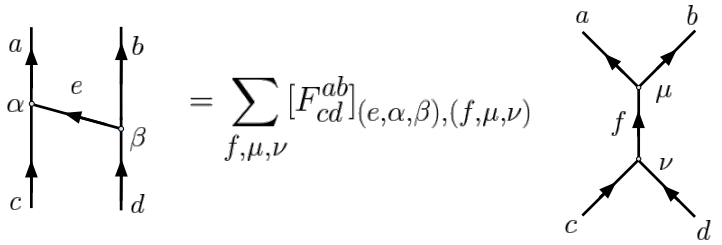

Figure 2.15: An F-move performed on rotated vertices, or "$H = I$"

$$[F_{cd}^{ab}]_{(e,\alpha,\beta),(f,\mu,\nu)} = \sum_{\alpha',\nu'} [A_e^{\hat{c}a}]^{-1}_{\alpha,\alpha'} [F_d^{\hat{c}ab}]_{(e,\alpha,\beta),(f,\mu,\nu')} [A_d^{\hat{c}f}]_{\nu',\nu}.$$

We also have through further computation that

$$[F_{cd}^{ab}]_{(e,\alpha,\beta),(f,\mu,\nu)} = \sqrt{\frac{d_e d_f}{d_a d_d}}[F_f^{ceb}]^{-1}_{(a,\alpha,\mu),(d,\beta,\nu)}.$$

Just as we have taken the convention that we omit flags in our computations, we will also take (the potentially confusing notation) where we use the described F-moves and omit our A and B maps. For the reader uncomfortable with this notation that can imagine we are in the case of a unimodal category (meaning all Frobenius-Schur indicators are trivial).

2.5 The Reshetikhin-Turaev Construction

2.5.1 An Overview

Here we follow much of the exposition of Turaev as described in his book [45]. The most striking result to take away is that every modular tensor category, denoted $\mathcal{C}$, gives rise to an anomaly-free $2+1$ dimensional TQFT:

$$\text{Modular Tensor Category} \qquad \mapsto \qquad (2+1) \quad \text{TQFT}.$$

The approach taken is to first define an invariant of framed links, which can be extended to an invariant of colored ribbon graphs in $\mathbb{R}^3$, or $\mathbb{R}^2 \times [0,1]$. Here a coloring means that each edge of the graph is given a simple object in $\mathcal{C}$ and each vertex is given an appropriate morphism. This is then extended to define an invariant of $3-$manifolds, making use of a surgery description of that $3-$manifold on a link in S^3. This can then be adapted to an invariant of a pair of (M,Ω) where Ω is a colored graph in M. From this type of invariant the jump to a TQFT is made. First a TQFT is found, which

has parametrized bases, meaning that surfaces have a homeomorphism to the standard closed surface of the same genus bounding a standard unknotted handlebody in $\mathbb{R}^3$. This is eventually lighted to weaker structures, like a Langrangian subspace of the $H_1(\Sigma;\mathbb{R})$.

2.5.2 Coloring a Ribbon Graph

Let $\mathcal{C}$ be a modular tensor category and G a ribbon graph.

Definition 2.5.1 *A* $\mathcal{C}$***-coloring*** *of G is an assignment of a simple object to each edge of G and an assignment to each vertex a vector in* $\mathrm{Hom}(\bigotimes_i a_i, 1)$*, where a_i are the labels of the edges incident to the vertex and the cyclic order is followed.*

Turaev has shown how the evaluation moves of a modular tensor category allow for the construction of a colored ribbon graph invariant in $\mathbb{R}^3$ or $\mathbb{R}^2 \times [0,1]$. In fact when the category is modular this ribbon graph invariant can be used to construct an entire $2+1$ (parametrized) topological quantum field theory. We won't go into the details of this construction and instead will use the relevant consequences.

2.5.3 3-Manifold Invariants

Of particular interest is the Kirby coloring ω, defined as seen in figure 2.16. This

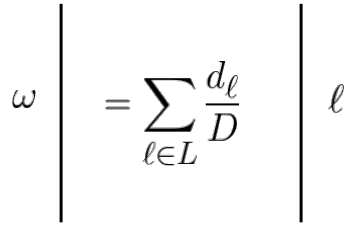

Figure 2.16: The definition of the Kirby Color

element allows for the construction of $3-$manifold invariatns using the surgery description

of the 3−manifold on a link in S^3 (Recall that a framed link is a special case of a ribbon graph). Then invariance under Kirby moves comes from special properties of coloring the link in question with ω, the proof of which can be seen in [48]. We will use the handle-slide invariance of ω in our later computations, which is illustrated in figure 2.17.

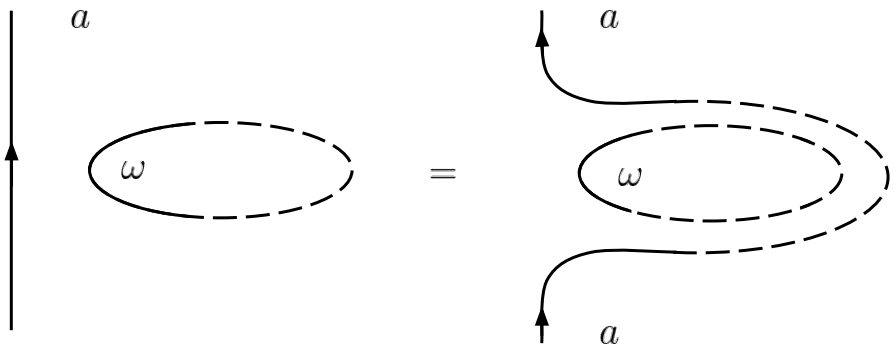

Figure 2.17: The handle slide invariance of ω

This 3−manifold invariant can be adapted further to give an invariant of pairs (M, Ω), where M is a 3−manifold, potentially with boundary, and Ω is a ribbon graph in M.

2.5.4 Module of States

Following the construction of Reshitikhin and Turaev we will describe the module of states, or TQFT vector space, $V(\Sigma_g)$ to any closed oriented surface of genus g [39, 40, 45]. Up to some homeomorphism into $\mathbb{R}^3$ we can take Σ_g to be in standard position in $\mathbb{R}^3$, meaning it bounds the standardly embedded handlebody H_g in $\mathbb{R}^3$. Then to Σ_g we assign a spine, S, of H_g, graph whose regular neighborhood is H_g. Then we take $V(\Sigma_g)$ to be the complex vector space having as a basis the $\mathcal{C}$-colorings of S.

The rose basis

The first basis we will describe is the basis corresponding to colorings of the rose on g petals. In particular, this graph has a single vertex. This allows for a description of the state space as a direct sum of these (potentially complicated) vertex Hom spaces, where the sum is over the edge labels. We see this basis in figure 2.18 and note that we abandon the labeling of vertices by greek indices in favor of a capital F to remind us that this Hom space is more complicated that those indexed by the structure constants of a fusion algebra.

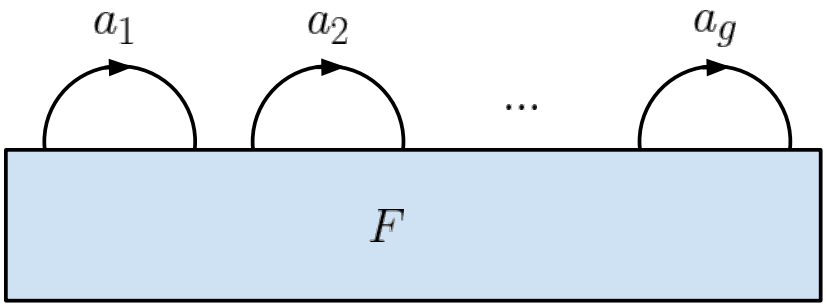

Figure 2.18: A basis element of $V(\Sigma_g)$ coming from the rose on g petals

The comb basis

The following basis is intimately related to the rose basis. Specifically, this basis comes from expanding the morphism F into the composition of the evaluation map corresponding to the label of the introduced edge, and the composition of two morphisms (corresponding to the two new vertex labels). This is seen in figure 2.19.

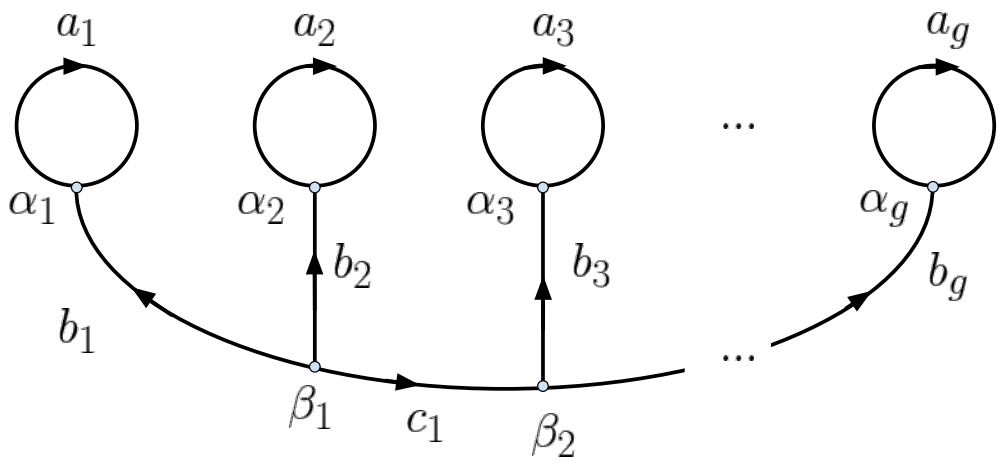

Figure 2.19: A basis element of $V(\Sigma_g)$ coming from expanding the vertex given in the rose basis

The eye-glasses basis

The choice of basis that will use most often in the following work is is shown in figure 2.20. We see that this is obtained by applying F-moves along b_2 through b_{g-1} in the comb basis.

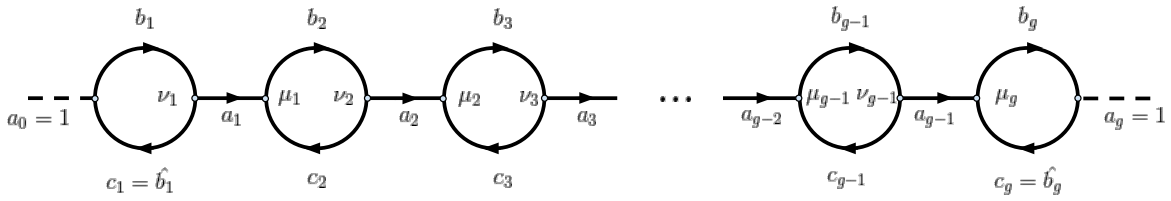

Figure 2.20: A basis element of $V(\Sigma_g)$

We denote a basis element of this type as

$$\vec{v} = (\vec{a}, \vec{b}, \vec{c}, \vec{\mu}, \vec{\nu})$$

$$= (a_1, ..., a_{g-1}, b_1, .., b_g, c_1, ..., c_g, \mu_2, ..., \mu_g, \nu_1, ..., \nu_{g-1}).$$

2.5.5 A Projective Action

This construction originates from the work description given in section 4 of [40]. Take an orientation preserving homeomorphism

$$h : \sigma \to \Sigma \in \mathrm{MCG}(\Sigma).$$

Then we look at the cylinder, $\Sigma \times [0, 1]$. We think of $\Sigma \times \{0\}$ as being parametrized by id and $\Sigma \times \{1\}$ as being parametrized by h. Now let H be the handlebody bounded by Σ, with colored spine S taken as a ribbon graph in H such that the colorings of S are the basis of $V(\Sigma)$. Then glue (H, S) to $\Sigma \times \{1\}$ along h and to $\Sigma \times \{0\}$ along the identity. Then this gives a pair (M, Ω) of a closed 3−manifold and a ribbon graph. This is seen in figure 2.21 for the case of a genus 2 surface and the rose basis.

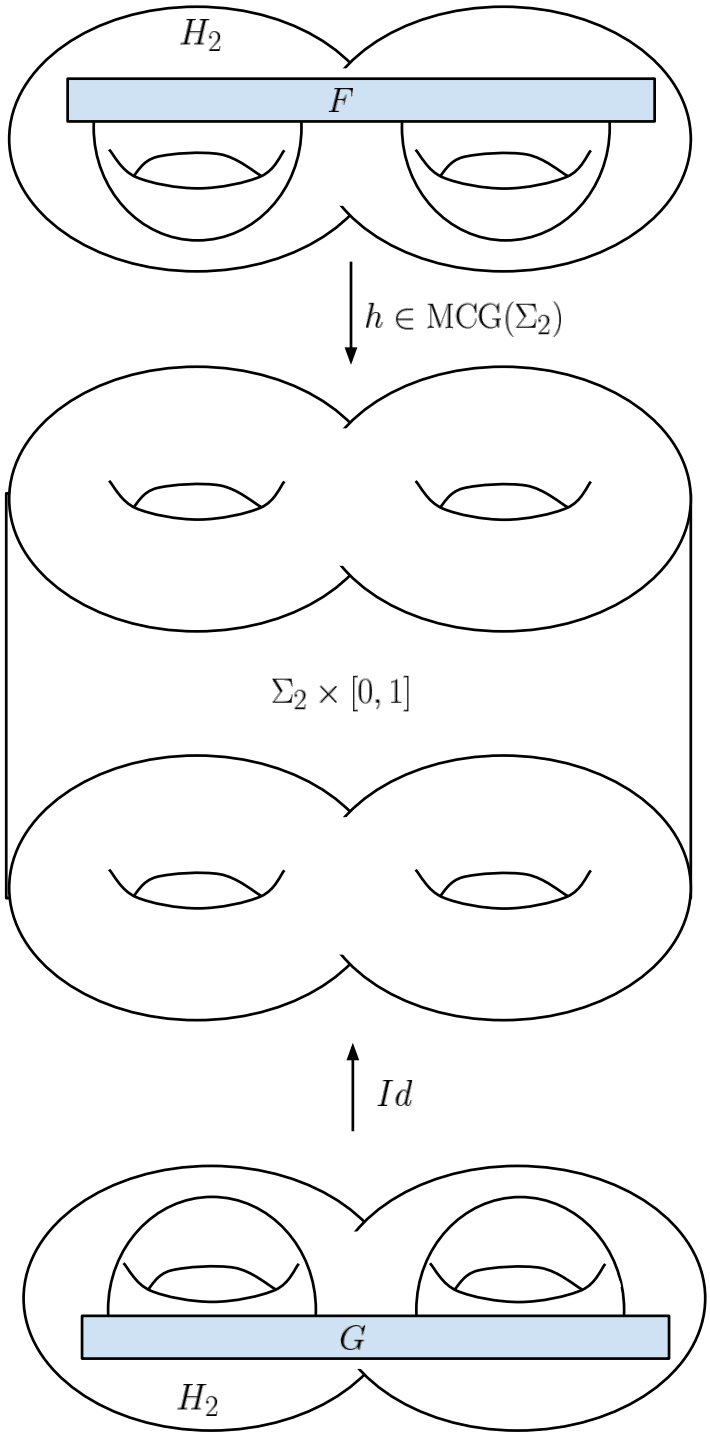
H_2
F
$h \in \mathrm{MCG}(\Sigma_2)$
$\Sigma_2 \times [0,1]$
Id
G
H_2

Evaluation of the invariant for this pair gives an operator

$$V_h : V(\Sigma) \to V(\Sigma)$$

This gives a (projective) representation of MCG(Σ), called a quantum representation. Our interest will be specifically in the case that h is a positive Dehn twist about a simple closed curve γ. This amounts primarily to understanding the surgery description of the mapping cylinder along a link L which is disjoint from the two spines. Then the evaluation is performed in S^3 of the invariant associated to L and the two ribbon graphs. In the case of the positive Dehn twist about γ, this is given by labeling γ with ω and giving it a -1 framing relative to the Σ, then evaluating the ribbon graph invariant, as well as the linking of the components of the ribbon graphs. As an example we will show how these computations can be realized for Dehn twists on the genus two surface in the rose basis. These can be seen in figures 2.22, 2.23, 2.24.

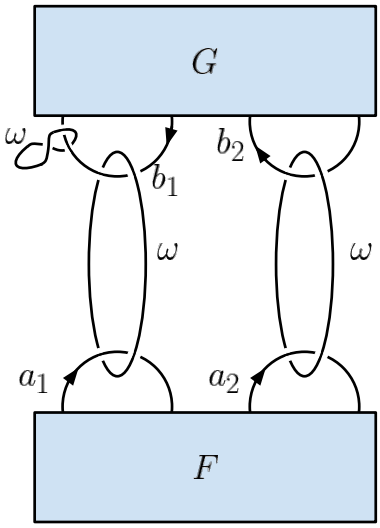

Figure 2.22: The action of the Dehn twist about the left meridian

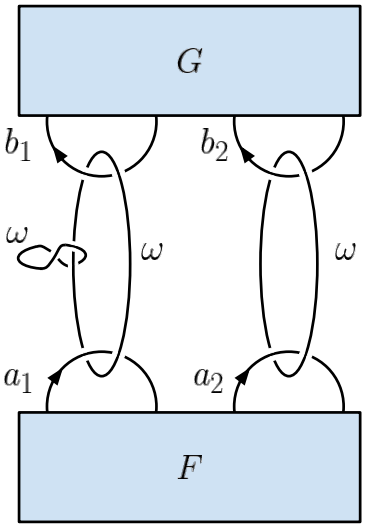

Figure 2.23: The action of the Dehn twist about the left longitude

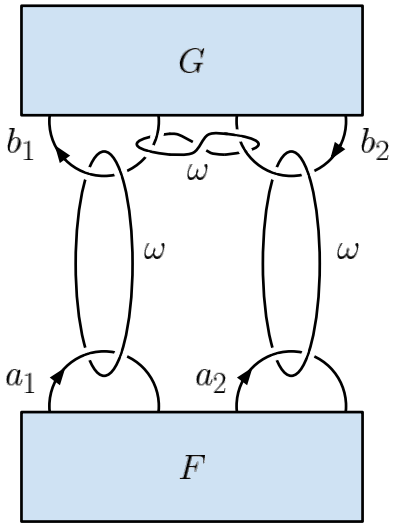

Figure 2.24: The action of the Dehn twist about the third Humphries generator

2.6 Spiders

Every pivotal tensor category gives rise to a Spider, in the sense of Kuperberg [33]. Following an approach that is closer to the world of planar algebras, [23], a single object

X would be chosen, then we would look at the full subcategory whose objects are tensor products of X and X^*. Diagrammatically this allows strands to labelled simply by an orientation rather than a label set. If X was chosen such that it is symmetrically self-dual, meaning $X = X^*$ and the frobenius-schur indicator associated to X is 1, then this gives an unoiented unshaded planar algebra [37]. For our purposes we won't choose a single object X, but rather a set of objects $\{X, Y, Z, ...\}$ along with their duals. This still gives rise to a full subcategory and diagrammatically it is closer to planar algebra with labeled strands. In some sense this is a middle ground between just using the graphical calculus of the original modular tensor category and making the full jump to the planar algebra approach.

2.6.1 Quantum Groups and Spiders

The spiders that we will be working with are built from the representation categories of quantum groups, denoted $Rep(U_q(\mathfrak{g}))$. We will primarily be working with the unimodal pivotal structure which can be put on this representation category, which we will denote $Rep^{uni}(U_q(\mathfrak{g}))$. This pivotal structure can be seen to exist by looking at the representation catgory as a subcategory of $sVec$ and taking the pivotal structure from the embedding. This tell us which pivotal tensor category we will be working with, and so we only need to specify a collection of simple objects to determine a spider. The fundamental representations, denoted V_{λ_i} or just λ_i will serve this role. Diagrammatically, we have objects are points on a line labeled with fundamental representations and morphisms are diagrams in a rectangle having the appropriate objects on the top and bottom, as seen in figures 2.25 and 2.26.

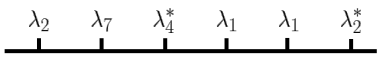

Figure 2.25: An object in our spider

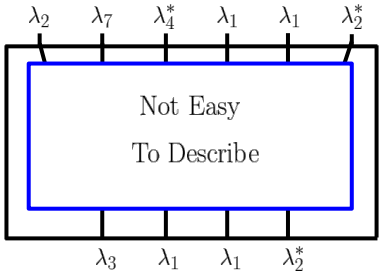

Figure 2.26: A morphism in our spider

Unfortunately, in the abstract there is very little control on what diagrams should be used to desribe these morphisms, so a "coupon" or box is used to hide our lack of understanding. There are some known combinatorial constructions of certain spiders that allow for a full description of these spaces. We will return to those examples after continuing our discussion in general.

2.6.2 What is lost in a Spider?

Our goal is to gain understanding of $Rep^{uni}(U_q(\mathfrak{g}))$ by working with the spider described above. It is then natural to ask: What do we lose? At first glance it would seem that in taking this subcategory we have lost nearly all of the irreducible representations of $U_q(\mathfrak{g})$. We will be able to recover these "lost" objects by looking at particular morphisms in our category. Let V_λ, where $\lambda = \sum_i a_i\lambda_i$ be the irreducible representation of $U_q(\mathfrak{g})$ with highest weight λ. Then in particular we know that there exists morphisms

$$\text{proj} : \bigotimes V_{\lambda_i}^{\otimes a_i} \to V_\lambda$$

the equivariant projection onto V_λ and

$$\text{inc} : V_\lambda \to \bigotimes V_{\lambda_i}^{\otimes a_i}$$

inclusion. Then composition of these morphisms, inc $\circ$ proj, is an idempotent morphism in our spider since we have taken a full subcategory. In particular, this is a minimal projection in the relevant endomorphism algebra. From here we can recover V_λ as a simple object by taking an idempotent completion of our spider. We will refer to these idempotents as clasps. When the spider at hand has a nice combinatorial description these clasps have diagrammatic descriptions in terms of minimal cut paths. This recovers the notion of a clasped-$\mathfrak{g}$ spider introduced by Kuperberg in his original paper [33]. With this idempotent completion in mind, it seems that we should have just taken the spider coming from all irreducible representations to begin with. We show in an example that when the combinatorial descriptions are available we can gain insight by taking this extra step. In figure 2.27 we see an example of two ribbon graphs colored with representations of $U_q(\mathfrak{sl}(3,\mathbb{C}))$. We see that different morphisms label the vertex, but no information about the multiplicity is provided.

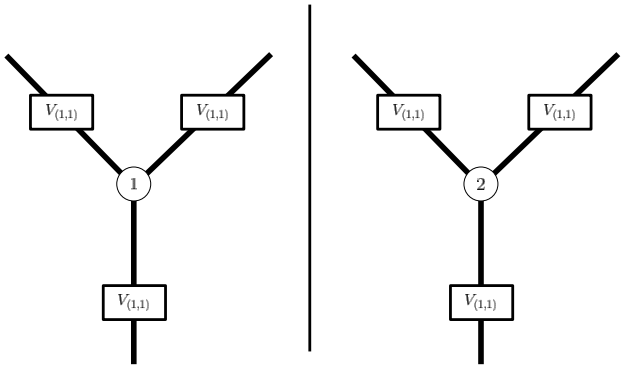

Figure 2.27: Multiplicity in $Rep^{uni}(U_q(\mathfrak{sl}(3,\mathbb{C})))$

In figures 2.28 and 2.29 we see these same coloring morphisms in the idempotent completed, or clasped, $\mathfrak{sl}(3,\mathbb{C})$ spider coming from the fundamental representations.

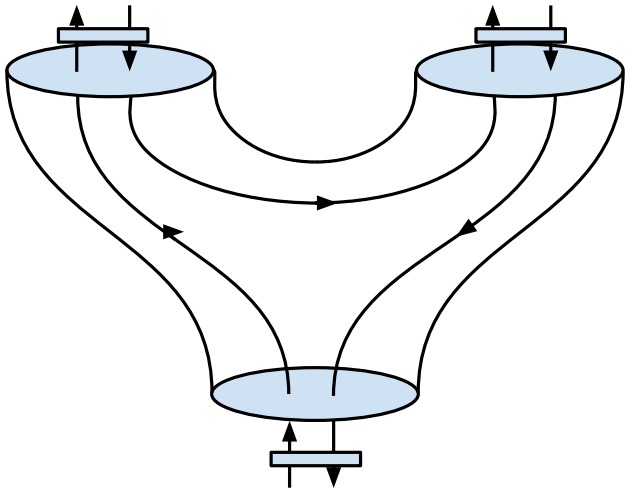

Figure 2.28: The morphism from the left of figure 2.27

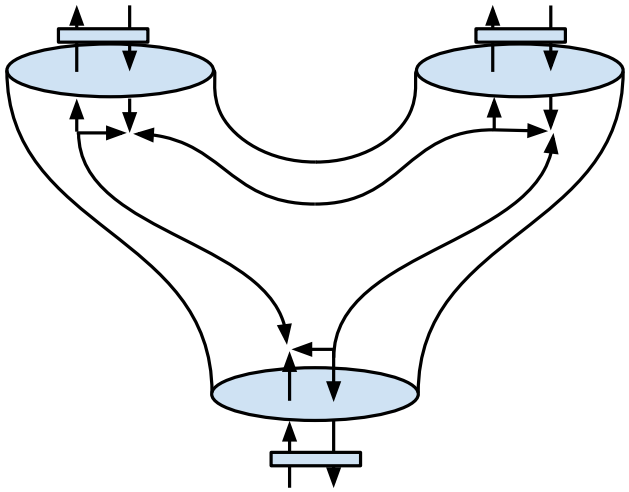

Figure 2.29: The morphism from the right of figure 2.27

2.6.3 Roots of Unity

As our goal is to examine the mapping class group representations coming from the clasped-$\mathfrak{g}$ spider we will need a modular tensor category. The first step from a spider towards a modular category is a semisimplification. This involves modding out the negligible morphisms, and in the language of clasped spiders this means modding out the clasps which has trace zero. The trace is shown in figure 2.5. When an appropriate root of unity is chosen reduces the number of simple objects to finitely many. Then this fusion category is modular when the $S-$matrix is nondegenerate. This is can be circumvented by showing that these categories satisfy certain modularization criteria. It should be noted that this is the first step where our spiders really need to be given a braiding. This is the rough outline of the procedure originating from work of Turaev and Wenzl [46, 47]. The work of Blanchet, (for A_n) in [7], and then Blanchet and Beliakova, (for B_n, C_n, and D_n) in [5], classifies the nonexceptional cases, meaning the categories coming from link invariants of type A_n, B_n, C_n, and D_n. This is the framework of where our clasped spiders will be used. For the remainder of our discussion a spider will mean a semisimplified clasped-$\mathfrak{g}$ spider evaluated at a root of unity, which is of type A_n, B_n, C_n, or D_n meaning we are able to apply the Reshetikhin-Turaev construction of a TQFT. We will take k to be the "level" of our construction. This means that q is a root of unity whose order is a function of k. The exact expression is not important for us here.

Chapter 3

Explicit Computation of Quantum Representations

Let $\mathcal{C}$ be a modular tensor category with "evaluation data" following the conventions from sections 2.4 and 2.5. We will be explicitly computing the action of Dehn twists on the eye-glasses basis. A description of these actions was given above for the specific matrix entry given two basis elements in the rose basis. We instead will compute the action on a basis element, and use that the pairing determined by the mapping cylinder constructing of the identity makes our basis orthogonal. This computation can be found in the work of the author in [12].

3.1 Mapping Class Group Generators

We will be working with the Humphries generators of the mapping class group of a genus g surface as seen in Fig. 3.1.

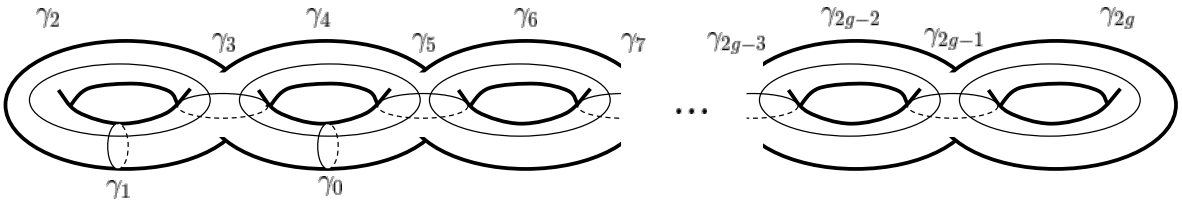

Figure 3.1: The Humphries generators

The actual generators of the mapping class group are positive Dehn Twists about these $2g+1$ curves. In particular we will fix the notation that T_i will stand for the image under the quantum representation of a positive Dehn twist about the curve γ_i.

3.2 T_0 and T_1

The local computation seen in Fig. 3.2 can be applied to the computations of T_0 and T_1.

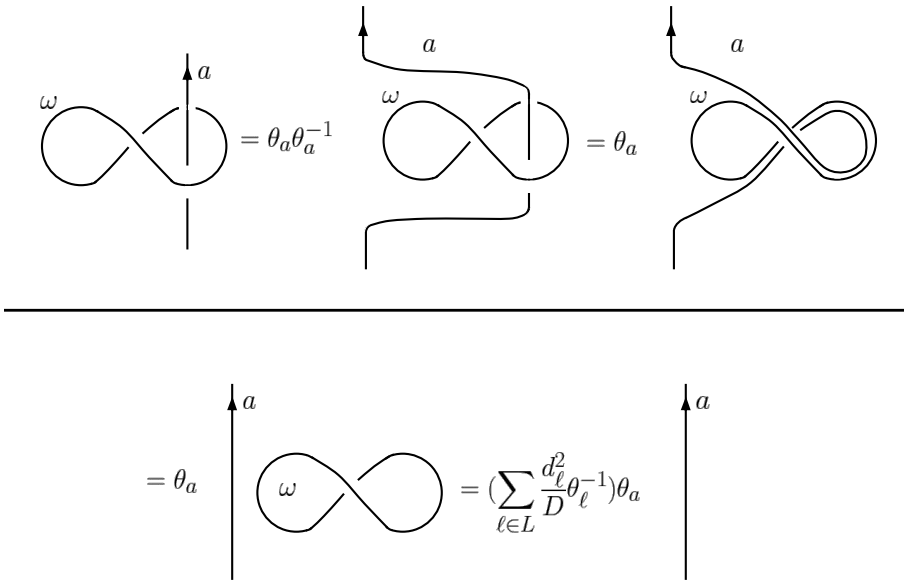

Figure 3.2:

In particular we see that

$$T_0(\vec{v}) = \frac{p_-}{D}\theta_{c_2}\vec{v}$$

and

$$T_1(\vec{v}) = \frac{p_-}{D}\theta_{c_1}\vec{v},$$

where

$$\frac{p_-}{D} = \sum_{a\in L}\frac{d_a^2}{D}\theta_a^{-1}$$

is a root of unity.

3.3 T_{2i+1} for $i = 1, ..., g-1$

The local computation shown in Fig. 3.3 and Fig. 3.4 can be applied to find T_{2i+1} for $i = 1, ..., g-1$.

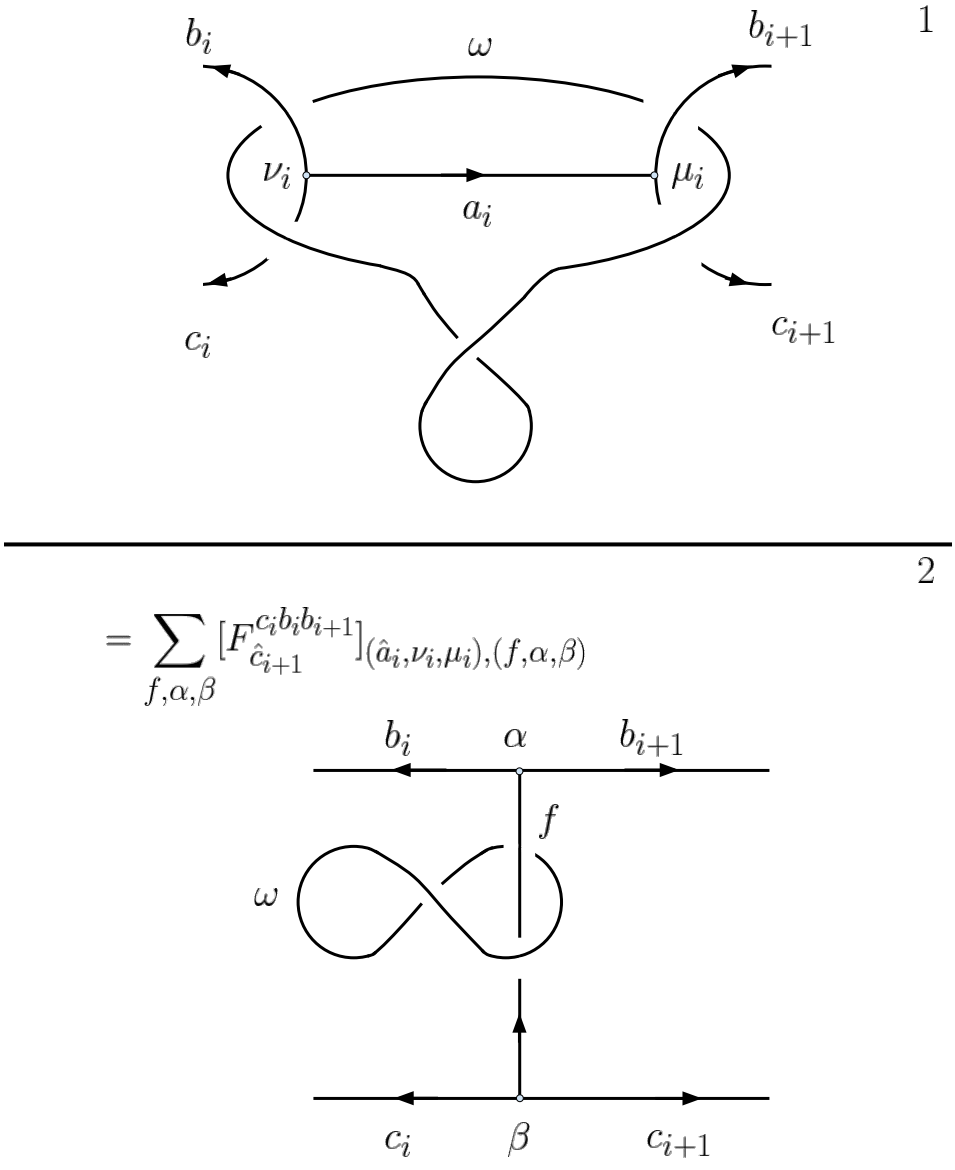

Figure 3.3: Steps 1 and 2

3

$$= \frac{p_-}{D} \sum_{f,\alpha,\beta} [F^{c_i b_i b_{i+1}}_{\hat{c}_{i+1}}]_{(\hat{a}_i,\nu_i,\mu_i),(f,\alpha,\beta)} \theta_f$$

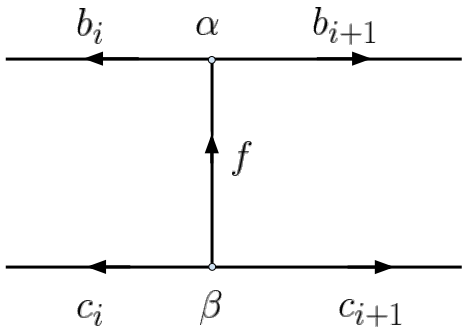

4

$$= \frac{p_-}{D} \sum_{\substack{f,\alpha,\beta \\ h,\sigma,\rho}} [F^{c_i b_i b_{i+1}}_{\hat{c}_{i+1}}]_{(\hat{a}_i,\nu_i,\mu_i),(f,\alpha,\beta)} \theta_f [F^{b_i b_{i+1} c_{i+1}}_{\hat{c}_i}]_{(f,\alpha,\beta,(h\sigma,\rho))}$$

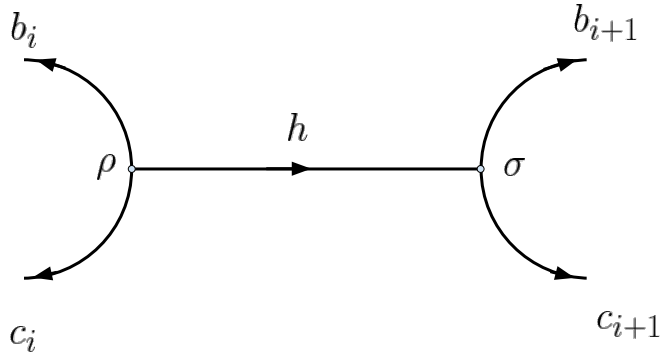

Figure 3.4: Steps 3 and 4

In particular we have

$$T_{2i+1}(\vec{v})$$

$$= \frac{p_-}{D} \sum_{f,\alpha,\beta,h,\sigma,\rho} [F^{c_i b_i b_{i+1}}_{\hat{c}_{i+1}}]_{(\hat{a}_i,\nu_i,\mu_{i+1}),(f,\alpha,\beta)} \theta_f [F^{b_i b_{i+1} c_{i+1}}_{\hat{c}_i}]_{(f,\alpha,\beta),(h,\sigma,\rho)} \vec{v}'_{h,\rho,\sigma},$$

where $\vec{v}'_{h,\rho,\sigma}$ is defined by changing $\vec{v}$ by the following: a_i to h, ν_i to ρ, and μ_{i+1} to σ.

3.4 T_{2i} for $i = 1, ..., g$

This computation is much more involved than the previous. This should be thought of as the generalization of $S-$matrices from the genus 1 case where the previous examples where more analogous to T matrices. To begin we look at the evaluation seen in Fig. 3.5 which will prove useful in our upcoming computation.

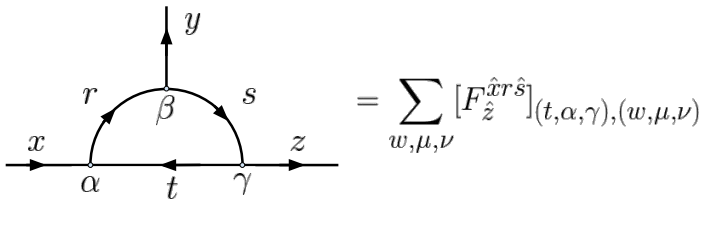

$$= \sum_{w,\mu,\nu} [F^{\hat{x}r\hat{s}}_{\hat{z}}]_{(t,\alpha,\gamma),(w,\mu,\nu)}$$

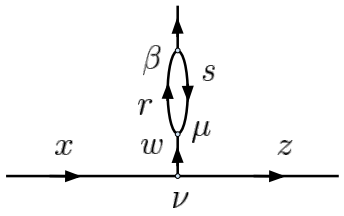

$$= \sum_{\nu} [F^{\hat{x}r\hat{s}}_{\hat{z}}]_{(t,\alpha,\gamma),(y,\beta,\nu)} \sqrt{\frac{d_r d_s}{d_y}}$$

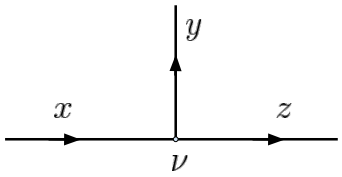

Figure 3.5: A useful computation

With this in mind we see in Fig. 3.6 ,Fig. 3.7,Fig. 3.8, and Fig. 3.9, a local calculation that allows us to realize the action of T_{2i}.

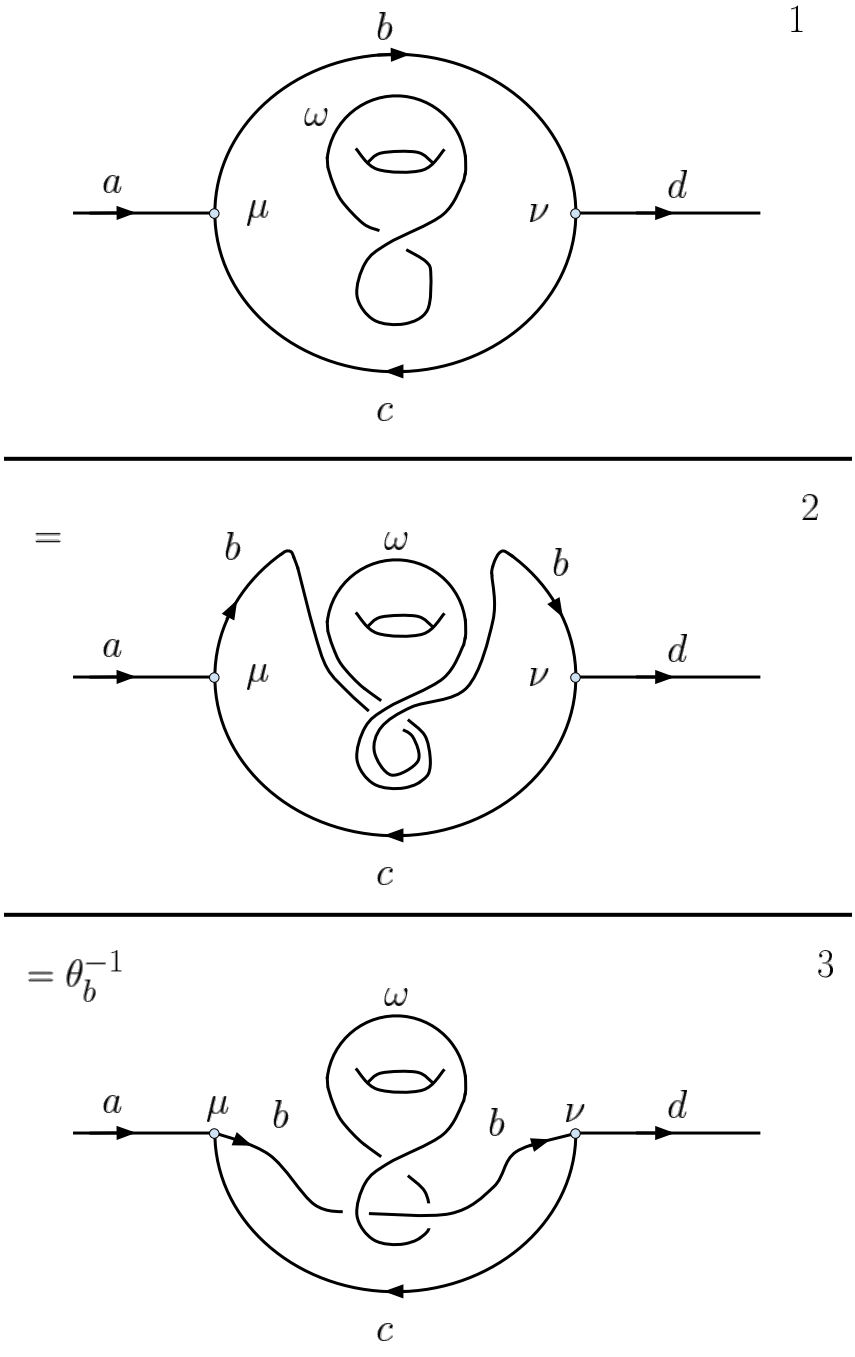

Figure 3.6: Steps $1, 2$, and 3

4

$$= \theta_b^{-1} \sum_{\ell \in L} \frac{d_\ell}{D}$$

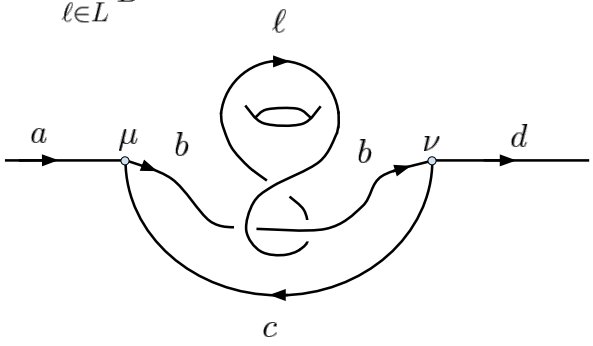

5

$$= \theta_b^{-1} \sum_{\ell,e,\alpha} \frac{d_\ell}{D} \sqrt{\frac{d_e}{d_b d_\ell}}$$

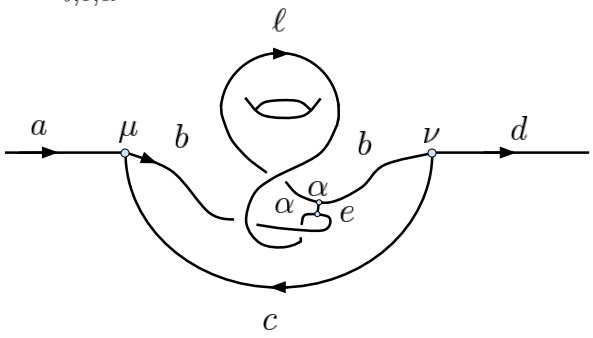

6

$$= \theta_b^{-1} \sum_{\ell,e,\alpha,\beta} \frac{d_\ell}{D} \sqrt{\frac{d_e}{d_b d_\ell}} [R^{\hat{b}\hat{\ell}}_{\hat{e}}]_{\alpha\beta} [R^{\hat{\ell}\hat{b}}_{\hat{e}}]_{\beta\alpha}$$

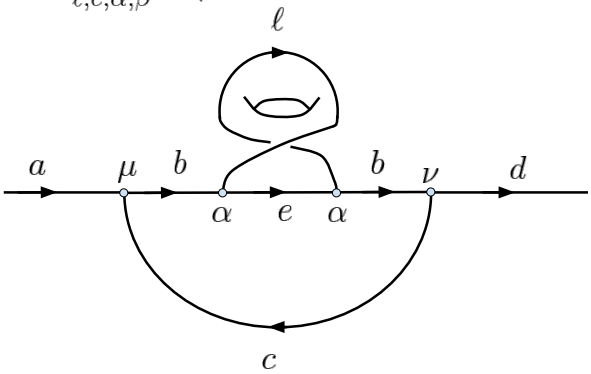

Figure 3.7: Steps 4, 5, and 6

7

$$= \theta_b^{-1} \sum_{\ell,e,\alpha} \frac{d_\ell}{D} \sqrt{\frac{d_e}{d_b d_\ell}} \frac{\theta_e}{\theta_\ell \theta_b}$$

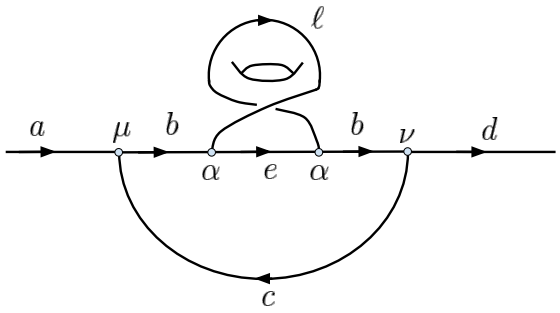

8

$$= \theta_b^{-1} \sum_{\substack{\ell,e,\alpha \\ f,\rho,\sigma}} \frac{d_\ell}{D} \sqrt{\frac{d_e}{d_b d_\ell}} \frac{\theta_e}{\theta_\ell \theta_b} [F_{\hat{b}}^{\hat{b}\hat{\ell}\ell}]_{(\hat{e},\alpha,\alpha),(f,\rho,\sigma)}$$

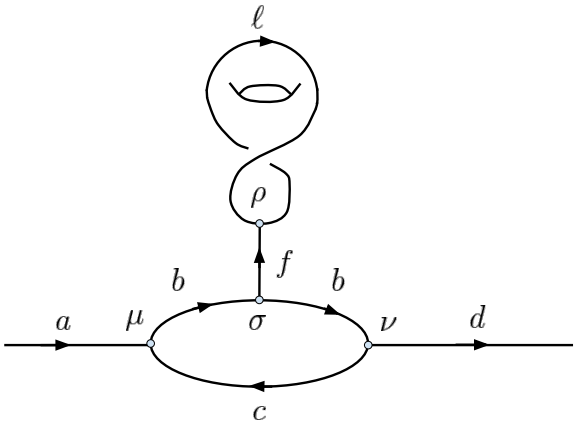

9

$$= \theta_b^{-1} \sum_{\substack{\ell,e,\alpha \\ f,\rho,\sigma \\ \eta}} \frac{d_\ell}{D} \sqrt{\frac{d_e}{d_b d_\ell}} \frac{\theta_e}{\theta_\ell \theta_b} [F_{\hat{b}}^{\hat{b}\hat{\ell}\ell}]_{(\hat{e},\alpha,\alpha),(f,\rho,\sigma)} [R_f^{\ell\hat{\ell}}]_{\rho\eta}$$

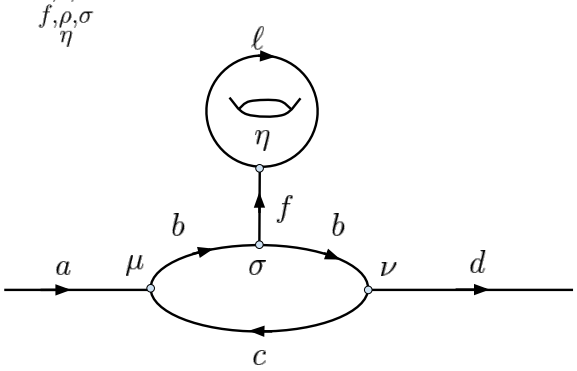

Figure 3.8: Steps 7, 8, and 9

10

$$= \theta_b^{-1} \sum_{\substack{\ell,e,\alpha \\ f,\rho,\sigma \\ \eta,\tau}} \frac{d_\ell}{D} \sqrt{\frac{d_e}{d_b d_\ell}} \frac{\theta_e}{\theta_\ell \theta_b} [F_{\hat{b}}^{\hat{b}\hat{\ell}\ell}]_{(\hat{e},\alpha,\alpha),(f,\rho,\sigma)} [R_f^{\ell\hat{\ell}}]_{\rho\eta} \; [F_{\hat{d}}^{\hat{a}b\hat{b}}]_{(c,\mu,\nu),(f,\sigma,\tau)} \sqrt{\frac{d_b d_b}{d_f}}$$

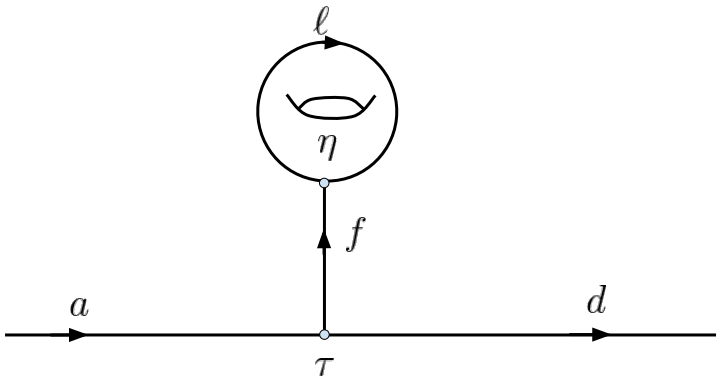

11

$$= \theta_b^{-1} \sum_{\substack{\ell,e,\alpha \\ f,\rho,\sigma \\ \eta,\tau \\ x,\lambda,\delta}} \frac{d_\ell}{D} \sqrt{\frac{d_e}{d_b d_\ell}} \frac{\theta_e}{\theta_\ell \theta_b} [F_{\hat{b}}^{\hat{b}\hat{\ell}\ell}]_{(\hat{e},\alpha,\alpha),(f,\rho,\sigma)} [R_f^{\ell\hat{\ell}}]_{\rho\eta} \; [F_{\hat{d}}^{\hat{a}b\hat{b}}]_{(c,\mu,\nu),(f,\sigma,\tau)} [F_a^{\hat{\ell}}]_{(f,\eta,\tau),(x,\lambda,\delta)}$$

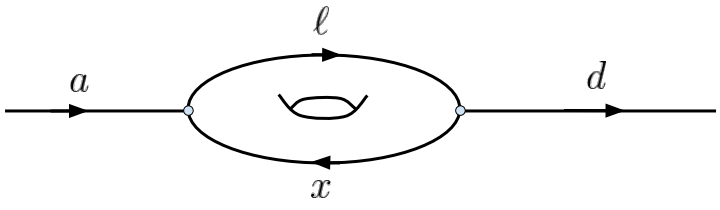

Figure 3.9: Steps 10 and 11

Then we see that

$$T_{2i}(\vec{v}) = \theta_{b_i}^{-1} \sum_{\substack{\ell,e,\alpha \\ f,\rho,\sigma,\eta,\tau \\ x,\lambda,\delta}} \frac{d_\ell}{D} \sqrt{\frac{d_e d_{b_i}}{d_f d_\ell}} \frac{\theta_e}{\theta_\ell \theta_{b_i}} [F_{\hat{b_i}}^{\hat{b_i}\hat{\ell}\ell}]_{(\hat{e},\alpha,\alpha),(f,\rho,\sigma)} [R_f^{\ell\hat{\ell}}]_{\rho\eta}$$

$$[F_{\hat{a_i}}^{\hat{a}_{i-1} b_i \hat{b_i}}]_{(c_i,\mu_i,\nu_i),(f,\sigma,\tau)} [F_{a_{i-1}}^{\hat{\ell}\ell a_i}]_{(f,\eta,\tau),(x,\lambda,\delta)} \vec{v}'_{\ell,x,\delta,\lambda},$$

where $\vec{v}'_{\ell,x,\delta,\lambda}$ is determined by changing b_i to $\hat{\ell}$, c_i to $\hat{x}$, μ_i to δ, and ν_i to λ.

3.5 Future Directions

These computations are done at face value. In one sense they are complete as they are in terms of only the defining data of a modular tensor category. They are also in many ways unsatisfactory. For example, a careful computation in terms of only only gauge invariant quantities would be more highly desired. Additionally there is much to be said about performing these computations in different bases. Unfortunately, the "interesting" basis is often tied to the specific modular tensor category being discussed. For example, having explicit bases which exhibit reducibility or for which the action of each Dehn twist is a monomial matrix. These types of properties are intimately related to whether the image of the representations is finite or not.

Chapter 4

Asymptotic Faithfulness

Definition 4.0.1 *The quantum representations, $\{\rho_k\}$, coming from a clasped $\mathfrak{g}-$spider are* **asymptotically faithful** *if for every non-central element, h, of the mapping class group, there exists an n such that for $k > n$ we have $\rho_k(h) \neq \alpha Id$.*

4.1 The AF Property

We begin to describe the AF property. This will be a niceness condition which we will put on a clasped-$\mathfrak{g}$ spider which will imply asymptotic faithfulness of the mapping class group representation coming from the Reshetikhin-Turaev construction. This can be thought of as combinatorial properties that are placed on the spider. In particular, one first needs a combinatorial description of the spider, meaning a description of the webs in terms of combinatorial generators and relations.

4.1.1 AF1

We say that a spider has property $AF1$ if there exists λ_i such that for every $\lambda = a\lambda_i + b\lambda_i^*$ we have

$$bP_\lambda = \alpha P_\lambda, \qquad \alpha \neq 0$$

for every braid b. The reader will notice that at first glance this equation is nonsense. In particular these cannot be equal at face value as $P_\lambda \in \mathrm{End}\bigotimes(V_{\lambda_i})$, but $bP_\lambda \in \mathrm{End}\bigotimes(V_{\sigma(\lambda_i)})$, where σ is the permutation induced by the braid b on the boundary points. What we truly mean by equality is there is an isomorphism between the appropriate $1-$dimensional vector space of diagrams. This isomorphism can be thought of as a choice of embedding into the disk, this will be rectified by the definition of segregated clasps given below. Now we have the following simplification if the λ_i in the definition of $AF1$ is self dual.

Theorem 1 *Let V_{λ_i} be a self dual representation of $\mathfrak{g}$ and $\lambda = \lambda_i^{\otimes n}$, then*

$$bP_\lambda = \alpha P_\lambda, \qquad \alpha \neq 0$$

for every braid b.

Proof: A braiding on our category tells us to recognize b as an element of $\mathrm{End}(\bigotimes V_{\lambda_i}^{\otimes a_i})$. The definition of clasps coming from the idempotent completion of an unclasped spider tells us that P_λ is an equivalence class of minimal idempotents. In particular we have that

$$P_\lambda \mathrm{End}(\bigotimes V_{\lambda_i}) P_\lambda = \mathbb{C} P_\lambda$$

and that we are looking at equivalence up to the following relation

$$P_1 \sim P_2$$

if $P_1 = uv$ and $P_2 = vu$ for $u, v \in \mathrm{End}(\bigotimes V_{\lambda_i}^{\otimes a_i})$. Then letting $u = bP_\lambda$ and $v = P_\lambda$, we have

$$bP_\lambda = bP_\lambda P_\lambda \sim P_\lambda bP_\lambda = \alpha P_\lambda$$

for some $\alpha \neq 0$. This proof can be seen diagrammatically in figure 4.1. ■

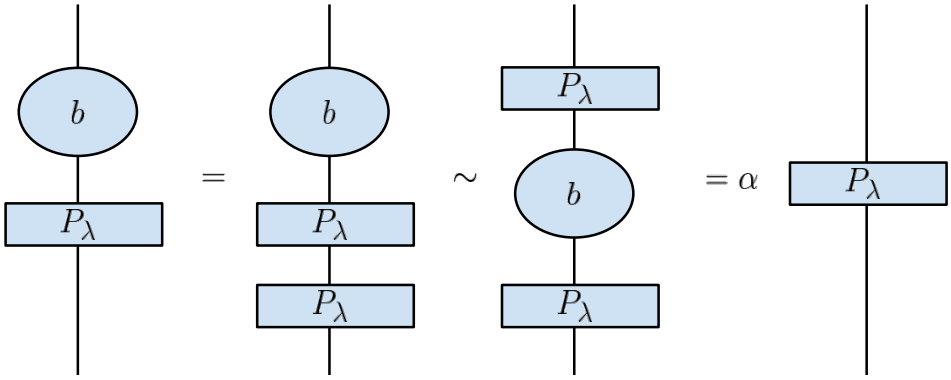

Figure 4.1: Property AF1 for self dual λ_i

Corollary 1 *Every spider with a self dual object has property AF*1*.*

This is our first example of things being greatly simplified when the desired λ_i is self dual. This will be a recurring theme and in showing a spider has the AF property finding a self dual representation will always be preferred. In other cases we will need the following definition adapted from Kim [28]:

Definition 4.1.1 *A clasp of weight $a\lambda_i + b\lambda_i^*$ is* **segregated** *if all of the strands labeled with λ_i are on the left of the "coupon" and strands labeled with λ_i^* are on the right.*

Then we can make sense of the above definition of bP_λ by talking about non-segregated clasps. Then we will look for a unique web connected to the top of a non-segregated clasp which will make the clasp segregated. Thus when we say a spider has property $AF1$ we

will be assuming the combinatorial description of the spider admits isomorphisms of all clasps to segregated clasps. This will be illuminated more in the "pillow" constructions used in the A_2 spider in figure 5.7.

In spiders which have a concrete combinatorial description the minimal idempotent property can be described in terms of annihilating diagrams with minimal cut paths of lower weight. This property can then be proved by showing that a braid decomposes as a sum of a multiple of the identity tangle and diagrams which introduce cut paths of lower weight.

4.1.2 AF2

We say that a spider has property AF2 if there exists an m, such that for $k > m$ there is some fundamental representation λ_i for which the combinatorial diagrams are linearly independent.

Definition 4.1.2 *A* **combinatorial diagram** *is a diagram which only encodes the combinatorial data of which clasps the strand begins and ends at. In order to make sense of linear independence, these diagrams have to exist, meaning there is a combinatorial model for the webs of the spider in which these diagrams can be interpreted. These diagrams for segregated clasps are shown in figure 4.2.*

We note specifically that in the case that the λ_i in the definition of property $AF2$ is self dual, then we are no longer keeping track of where a strand begins and ends, but only which clasps it connects, as seen in figure 4.3.

As this is a single diagram the question of linear independence can be answered by showing this diagram is nonzero. This can be done by showing this morphism is not negligible. This comes down to calculating $\theta(P_{a\lambda}, P_{b\lambda}, P_{c\lambda})$ as seen in figure 4.4.

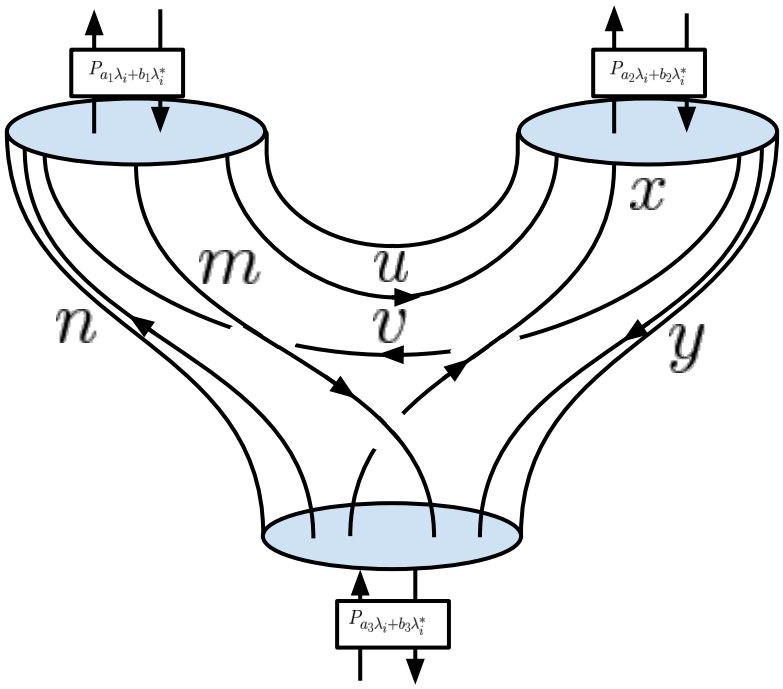

Figure 4.2: Combinatorial Diagrams

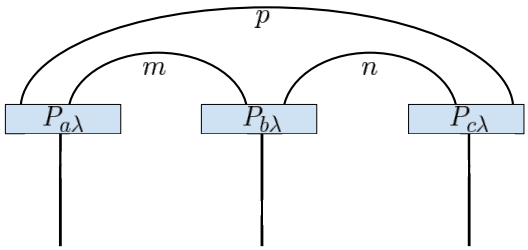

Figure 4.3: The Combinatorial Diagram for a Self Dual Object

When a recursive description of $P_{a\lambda}$ this constant can be calculated using the recursion.

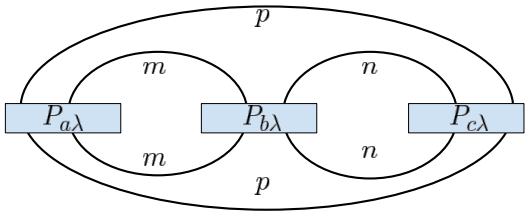

Figure 4.4: $\theta(P_{a\lambda}, P_{b\lambda}, P_{c\lambda})$

4.1.3 The AF Property

We then say that a spider has the AF property if there exists a λ_i such that property $AF1$ and property $AF2$ are satisfied using this λ_i

4.2 The State Space

Let Σ be a closed orientable surface. We specialize the construction of the state space $V(\Sigma)$ given in the introduction to the specific case of spiders. Up to a homeomorphism into Euclidean space, we can think of Σ as bounding a standardly embedded handlebody H. Then we associate to Σ a spine of H, namely a trivalent graph whose regular neighborhood is H. The choice of a particular trivalent graph corresponds to choosing a pants decomposition of Σ by looking at the disk dual to the edge. Now we define an admissible labeling of this trivalent graph. At each edge of the graph we assign a clasp in our spider and each vertex is given a web in the triple clasped space of the three incident edges. Then we define $V_k(\Sigma)$ as the free complex vector space having a basis of admissible labels. We note that as k increases the order of q increases as well and more clasps are included in this construction.

4.3 Curve Operators

We look to define a class of operators on $V(\Sigma)$ called curve operators. Let γ be an oriented simple closed curve on Σ and V_λ be a fundamental representation of $\mathfrak{g}$. Then we define

$$C_\lambda(\gamma) = Z(\Sigma \times I, (\gamma)_\lambda \times \{1/2\} \in V(\Sigma) \otimes V(-\Sigma) = \mathrm{End}(V(\Sigma))$$

where $(\gamma)_\lambda$ is defined to be the curve γ colored with the P_λ clasp. Where we often drop the label λ is the choice is not relevant. If V_λ is self dual then we are able to ignore the orientation given to γ. We have the following lemma:

Lemma 1 *Let $h : \Sigma \to \Sigma$ be an orientation preserving homemorphism. Then we have*

$$V_h C(\gamma) V_h^{-1} = C(h(\gamma))$$

Proof: WLOG we may assume that h is a positive Dehn twist about some curve α. Then the description of the action from the introduction tells us we have the web made of a framed α colored with ω stacked over the curve γ stacked over the curve α colored with ω and frame with the opposite framing. This can be seen in the left-most column of figure 4.5. Then as ω is specifically the color making this curve invariant under Kirby moves we see that through a handleslide we can pass γ to the lowest level. This is seen in column two of figure 4.5. Then finally the balanced stabilization property of ω allows for the cancellation of the oppositely framed α curves. ■

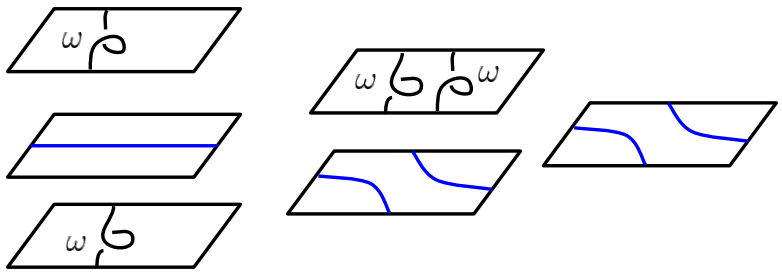

Figure 4.5: Conjugating Curve Operators

4.4 Graph Geodesic

We will need the following useful lemma.

Lemma 2 *Let a and b be two non-trivial, non-isotopic simple closed curves on a closed orientable surface Σ. Then there exists a pants decomposition of Σ such that a is one of the decomposing curves and b is a non-trivial graph geodesic with respect to the decomposition, meaning that b does not intersect any curve of the decomposition twice in a row.*

This is lemma 4.1 in [19]. This is illustrated in figure 4.6.

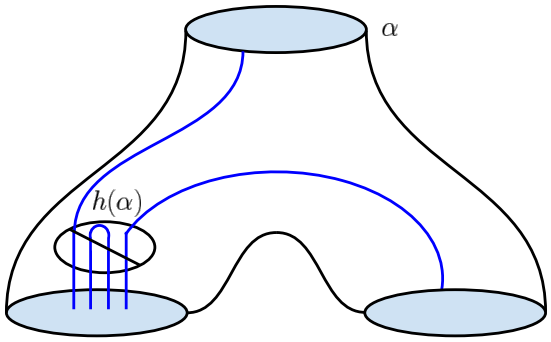

Figure 4.6: An illustration of Lemma 2

4.5 Utilizing Semisimplicity

We observe how in a spider (as we have defined it) the identity tangle factors through a sum of clasps of lower weight. This fact follows directly from the semisimplification procedure. In particular we have

Lemma 3

$$\bigotimes V_{\lambda_i}^{\otimes a_i} = \bigoplus V_\eta$$

Looking at the weights of both sides we have that the sum on the RHS is taken over η where of lower weight than the LHS and the coefficient in front of V_λ is 1.

This is seen in the graphical calculus in figure 4.7, where x_η^λ and y_λ^η are just connecting diagrams. This property can be proven inductively when a nice recursive description is given for the clasps in the combinatorial setting.

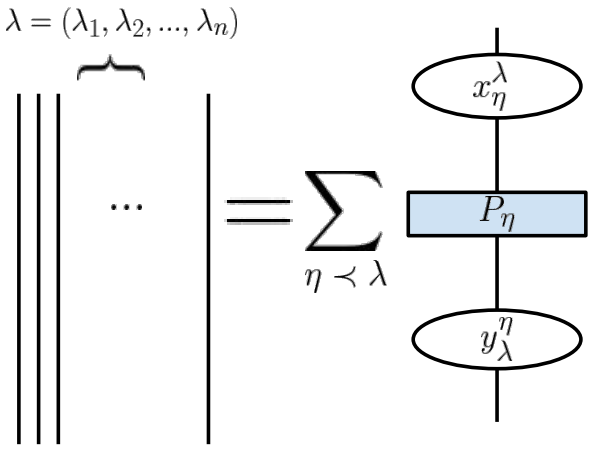

Figure 4.7: Factoring the identity tangle

4.6 Main Result: Asymptotic Faithfulness

This work is a generalization of that of the author in [11, 9]. As such many of the figures, and wording of certain arguments are adapted from there. In summary, we will construct a "comparison vector" from the combinatorial properties of the spider that will allow us to show we will not be acting trivially.

Theorem 2 *Let $\mathfrak{g}$ be such that the $\mathfrak{g}$-spider satisfies the AF property. Let Σ be a closed, oriented surface, h an orientation preserving homeomorphism, and V_h the action of h on the vector space $V(\Sigma)$ coming from the $\mathfrak{g}$-spider. Suppose there exists a simple closed curve $a \subset \Sigma$ such that $h(a)$ is not isotopic (as a set) to a. Then V_h is a multiple of the identity for at most finitely many k. That is, h is eventually detected as k increases.*

Proof: Let V_λ be the fundamental representation used to satisfy the AF property for $\mathfrak{g}$-spider. Then let C denote the curve operator coming from V_λ. Since

$$V_h C(a) V_h^{-1} = C(h(a)),$$

it suffices to show that for some k, $C(a) \neq C(h(a))$.

By the graph geodesic lemma above 2, there exists a handlebody H boudned by Σ such that a bounds an embedded disk in H and $h(a)$ is a non-trivial graph gedesic with respect to a pants decomposition of Σ. Dual to this pants decomposition is a spine of H, namely a trivalent graph whose tubular neighborhood is H.

Now let $Z(H) \in V(\Sigma)$ be the vector determined by H with the empty labeling. We also have $Z(H, h(a))$ is the vector determined by the pair $(H, h(a))$ where $h(a)$ is pushed into the interior of H and the labelings are determined by resolving webs. Then we have

$$C(a)(Z(H)) = Z(H, a) = dZ(H)$$

as a is taken to bound an embedded disk in H. It is also true that

$$C(h(a))(Z(H)) = Z(H, h(a)),$$

meaning it suffices to show that $Z(H, h(a))$ is not a multiple of $Z(H)$.

We look to build comparison vectors that will be used against $Z(H, h(a))$. To each edge e of the spine given by the graph geodesic lemma let p_e be the number of times that $h(a)$ passes through the dual disk to e with orientation given by the right hand rule and q_e denote the number of times with the opposite orientation. Then locally, along each edge we have an identity tangle of type (p_e, q_e). Now for our comparison vector w, let w_e be labeled by the clasp $P_{(p_e,q_e)}$. Then at each vertex we assign the labeling arising from the corresponding combinatorial diagram, all of which are nonzero by $AF2$, where we are now assuming that k larger than the m furnished by property $AF2$. We can think of $h(a)$ pushed into the corresponding pair of paints to the vertex, then the graph geodesic property tells us that any strand must attach two distinct boundary components. These

are exactly the desired diagrams. When let the label given to the vertex be the diagram determined by $h(a)$. Let b_w be the basis vector of $V(\Sigma)$ corresponding to the label w.

Now we claim

$$Z(H, h(a)) = \lambda b_w + v,$$

where $\lambda \neq 0$ and v consists of multiples of b_x where x is a label having $(m_e, n_e) \succ (p_e, q_e)$ at each edge e of the spine, where (m_e, n_e) is the labeling coming from x. Now applying semisimplicity as in Lemma 4.5 to the local identity tangle along each edge we have the desired factoring. Finally we have that λ is not zero as any additional braiding contributes some nonzero scalar by property $AF1$. Thus we have

$$Z(H, h(a)) = \lambda b_w + v,$$

and so $Z(H, h(a))$ is not a multiple of $Z(H)$, and our desired result is proven. ■

Corollary 2 *Let σ be a closed connected oriented surface and $MCG(\Sigma)$ its mapping class group. For every non-central $h \in MCG(\Sigma)$, then there exists some $k_0(h)$ such that for any $k \geq k_0(h)$, the operator*

$$V_h : V_k(\Sigma) \to V_k(\Sigma)$$

is not the identity, meaning

$$V_h \neq 1 \in \mathcal{P}End(V(\Sigma)),$$

the projective endomorphisms. In particular, any infinite direct sum of these quantum representations will faithfully represent these mapping class groups modulo their center.

Proof: If h fixes all simple closed curves then h must commute with all possible

Dehn twists. As Dehn twists generate the mapping class group, then h must be in the center. Thus for any non-central $h \in MCG(\Sigma)$ we have that $h(a)$ is not isotopic to a for some simple closed curve, and the main theorem can be applied. ■

4.7 Future Directions

The pressing direction is to prove that all $\mathfrak{g}-$spiders have the AF property, but this will be discussed more in the next chapter and as such we will avoid it here. One potential question leading towards this is whether or not asymptotic faithfulness implies the AF property. At the current time it seems difficult to the author for asymptotic faithfulness alone to allow for the construction of the necessary combinatorial model.

Chapter 5

Specializing to Low Rank Examples

We will introduce a change in notation. In particular we will often call refer to a clasped $\mathfrak{g}-$spider by it's classifying Dynkin diagram, for example the A_2 spider is the clasped $\mathfrak{sl}(3,\mathbb{C})-$spider.

Definition 5.0.1 *A* **quantum integers** *is*

$$[n] = \frac{q^n - q^{-n}}{q - q^{-1}}$$

and the **quantum factorial** *is*

$$[n+1]! = [n+1] \cdot [n]!.$$

We note that this definition depends only on q, but when specializing to spiders we will actually be choosing roots of q as we will see below.

5.1 The A_1 Spider

In this section we recover the results of Freedman Walker and Wang, in [19]. This is nearly circular as our approach is heavily influenced by theirs, and even a generalization.

5.1.1 The Combinatorial Description

The A_1 spider is the most studied of all spiders. This theory is also called the Temperley-Lieb-Jones theory as described in [48]. There is a braided monoidal equivalence

$$Rep^{uni}(U_s(\mathfrak{sl}(2,\mathbb{C}))) \cong \mathcal{TL}(-is),$$

as seen in [36]. Here the s is used rather than q as there are particular choices that depend on which root of q is being taken. In particular we have $s^2 = q$ so

$$[n] = \frac{s^{2n} - s^{-2n}}{s^2 - s^{-2}}.$$

It is important to note that not only is the pivotal structure changing but also $s \mapsto -is$ which changes the underlying fusion category. This immediately takes care of the question of modularity for the semisimple categories we will be working with. The combinatorial description of webs is given by non-crossing planar matchings called Temperley-Lieb diagrams. Specifically $\mathrm{Hom}(m,n)$ is given by the non-crossing planar matchings in the rectangle having m points on the bottom of the rectangle and n points on the top as seen in figure 5.1.

5.1.2 The Clasped A_1 Spider

The clasps in the A_1 spider are very well understood. These are the Jones-Wenzl projectors in the Temperley-Lieb algebras.

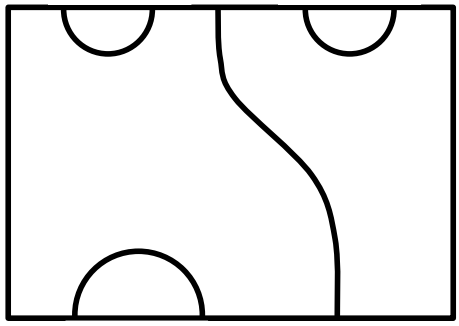

Figure 5.1: An element of Hom(3, 5) in the A_1 spider

Theorem 3 (Wenzl [49]) *The Jones-Wenzl projectors satisfy the recurrence relation shown in figure 5.2.*

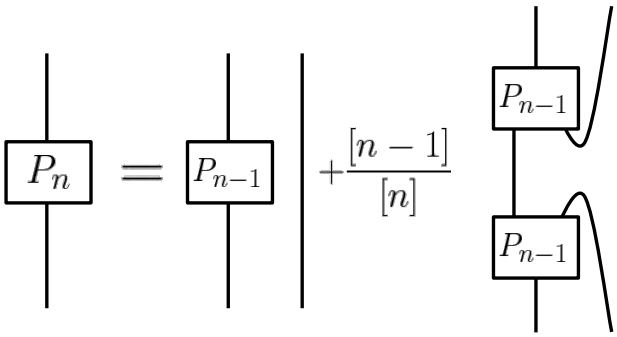

Figure 5.2: The Wenzl Recursion Formula

5.1.3 The AF Property For A_1

As the fundamental representation for $\mathfrak{sl}(2,\mathbb{C})$ is self dual this amounts to showing $\theta(a,b,c) \neq 0$ for some large enough k, for admissible a, b, c. Explicit formula for these θ symbols can be found in [27], and in particular

$$\theta(a,b,c) = (-1)^{(\frac{1}{2}a+b+c)} \frac{[\frac{1}{2}(a+b+c)+1]![\frac{1}{2}(a+c-b)]![\frac{1}{2}(a+b-c)]![\frac{1}{2}(b+c-a)]!}{[a]![b]![c]!}$$

We additionally have that $[n] \neq 0$ when $n \leq k+1$, and thus we need only find the largest factor in the numerator. So we have

$$\frac{1}{2}(a+b+c)+1 \leq k+1$$

or

$$a+b+c \leq 2k$$

which is the standard level k admissibility for the Temperley-Lieb-Jones theory. This tells us that as long as m is larger than $\frac{a+b+c}{2}$ then $\theta(a,b,c) \neq 0$. As we used a self dual object we can apply 1 to guarantee $AF1$. Thus we have that the A_1 has the AF property and so:

Theorem 4 *The Reshetikhin-Turaev quantum mapping class group representation coming from the A_1 spider is asymptotically faithful.*

This recovers the results of Freedman, Walker, and Wang [19].

5.2 The A_2 Spider

5.2.1 The Combinatorial A_2 Spider

This section recovers work of the author in [11]. As such many of the figures are taken from there. Kuperberg showed, in [33], the A_2 spider is generated by the following two webs seen in Figure 5.3

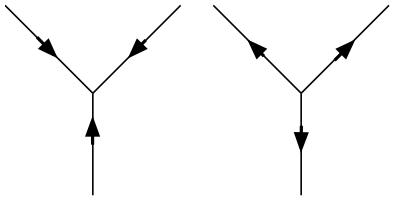

Figure 5.3: Sinks and Sources

subject to the following relations in Figure 5.4.

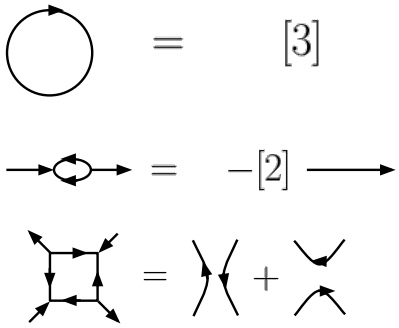

Figure 5.4: $SU(3)$ Relations

We recall what this means. We will be looking at disks where the boundary is some sequence of +s and −s which correspond to V and V^* where V is the fundamental defining representation of $\mathfrak{sl}(3,\mathbb{C})$. Then our webs are trivalent graphs embedded into the disk with an orientation where edges meet the boundary of the disk and the embedded graph is subject to the listed local relations. An alternative interpretation is to take take the sequences of +'s and −'s as objects in our category and looking at these embedded graphs as corresponding to morphisms between the corresponding tensor products of V's and V^*'s.

5.2.2 The Clasped A_2 Spider

The work of Kim developed the theory of Jones-Wenzl idempotents for rank 2 Lie algebras, and in particular for A_2 [28]. These are the minimal projectors in the skein algebra of the disk, alternatively the endomorphism algebras corresponding to the boundary components. They satisfy the annihilation axiom as well, under both $Y's$ and caps. We introduce the notation (m, n) for the fundamental projector indexed by m and n.

Theorem 5 (Kim [28]) *For $a, b \geq 1$, the fundamental projectors satisfy the recursion given in figure 5.5.*

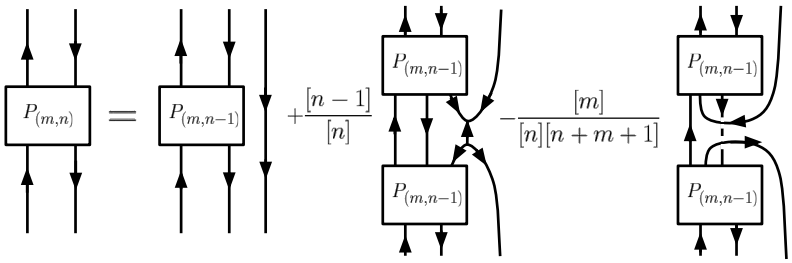

Figure 5.5: The fundamental projectors for A_2

Where we note that the crossing is used for convenience and expanding into the standard basis would and using the annihilation property of the projectors would yield the unique maximal cut out from the hexagonal tiling with the appropriate boundary.

5.2.3 The AF Property of For A_2

To build up the theory of the intertwiner spaces in the A_2 web in the classic case, we turn our attention to

$$I((m_1, n_1), (m_2, n_2), (m_3, n_3))$$

$$\cong Hom((m_1, n_1) \otimes (m_2, n_2) \otimes (m_3, n_3), (0, 0))$$

$$\cong Hom((m_1, n_1) \otimes (m_2, n_2), (n_3, m_3)).$$

Corresponding to the disc with $m_1 + m_2 + m_3$ entries and $n_1 + n_2 + n_3$ exits, where these boundary points are organized into three groups, the projector (m_i, n_i) is placed on the corresponding grouping. Up to an invertible scalar from above, this construction gives us an isomorphism class of vector spaces, called the intertwiner space of type $((m_1, n_1), (m_2, n_2), (m_3, n_3))$, denoted $I((m_1, n_1), (m_2, n_2), (m_3, n_3))$, which will be referred to as the fusion or triangle space $((m_i, n_i))$.

A necessary condition for the intertwiner spaces to be nontrivial is

$$|(m_1 + m_2 + m_3) - (n_1 + n_2 + n_3)| = 3\ell$$

where ℓ is a parameter of the space. Suppose that $m_1 + m_2 + n_2 = n_1 + n_2 + m_3 = s$, and let $\ell \geq 0$, then denote by $I_\ell(m_i, n_i)$ the triangle space $I((m_i + \ell, n_i))$, and by $I^\ell(m_i, n_i)$ the triangle space $I((m_i, n_i + \ell))$. Define $p_i = s - m_i - n_i$.

Theorem 6 (Suciu [43]) *1. $I_\ell((m_i, n_i))$ is nontrivial if and only if $p_i \geq 0$*

2. $dim(I_\ell((m_i, n_i))) = \min(m_i, n_i, p_i) + 1$.

A proof of the theorem can be found in [43]. The proof revolves around computing theta symbols through a fairly involved recursion. This is analogous to computing the theta symbols in Temperley-Lieb recoupling theory.

An admissible $6-$tuple (x, y, a, b, u, v) is an ordered set of six non-negative integers such that the following holds

$$a + v = m_1, \quad x + u = n_1$$

$$u + b = m_2, \quad v + y = n_2$$

$$a + b = m_3, \quad x + y = n_3$$

There are exactly $\min(m_i, n_i, p_i) + 1$ of these admissible $6-$tuples, which form a basis for $I((m_i, n_i))$, which are exactly the combinatorial diagrams as seen in figure 5.6.

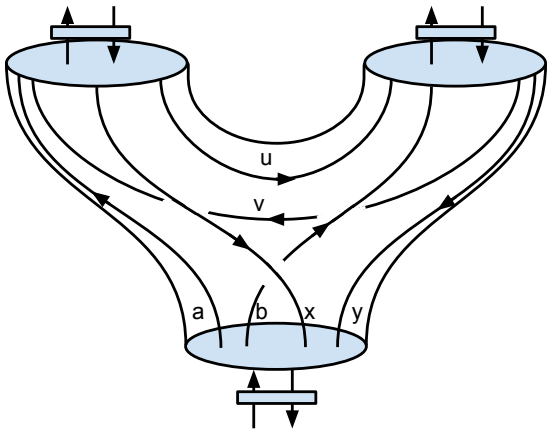

Figure 5.6: The Combinatorial Diagrams for A_2

This particular representation of the intertwiner space has been chosen as it will be most hopeful when applying to the construction described below. A second, potentially more precise figure, utilizes the diagrammatic trick of "pillows", as seen in figure 5.7.

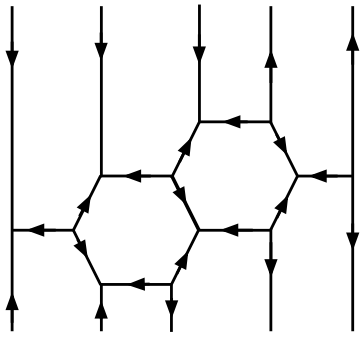

Figure 5.7: A pillow changing the ordering of boundary points from $(2, 3)$ to $(3, 2)$

A pillow allows for the reordering of boundary strands, and can be thought of as an

isomorphism of the skein space of the disk depending on the realization we are using. This is exactly the construction of segregating clasps described in the $AF1$ property. Combining this we have a more precise picture for basis diagrams, as seen in figure 5.8.

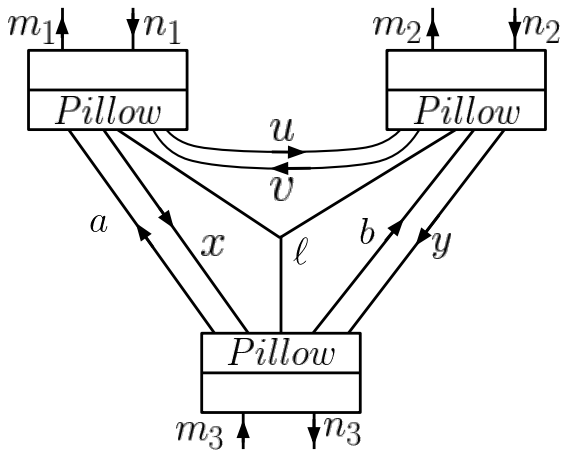

Figure 5.8: A $I(m_i, n_i)$ basis using a pillow construction

The case of $\ell \neq 0$ can be seen by adding in an $\ell-$fold triple point in the skein space as well. Then the annihilation property of "turn backs", meaning cups/caps and Ys, along with the segregation properties of the pillow property imply property $AF1$ for the A_2 spider.

Fixing a Level

Let A be a $6r^{\text{th}}$ primitive root of unity where $r = k+3$, with k the level of our theory. In particular,

$$[n] = \frac{A^{3n} - A^{-3n}}{A^3 - A^{-3}}.$$

This leads to new identities in the level k instance

$$[3r] = 0, \qquad [3r - n] = [n], \qquad [3r + n] = -[n], \qquad [n + 6r] = [n].$$

Recall that

$$\mathrm{Tr}((m,n)) = \langle (m,n),(m,n)\rangle = \frac{[m+1][n+1][m+n+2]}{[2]}$$

This implies that as long as $m+n \leq k$ the fundamental projectors are not killed in the semisimplification. Then further analysis detailed in chapter 6 of [43] implies that as long as $s+\ell \leq k$ the triangle spaces unaffected by the semisimplification process. Thus we have that the combinatorial diagrams and nonzero, when $m > s+\ell$, and in particular for the combinatorial diagrams where $\ell = 0$ we have $k > s = m_1 + m_2 + n_3$. So we have that the A_2 spider satisfies property $AF2$.

Asymptotic Faithfulness

Theorem 7 *The Reshetikhin-Turaev quantum mapping class group representation coming from the A_2 spider is asymptotically faithful.*

5.3 The C_2 Spider

This section is closely related to the work of the author in [9], and the proof that property $AF2$ holds is based on the work [10]. This was work completed through the mentorship of Andres Mejia during the REU program at Santa Barbara in the summer of 2017. As such many of the arguments and figures are adapted from there.

5.3.1 The Combinatorial C_2 Spider

The combinatorial construction of this spider is in many ways closer to A_1 than A_2. There are two strand types, one associated to each fundamental representation of $U_q(\mathfrak{sp}(4))$. As in Kuperberg's original work, [33], we will use a single strand and a double

strand to diagrammatically represent these two strand types. Then we have that the C_2 spider is generated by a single trivalent vertex type, as seen in figure 5.9.

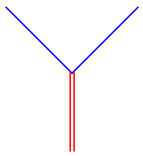

Figure 5.9: The generator of the C_2 spider

The relations seen in figure 5.10 then complete the description of the C_2 spider. These

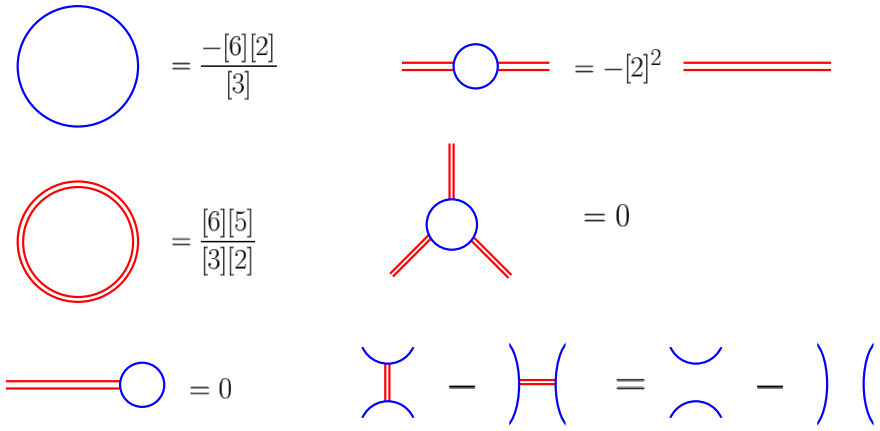

Figure 5.10: The relations in the C_2 spider

webs admit the same description in the A_2 case, but now rather than $+$'s and $-$'s we have red and blue, or equivalently single and double, points on the boundary. These correspond to the morphisms between the appropriate tensor products of V's and W's (the two fundamental representations).

5.3.2 Clasped C_2 Spider

While the existence of these clasps was proven in Kuperberg's original work, explicit constructions of the clasps, making use of the combinatorial structure, were partially given by Kim [28]. Partial results in this case mean that constructions are only found for clasps of the type $(p, 0)$ and $(0, q)$. In order to best state these results the change of basis seen in figure 5.11 is introduced.

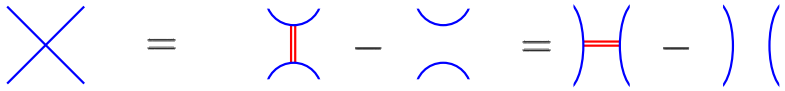

Figure 5.11: Defining a tetravalent vertex formally

Theorem 8 (Kim [28]) *The clasps of type* $(n, 0)$ *satisfy the recursive relationship given in Figure 5.12.*

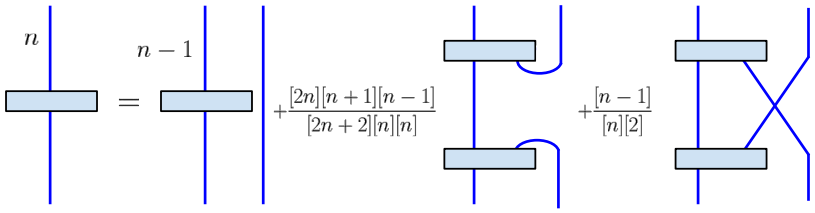

Figure 5.12: A recursive description of a $(n, 0)$ clasp

The key property of these clasps is the annihilation of webs which create a cut path with weight lower than the clasp. This should be thought of as the generalization of the annihilation of "cups" and "caps" by Jones-Wenzl projectors.

5.3.3 The AF Property For C_2

We begin by immediately noting that either choice of fundamental representation is self dual so we immediately see the C_2 spider has property $A1$, applying 1. From here we will choose the fundamental representation of type 1, meaning single strand or blue in our above notation. Then we will also introduce the notation that $a := (a, 0)$ for simplicity. We will recall the definition of $\theta(a, b, c)$ specialized to our setting, seen in figure 5.13.

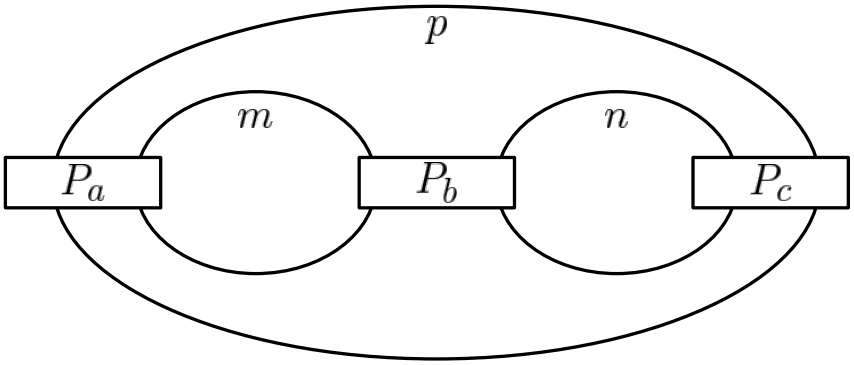

$$m = \frac{a+b-c}{2} \qquad n = \frac{b+c-a}{2} \qquad p = \frac{a+c-b}{2}$$

Figure 5.13: The Theta symbol in the C_2 spider

We introduce the notation $Net(m, n, p)$, based on figure 5.13, to help when we are working with m, n, and p more than a, b, and c. From here we begin our start of the calculation of $Net(m, n, p)$. This is a generalization of the recoupling theory and recursion done for the A_1 case by Kauffman and Lins [27].

Lemma 4

$$\mathrm{Tr}(P_{p,0}) = \left(\frac{[2p+4]}{[4]}\right)\left(\frac{[3+p][p+1]}{[3]}\right).$$

Proof: We proceed by induction, using the recursive definition given by Kim, in Theorem 8.

The base case is clear, since the trace of P_1 is nothing but a loop that evaluates to $\frac{-[6][2]}{[3]}$ which agrees with the formula above. This can be calculated as follows, using Kim's double clasp expansion and taking the trace, as seen in figure 5.14.

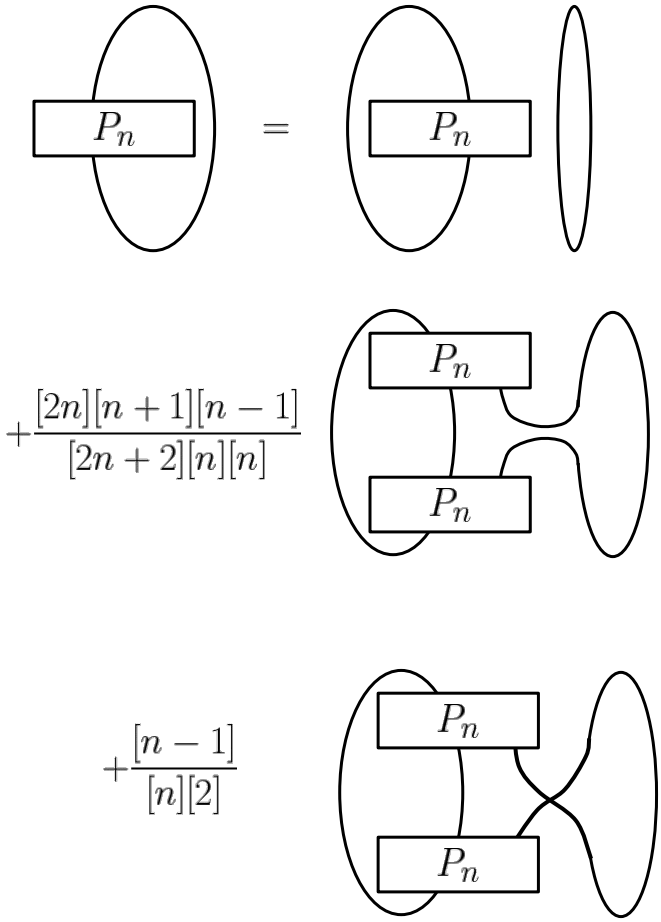

Figure 5.14: The trace of a clasp in C_2

Wee see taking the trace amounts to the trace of the $P_{n-1,0}$ along with some factors: we resolve the first summand by multiplying by the loop constant $-\frac{[6][2]}{3}$; we resolve the second by using idempotence, so it is merely $P_{n-1,0}$; we resolve the third by multiplying $\frac{[6][2]}{3}$ (changing basis again, we see that one summand dies, and the second subtracts off a loop constant.)

From this, we obtain that

$$\begin{aligned} P_n &= \mathrm{Tr}(P_{n-1}) \left(\frac{-[6][2]}{[3]} + \frac{[2n][n+1][n-1]}{[2n+2][n]} + \frac{[n-1][6][2]}{[n][2][3]} \right) \\ &= \left(\frac{[4+n][n]}{[3]} \cdot \frac{[2n+2]}{[3]} \right) \cdot \left(\frac{-[6][2]}{[3]} + \frac{[2n][n+1][n-1]}{[2n+2][n]^2} + \frac{[n-1][6][2]}{[n][2][3]} \right) \\ &= \frac{[2n+4]}{[4]} \cdot \frac{[3+n][n+1]}{[3]}, \end{aligned}$$

as desired. ■

Theorem 9 $Net(m,n,0) = Tr(P_{m+n})$

Proof: This is given in figure 5.15 ■

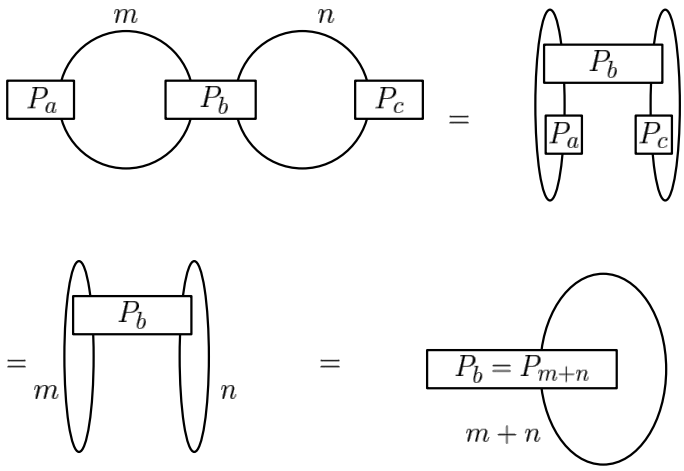

Figure 5.15: The proof of Theorem 9

We will abbreviate the expansion coefficients for P_n by defining

$$\alpha_n := \frac{[2n][n+1][n-1]}{[2n+2][n]^2} \qquad \beta_n := \frac{[n-1]}{[n][2]},$$

and for further convenience, we will define

$$A_i := -\frac{[6][2]}{[3]} + \alpha_{m+i} + \alpha_{n+i} + \frac{[6][2]}{[3]}(\beta_{n+i} + \beta_{m+i}) - [4][2]\beta_{n+i} \cdot \beta_{m+i} \quad B_i := \alpha_{n+i} \cdot \alpha_{m+i}$$

definitions that will be made clear by the next few lemmas. The first step of our recursion is easy:

Lemma 5 $Net(m, n, 1) = A_1 \cdot Net(m, n, 0)$

Proof: Using the double clasp expansion we obtain the equation

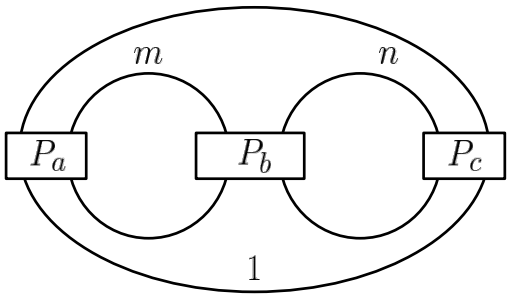

$=$

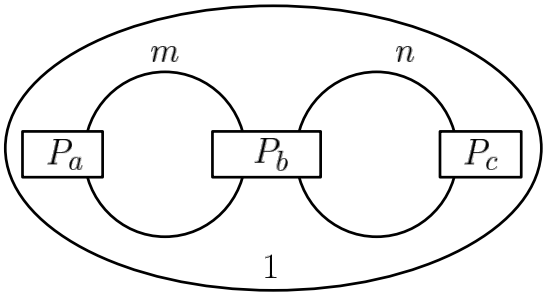

$+(\alpha_{n+1} + \alpha_{m+1})$

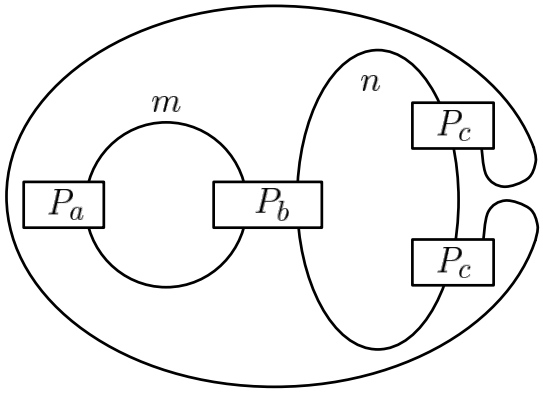

$+(\beta_{n+1} + \beta_{m+1})$

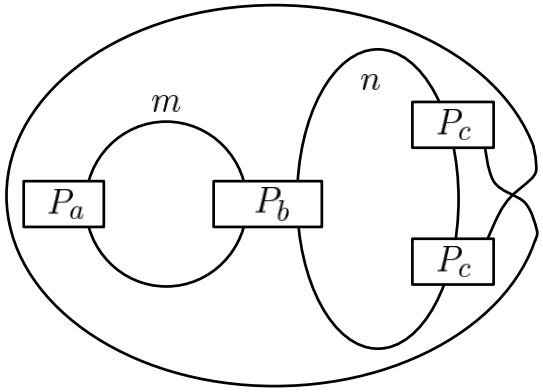

$+\alpha_{n+1}\alpha_{m+1}$

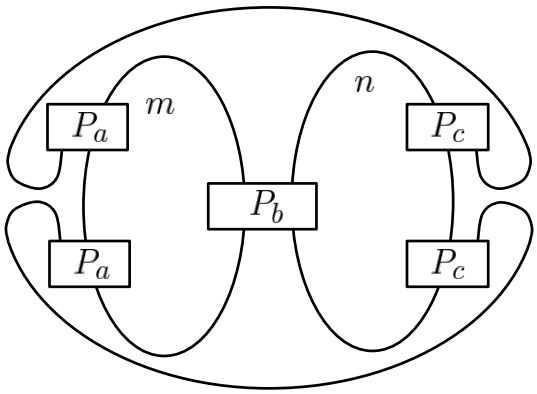

$+(\alpha_{m+1}\beta_{n+1} + \beta_{m+1}\alpha_{n+1})$

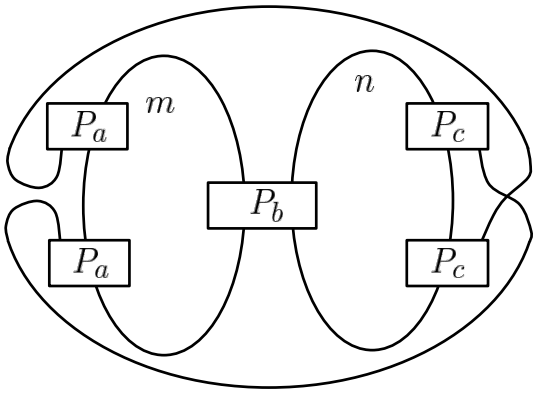

$+\beta_{n+1}\beta_{m+1}$

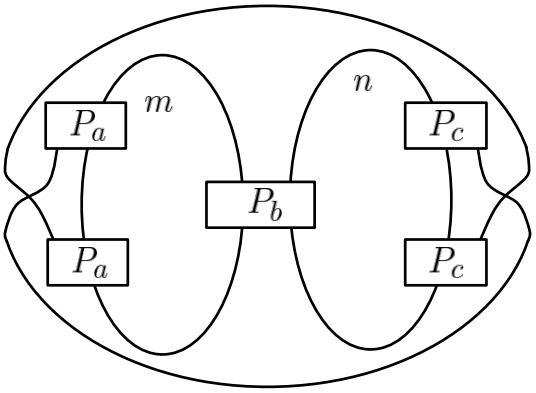

where the diagrams with sums are collected by symmetry. One can easily check that the diagrams with $\alpha_{n+1}\alpha_{m+1}$ and $\beta_{n+1} + \beta_{m+1}$ annihilate by the cut path property; the diagram with $\alpha_{n+1} + \alpha_{m+1}$ is just $Net(m, n, 0)$; the diagram with $\beta_{n+1} + \beta_{m+1}$ is just $\frac{[6][2]}{[3]} Net(m, n, 0)$, and the first diagram is just $-\frac{[6][2]}{[3]} Net(m, n, 0)$. As for the last diagram with $\beta_{n+1}\beta_{m+1}$, we use the following important trick (which we will continue to use liberally without mention):

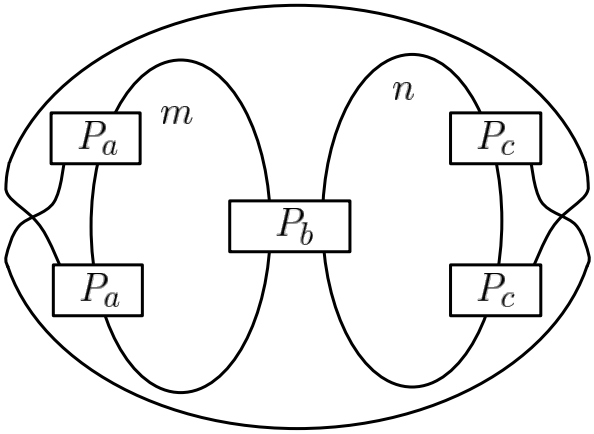

$=$

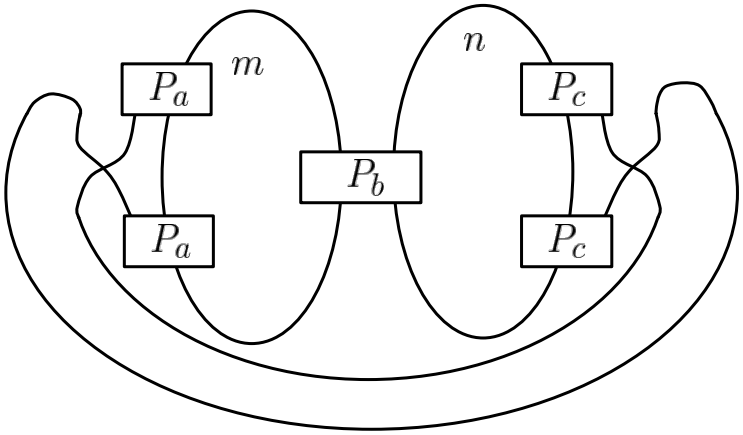

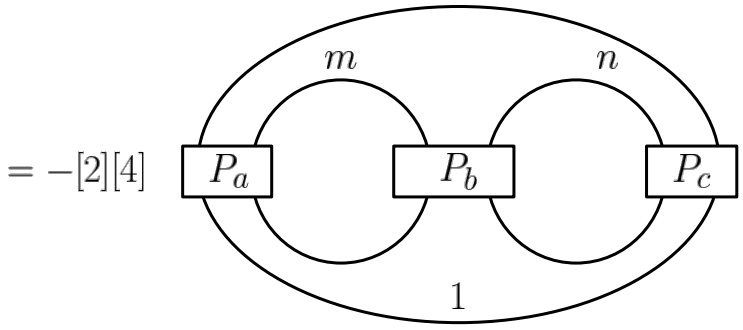

where the final equality follows from expanding the diagram with the relation

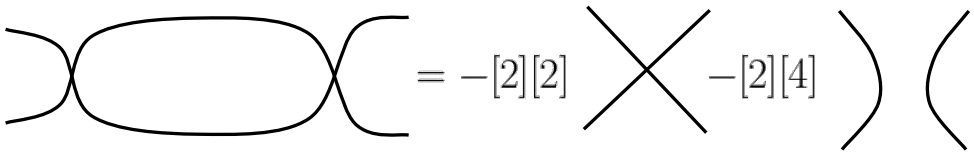

and noting that the first summand dies by the cut path property.

Putting all of this together, we see that

$$Net(m,n,1) = (-\frac{[6]}{[2]}[3]+\alpha_{n+1}+\alpha_{m+1}+\frac{[6]}{[2]}[3](\beta_{n+1}+\beta_{m+1})-[4][2]\beta_{n+1}\beta_{m+1})Net(m,n,0)$$

$$= A_1 Net(m,n,0),$$

as desired. ■

Our next goal is to determine the value of $Net(m,n,p)$ inductively. Unfortunately, it is too hopeful that this can done directly and for this end we must define a slightly new type of net shape

Definition 5.3.1

$$Net(m, n, p_e + 1, p_i - 1) =$$

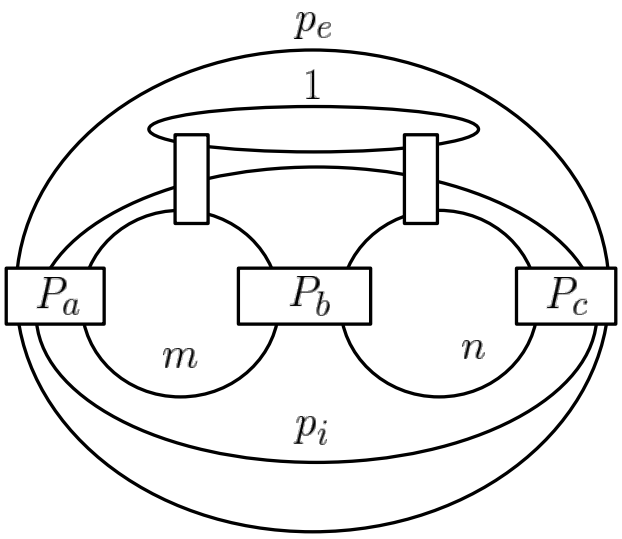

where $p_i + p_e = p - 1$.

Equipped with this, we can state and prove the next lemma, where we will care especially about the case $p_i = 1$ and $p_e = p - 2$.

Lemma 6 $Net(m, n, p) = A_p Net(m, n, p - 1) + B_p Net(m, n, 1, p - 2)$.

Proof: The proof method here is very similar, and we begin by isolating the outermost strands into $p - 1$ and 1 to obtain that

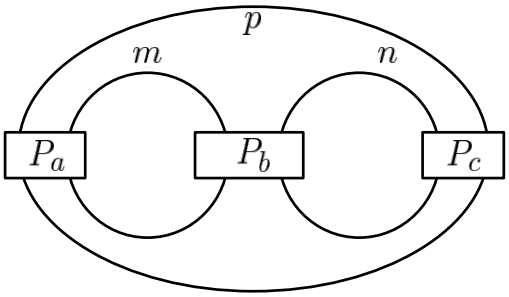

$=$

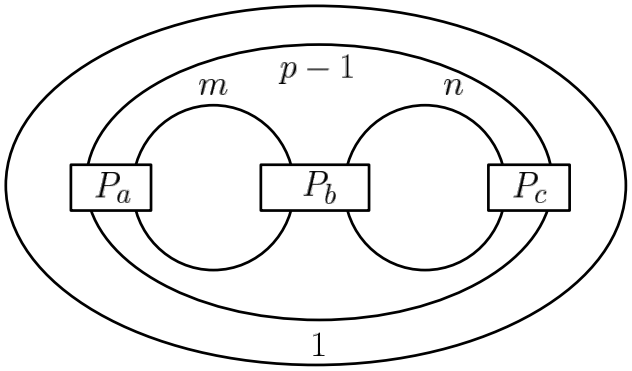

$+(\alpha_{n+p} + \alpha_{m+p})$

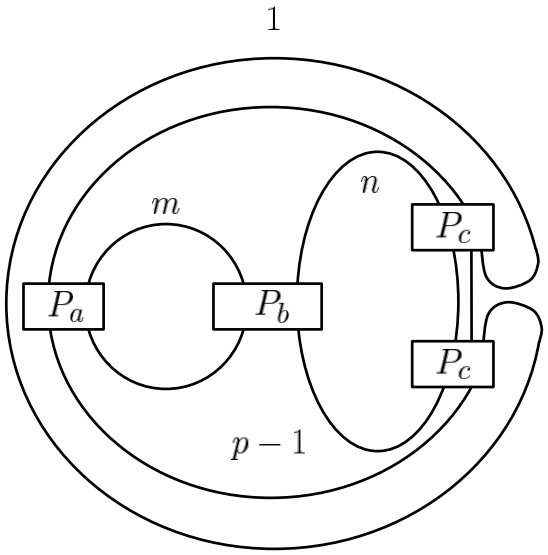

$+(\beta_{n+1}+\beta_{m+1})$

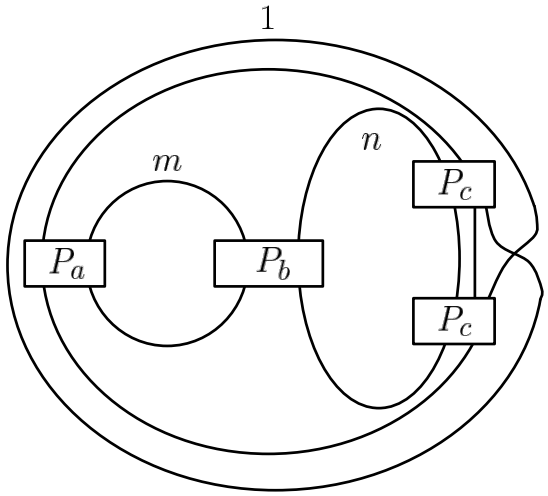

$+\alpha_{n+p}\alpha_{m+p}$

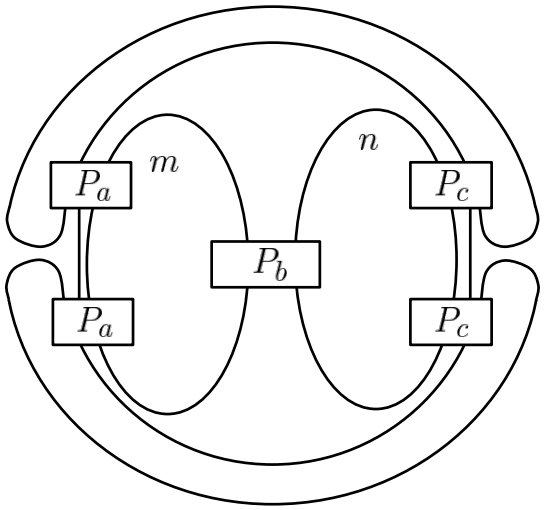

$+(\alpha_{m+p}\beta_{n+p} + \beta_{m+p}\alpha_{n+p})$

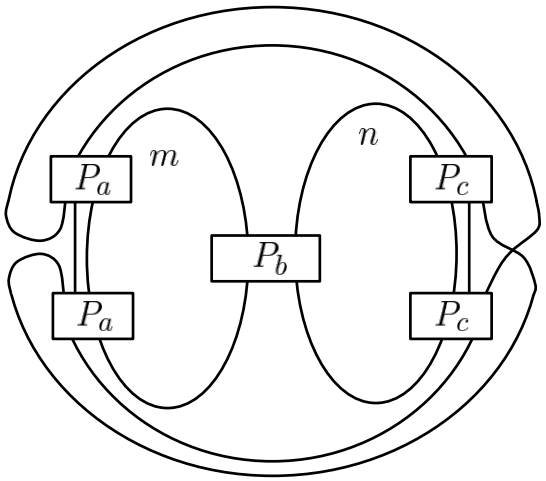

$+\beta_{n+p}\beta_{m+p}$

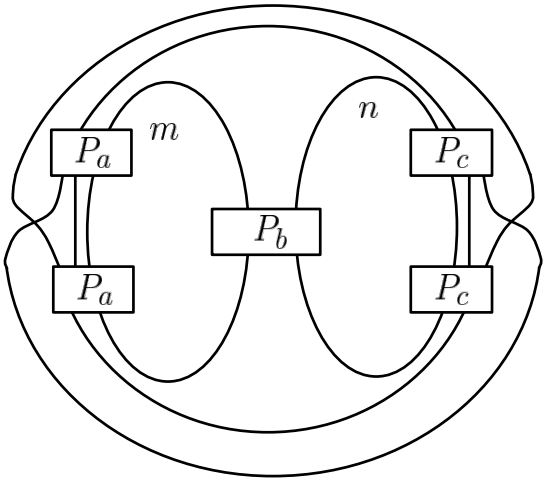

We handle the first three summands precisely as before and notice that the last one can also be handled with the "double cross trick." Collecting terms, we see that we obtain precisely $A_pNet(m, n, p-1)$. The fourth summand is precisely $Net(m, n, 1, p-2)$ up to isotopy, giving us the term $B_pNet(m, n, 1, p-2)$ as claimed. Finally, the penultimate summand dies by the cut path property, proving the claim. ■

Our idea will now be to calculate $Net(m, n, p-1, 0)$ and to reduce our calculation of $Net(m, n, 1, p-2)$ to this case by recursively expressing $Net(m, n, p_e, p_i)$ in terms of $Net(m, n, p_e+1, p_i-1)$. To this end, we prove the following two lemmas

Lemma 7 $Net(m, n, p-1, 0) = A_1Net(m, n, p-1)$

Proof:

$$Net(m, n, p-1, 0) =$$

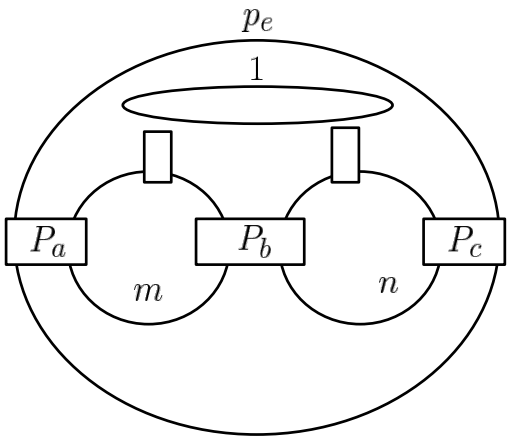

$+(\alpha_{n+1} + \alpha_{m+1})$

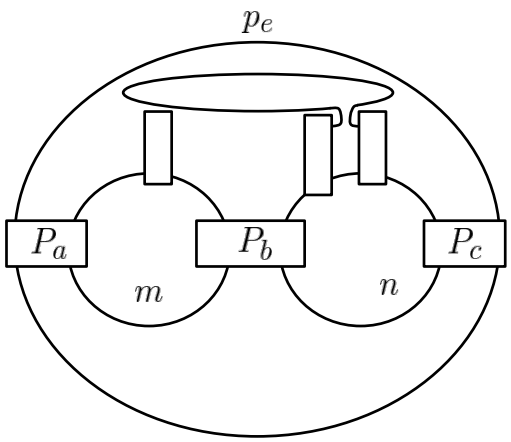

$+\alpha_{n+1}\alpha_{m+1}$

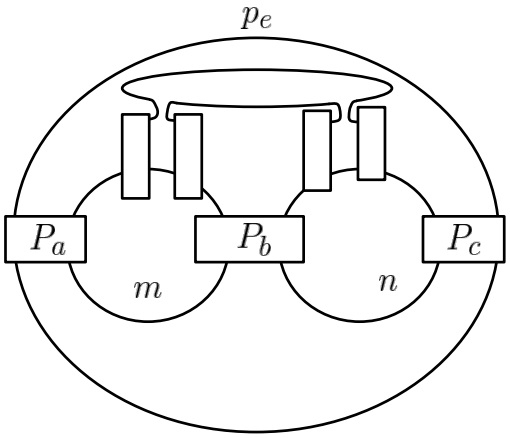

$+(\beta_{n+1} + \beta_{m+1})$

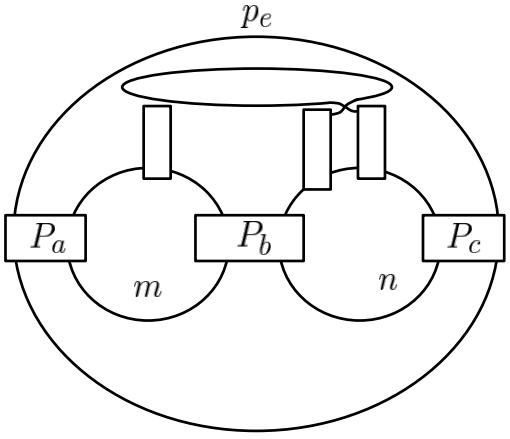

$+\beta_{n+1}\beta_{m+1}$

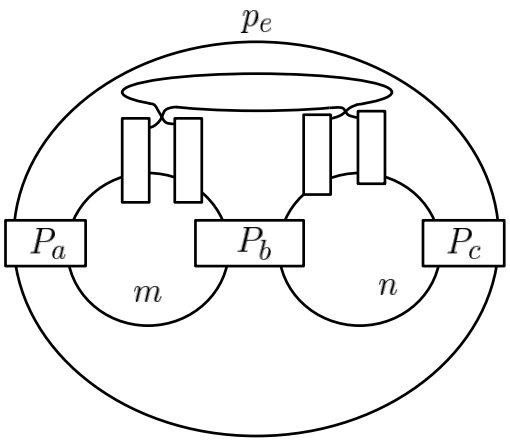

$+(\alpha_{m+1}\beta_{m+1}+\alpha_{m+1}\beta_{m+1})$

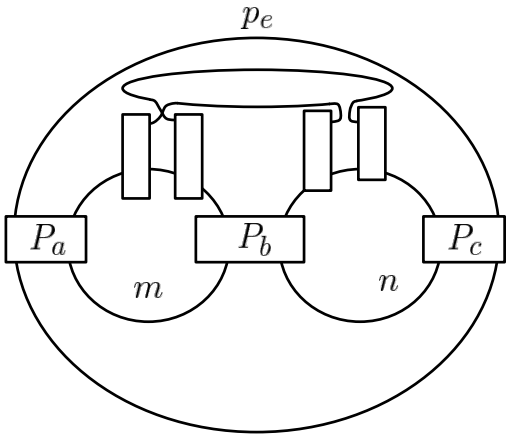

which all reduce exactly as claimed by the annihilation property and calculations similar to those in previous lemmas.

■

We now arrive at the final lemma needed for our recursive evaluation:

Lemma 8 $Net(m, n, p_e, p_i) = A_{p_i+1} Net(m, n, p-1) + B_{p_i+1} Net(m, n, p_{e+1}, p_{i+1})$

Proof:

$$Net(m, n, p_e, p_i) =$$

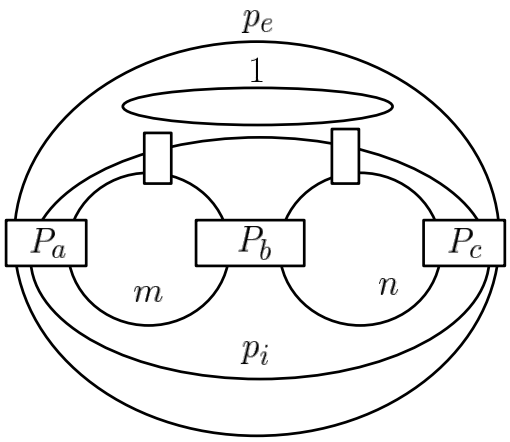

$+(\alpha_{n+1}+\alpha_{m+1})$

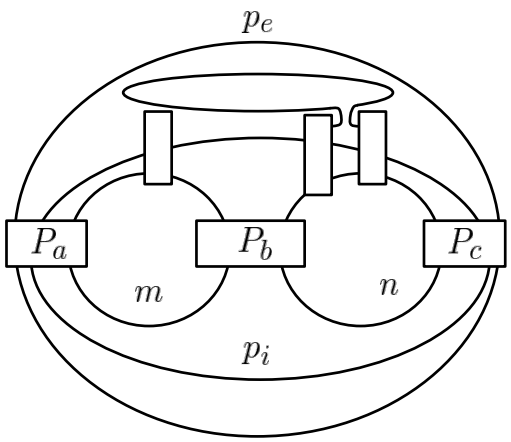

$+\alpha_{n+1}\alpha_{m+1}$

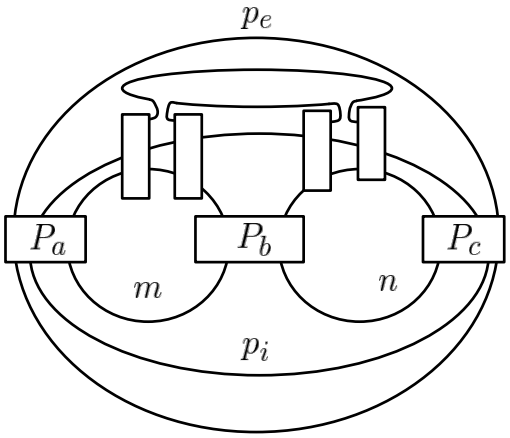

$+(\beta_{n+1}+\beta_{m+1})$

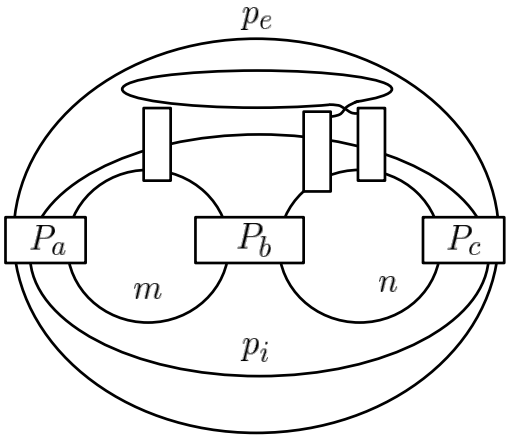

$+\beta_{n+1}\beta_{m+1}$

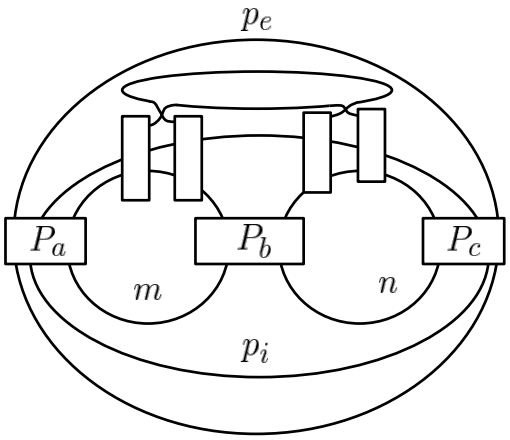

$+(\alpha_{m+1}\beta_{m+1} + \alpha_{m+1}\beta_{m+1})$

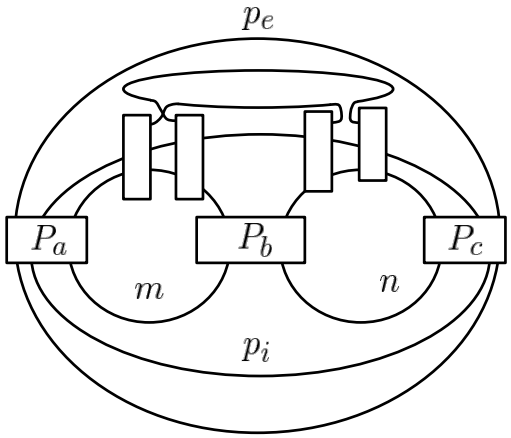

■

Putting the above formulas together, we can define the recursive evaluation:

$$Net(m,n,p) = \left(A_p + \sum_{i=1}^{p-1} A_i \prod_{k=i+1}^{p} B_k \right) Net(m,n,p-1)$$

and by direct calculation, we see that

$$\prod_{i+1}^{p} B_k =$$

$$\left(\frac{[2m+2i+2][m+i][n+i][2n+2i+2]}{[m+i+1][n+i+1]} \right) \left(\frac{[m+p+1][n+p+1]}{[2m+2p+2][2n+2p+2][n+p][m+p]} \right)$$

simplifying the expression further to

$$A_p + \left(\frac{[m+p+1][n+p+1]}{[2m+2p+2][2n+2p+2][n+p][m+p]} \right)$$
$$\cdot \left(\sum_{i=1}^{p-1} A_i \left(\frac{[2m+2i+2][m+i][n+i][2n+2i+2]}{[m+i+1][n+i+1]} \right) \right)$$

when q is a sufficiently large root of unity ($N = 4 \cdot (m+n+p+1)$), the left factor is always positive, as is the product, so it sufficient to check that A_i is nonnegative for all $1 \leq i \leq p$. So, using the formulas

$$\alpha_n := \frac{[2n][n+1][n-1]}{[2n+2][n]^2} \qquad \beta_n := \frac{[n-1]}{[n][2]},$$

and

$$A_i := -\frac{[6][2]}{[3]} + \alpha_{m+i} + \alpha_{n+i} + \frac{[6][2]}{[3]}(\beta_{n+i} + \beta_{m+i}) - [4][2]\beta_{n+i} \cdot \beta_{m+i} \quad B_i := \alpha_{n+i} \cdot \alpha_{m+i}$$

And by substitution, we see that

$$A_i = -\frac{[6][2]}{[3]} + \frac{[2(m+i)][m+i+1][m+i-1]}{[2m+2i+2][m+i]^2} + \frac{[2(n+i)][n+i+1][n+i-1]}{[2n+2i+2][n+i]^2}$$
$$+ \frac{[6][2]}{[3]}\left(\frac{[m+i-1]}{[m+i][2]} + \frac{[n+i-1]}{[n+i][2]}\right) - [4][2]\left(\frac{[m+i-1]}{[m+i][2]}\frac{[n+i-1]}{[n+i][2]}\right).$$

Theorem 10 *When q is a root of unity of order greater than $2(a+b+c)+4$, we have that $\theta(a,b,c) \neq 0$.*

Proof: Making the substitution $q = e^{2\pi i/2(2k+6)}$, we let $N := 2(2k+6)$ and replace each quantum integer with

$$[s] = \frac{\sin(2\pi s/N)}{\sin(2\pi/N)}$$

and collecting terms in the denominator, and using the fact that the denominator is non-vanishing and positive, we see that it is sufficient to check

$$A_i = \sin(4s \cdot \pi/N)\sin((s+1) \cdot 2\pi/N)\sin((s-1) \cdot 2\pi/N)\sin((2j+2) \cdot 2\pi/N)$$

$$\cdot \sin^2(j \cdot 2\pi/N)\sin(6\pi/N)\sin(4\pi/N)\sin(2\pi/N) + \sin(4j \cdot \pi/N)\sin((j+1) \cdot 2\pi/N)$$

$$\cdot \sin((j-1) \cdot 2\pi/N)\sin((2s+2) \cdot 2\pi/N)\sin^2(s \cdot 2\pi/N)\sin(6\pi/N)\sin(4\pi/N)$$

$$\cdot \sin(2\pi/N) + \sin((s-1) \cdot 2\pi/N)\sin((2s+2) \cdot 2\pi/N)\sin(k \cdot 2\pi/N) \cdot \sin((2j+2)$$

$$\cdot 2\pi/N)\sin^2(j\cdot 2\pi/N)\cdot\sin(12\pi/N)\sin(4\pi/N)\sin(2\pi/N)+\sin((j-1)\cdot 2\pi/N)$$

$$\cdot\sin((2j+2)\cdot 2\pi/N)\sin(j\cdot 2\pi/N)\sin((2s+2)\cdot 2\pi/N)\sin^2(s)\sin(12\pi/N)\sin(4\pi/N)$$

$$\cdot\sin(2\pi/N)-\sin((s-1)\cdot 2\pi/N)\sin((j-1)\cdot 2\pi/N)\sin((2s+2)\cdot 2\pi/N)$$

$$\cdot\sin((2j+2)\cdot 2\pi/N)\sin(s\cdot 2\pi/N)\sin(j\cdot 2\pi/N)\sin(6\pi/N)\sin(2\pi/N)\sin(8\pi/N)$$

$$\sin(12\pi/N)\sin^2(4\cdot pi/N)\sin((2s+2)\cdot 2\pi/N)\sin((2j+2)\cdot 2\pi/N)\sin^2(j\cdot 2\pi/N)\sin^2(s\cdot 2\pi/N)$$

where $s := n + i$ while $j := m + i$.

We claim that this is is nonzero for $N > 4(m + n + i + 1)$. This computation seems unwieldy, but is actually in a form that allows us to conclude our result. To see this, one should note that the restriction that $N > 4(m+n+i+1)$ gives that for every value of x as appears above, $\sin(x) \in (0, \pi/2)$. This implies that each among the sin are monotonic. Then we see that the function is strictly negative, and thus along the discussion above we have that $\theta(a, b, c)$ is strictly nonzero. ■

Corollary 3 *The C_2 spider satisfies property $AF2$.*

Theorem 11 *The Reshetikhin-Turaev quantum mapping class group representation coming from the C_2 spider is asymptotically faithful.*

5.4 Future Directions

5.4.1 The G_2 Spider

This is the final of the rank 2 spiders studied by Kuperberg [33]. There has also been extended interest in the link invariant associated to this spider [32]. We quickly see that the G_2 spider satisfies property $AF1$ as both fundamental representations are self dual

and applying 1. Without a concrete description of clasps it seems very difficult to prove that property $AF2$ holds.

5.4.2 A_n

A combinatorial construction of the A_n spider has been completed by Cautis, Kamnitzer, and Morrison [14].

The AF Property of A_n

There is little progress hinting towards how to proceed to prove property $AF1$ or property $AF2$. Although for n even there is a self-dual fundamental representation that could be used to ensure property $AF1$.

5.4.3 Clasps

Work has been done on constructing the clasps for the A_n spider, but the focus has been on their categorification and applications in knot homology [41]. Building these clasps recursively could help in proving the AF property.

5.4.4 Changing Pivotal Structure and More

Parallel results on asymptotic faithfulness have been proven by Anderson for the A_n case [1], using the underlying modular tensor category $\mathcal{C} = Rep(U_q(\mathfrak{sl}(N, \mathbb{C})))$. In particular these parallel results come through not only the changing of pivotal structure, but also a subsequent change of the underlying specialization. This can be seen in the equivalence

$$Rep^{uni}(U_s(\mathfrak{sl}(2, \mathbb{C}) \cong \mathcal{TL}(-is).$$

This change in the root of q being chosen actually results in an entirely different fusion category with the same underlying fusion ring. This can be seen explicitly as the Frobenius-Schur indicators differ, which are defined in terms of $F-$moves. While it seems shocking that the pivotal structure would be able to affect the kernel of the quantum representations the author is not aware of any proof given literature which this fact. We also note that the underlying fusion rings are the same which implies the dimension of the vector space being acted on is the same, so there is a possibility these representations are equivalent.

Chapter 6

Applications

6.1 Applications to Topology

The results of this section recover the work of Andersen in [2]. His approach is through geometric quantization, but it is mentioned at the end of [2] "One can translate our proof of Theorem 4 into a BHMV-skein model proof of Theorem 8". Perhaps this could be considered some version of that translation, but the author cannot claim to be comfortable enough with the details of geometric quantization to ensure this.

6.1.1 Nielsen-Thurston Type

The Nielsen-Thurston classification, [44], is a way of classifying the elements of the mapping class group of a compact oriented surface. We have three types of elements. Let ϕ be a mapping class then either

1. ϕ is periodic, meaning it is finite order, meaning some power of ϕ is the identity.

2. ϕ is reducible, meaning ϕ preserves some finite union of disjoint simple closed curves on the surface.

3. ϕ is pseudo-Anosov, meaning that there exists $\lambda > 1$, two transverse measured foliations F^s and F^u on the surface and a diffeomorphism f of the surface, which represents ϕ, such that

$$f_*(F^s) = \frac{1}{\lambda}F^s$$

and

$$f_*(F^u) = \lambda F^u.$$

In the Pseudo-Anosov case we call λ the stretching factor and it is uniquely determined by ϕ. The reducible case one continues the analysis of ϕ by cutting the surface along the preserved simple closed curves to give a surface with boundary. Then we know there exists a diffeomorphism f which represents ϕ and induces a diffeomorphism on the resulting components after cutting, which on each peace is either finite order or Pseudo-Anosov.

6.1.2 Applying Asymptotic Faithfulness

If $\{\rho_k\}$ is an asymptotically faithful family of quantum representations then ϕ is determined entirely by $(\rho_k(\phi))_{k\in\mathbb{N}}$. This should tell us that the Nielsen-Thurston classification can be determined by analyzing this sequence.

Theorem 12 *For any mapping class ϕ of Σ we have that there exists an integer M such that*

$$(\rho_k(\phi))^M \in \mathbb{C}Id$$

for all k if an only if $\phi^M = 1$.

Proof: First assume there exists an integer M such that

$$(\rho_k(\phi))^M \in \mathbb{C}Id$$

for all k. Asymptotic faithfulness tells us that $\rho_k(\phi^M)$ being a multiple of the identity for all k implies $\phi^M = 1$.

Then assuming $\phi^M = 1$, we have

$$\rho_k(\phi)^M = \rho_k(\phi^M) = \rho_k(1) \in \mathbb{C}Id.$$

■

This deals with the case of ϕ being periodic. We are left to separate reducible elements from Pseudo-Anosov elements. The key will be to determine when an element is reducible.

Theorem 13 *For any mapping class ϕ and any non-trivial homotopy class γ of a simple closed curve on Σ we have that ϕ is reducible along γ, meaning $\phi(\gamma) = \gamma$ if and only if*

$$[\rho_k(\phi), C_k(\gamma)] = 0$$

for all k. Where we know γ is a simple closed curve in Σ, and $C(\gamma) \in End(V_k(\Sigma))$ is the curve operator associated the the fundamental representation V_λ the fulfills the AF property. In particular we have

$$C(\gamma) = Z(\Sigma \times I, \gamma \times \{1/2\}) \in V(\Sigma) \otimes (V(-\Sigma)) = End(V(\Sigma))$$

where the k has been left out as it is fixed.

Proof: This fallows along the same line as the conjugation of curve operators seen in Lemma 1. Assume

$$[\rho_k(\phi), C_k(\gamma)] = 0,$$

meaning

$$V_\phi C(\gamma) = C(\gamma) V_\phi.$$

Then we have

$$V_\phi(C(\gamma)V_\phi^{-1} = C(\gamma)$$

which implies

$$C(\phi(\gamma)) = C(\gamma)$$

Now assume by way of contradiction that $\phi(\gamma)$ is not isotopic as a set to γ, meaning that as homotopy classes we have $\phi(\gamma) \neq \gamma$. Then we are able to follow through our argument seen at the beginning of our proof for asymptotic faithfulness. To get that $C(\gamma)$ is not a multiple of $C(\phi(\gamma))$, a contradiction. Thus we have that $\phi(\gamma) = \gamma$ and ϕ is reducible.

Now assuming that $\phi(\gamma) = \gamma$ then we can start from

$$C(\phi(\gamma)) = C(\gamma)$$

and run the argument in reverse. ■

This is admittedly a disappointing recovery of the Nielson Thurston type. In principle, asymptotic faithfulness implies that all properties of a mapping class should be recoverable from the family of quantum representations, but the proof provided here does nothing to show how the stretching factor can be obtained.

6.2 An Introduction to TQC

This section is based on the work of the author in [12]. As such the figures and arguments have been adapted from there.

6.2.1 Classical Computing

Definition 6.2.1 *A* **bit string** *is a vector $x \in \mathbb{Z}_2^n$, where $\mathbb{Z}_2$ is the finite field of 2 elements.*

In the world of classical computers, this has a very concrete description. In many ways a bit string should be thought of as a piece of "information". Each bit, or component, of the bit string can be thought of as a clear "yes" or "no", similarly "on" or "off". The most common implementation of this model is in the use of the use of transistors in digital circuits as switch.

Definition 6.2.2 *A* **computing problem** *is a family of Boolean functions, denoted*

$$f : \mathbb{Z}_2^n \to \mathbb{Z}_2^n$$

or more precisely

$$\{f_i : \mathbb{Z}_2^n \to \mathbb{Z}_2\}_{i=1}^n.$$

There is a question of the computability of f, but we will assume all of our computing problems are computable as this property is not changed even when jumping to quantum computing. Thus our goal is to compute $f(N)$ for any bit string N.

6.2.2 Quantum Computing

We will take the underlying principle of quantum computing to be "linearizing" classical computing. This means we will be lifting from $\mathbb{Z}_2$ to $\mathbb{C}$, and really $\mathbb{P}^1$ as we will be uninterested in overall phases.

Definition 6.2.3 *A* **qubit** *is a non-zero vector in $\mathbb{C}^2 = \mathbb{C}[\mathbb{Z}_2]$. Similarly an $n-$***qubit** *is a non-zero vector in $(\mathbb{C}^2)^{\otimes n} = \mathbb{C}[\mathbb{Z}_2^n]$, which has as basis vectors the bit strings of length*

n.

So generally we have gone from bit strings to linear combinations of bit strings, these can be thought of as superpositions of bit strings. This step of turning the classical information of bit string N to a quantum state $|N>$ will be called an encoding.

Definition 6.2.4 *Let us take an encoding, $x \mapsto |x\rangle \in (\mathbb{C}^2)^n$, and a computing problem f. Then we say that $U_x \in U(2^n)$ is an implementation of f if $U_x|x\rangle$ is near $|f(x)\rangle$, in $(\mathbb{C}^2)^n$, alternatively we can think of*

$$U_x|x\rangle = \sum_j a_j|j\rangle.$$

Then $|a_j|^2$ is the probability of $U_x|x\rangle$ being $|j\rangle$, so U_x is an implementation of f if $|af(x)|^2 >> 0$.

Definition 6.2.5 *An* **encoding** *of a computation model will consist of an encoding of the the classical information as quantum states (as described above), as well as a collection of gates (unitary matrices), which are used to generate potential implementations of computing problems.*

Definition 6.2.6 *If an encoding lies as a subspace inside of a larger Hilbert space, we call our encoding the* **computational subspace**.

Definition 6.2.7 *We say that our encoding has* **leakage** *if the computation subspace is not invariant under the gate set.*

6.2.3 Introducing Topology

The main issue facing quantum computing is decoherence. In short, this means interactions with the nearby environment introducing errors.

Definition 6.2.8 *We will say that an encoding is* **topological** *if for any given N, the corresponding state $|N\rangle$ and potential gates correspond to some topologically invariant structure.*

The most common example of a topological encoding, will be isotopy classes. An example of particular interest to us will be isotopy classes of ribbon graphs.

A Brief Historical Aside

The idea of topologically protected quantum computing should be attributed both to Kitaev and Freedman independently. Kitaev proposed using anyons to encode quantum memory and provided a collection of gates, coming from braids, that were exponentially precise [31]. Freedman's computational model was rooted in topological quantum field theory. Freedman, Larsen, and Wang then provided a universal gate set from braiding, and showed that this new proposal recovers the computational power of ordinary quantum computing [20]. This is what is called topological quantum computing. One key insight into Freedman's approach is the hope of implementing this computational model using topological matter.

This description of topological quantum computing is exactly the situation we are working in. In particular, Unitary modular tensor categories are the mathematical foundation for anyonic systems, and as we have seen the algebraic input of Unitary TQFTs.

6.3 Clifford Groups

We follow the exposition given in [6]. We begin by generalizing the qubit setting described above. Let G be a finite abelian group, decomposed as

$$G = \mathbb{Z}/m_1\mathbb{Z} \times ... \times \mathbb{Z}/m_s\mathbb{Z}.$$

We consider the complex vector space

$$\mathcal{H}_G = \mathbb{C}^{m_1} \otimes ... \otimes \mathbb{C}^{m_s}.$$

We note that $x \in \mathcal{H}_G$ is represented as some $g \in G$ and so we have the notation:

$$\mathcal{H}_G = \text{span}\{|g\rangle : g \in G\}.$$

We also have the following relationship

$$\mathcal{H}_G^{\otimes n} = \mathcal{H}_{G^n},$$

where we are using the notation that

$$G^n := \bigoplus_{i=1}^{n} G.$$

Thus rather than encoding bits, we are encoding a finite abelian group. When this finite abelian group is $\mathbb{Z}_d$ we call non-zero vectors in $\mathcal{H}$, qudits.

6.3.1 Pauli Group over G

Let $\gamma = e^{\frac{\pi i}{|G|}}$.

Definition 6.3.1 *A **Pauli operator** over G is any unitary operator on $\mathcal{H}_G$ of the form*

$$\sigma(a, g, h) := \gamma^a Z_g X_h$$

where

$$X_g(|x\rangle) = |g + x\rangle$$

$$Z_h(|x\rangle) = \chi_h(x)|x\rangle$$

where χ_h is a character of G.

Definition 6.3.2 *The **Pauli group over** G is the subgroup of $U(\mathcal{H}_G)$ generated by all Pauli operators, denoted $P_{1,G}$. Then we have*

$$P_{n,G} := P_{1,G}^{\otimes n} \subset U(\mathcal{H}_G^{\otimes n}) = U(\mathcal{H}_{G^n})$$

*called the n^{th} **Pauli Group over** G*

6.3.2 Clifford Group over G

Definition 6.3.3 *The n^{th} **Clifford group over** G, denoted as $C_{n,G}$, is the normalizer of $P_{n,G}$ in $U(\mathcal{H}_{G^n})$, and actually as operators differing by only a phase will not contribute to a conjugation $PU(\mathcal{H}_{G^n})$.*

6.3.3 Normalizer Circuits

Definition 6.3.4 *A **normalizer circuit over** G is a member of the group, N_G, generated by*

- *Group automorphism gates:*

  $$|g\rangle \mapsto |\psi(g)\rangle$$

  for $\psi(g)$ a group automorphism.

- *Quadratic phase gates:*

  $$|g\rangle \mapsto \zeta(g)|g\rangle$$

where $|\zeta(g)| = 1$ *and*

$$\zeta(g+h) = \zeta(g)\zeta(h)B(g,h)$$

where

$$B(x+y,g) = B(x,g)B(y,g)$$

$$B(g,x+y) = B(g,x)B(y,g).$$

- *Quantum Fourier Transforms:*

$$\mathcal{F} : |g\rangle \mapsto \frac{1}{|G|}\sum_{x\in G}\chi_x(g)|x\rangle$$

Where χ_x *are characters of the group.*

Theorem 14 *[6]*

$$N_G \leq C_{1,G}$$

Conjecture 6.3.1 *[6]*

$$N_G = C_{1,G}$$

6.4 An Encoding for Quantum Representations of MCGs

We propose a topological qudit encoding based on the Reshetikhin Turaev state space. This should be thought of as generalizing the use of anyons with their exchange statistics to the case of mapping class group representations. The difficulty lies in finding how to encode qudits into the relevant Hilbert space.

Definition 6.4.1 *Let* $\mathcal{C}$ *be a rank* d *modular tensor category, meaning* $\mathcal{C}$ *has* d *isomorphism classes of simple objects or anyon types, and* $V_g = V(\Sigma_g)$ *be the Reshetikhin Turaev*

state space of the genus g closed surface. Then our encoding of qudits will refer to the subspace of V_g in which every basis vector has only the longitudinal edges of the spine colored by non-trivial labels. This can be seen in figure 6.1.

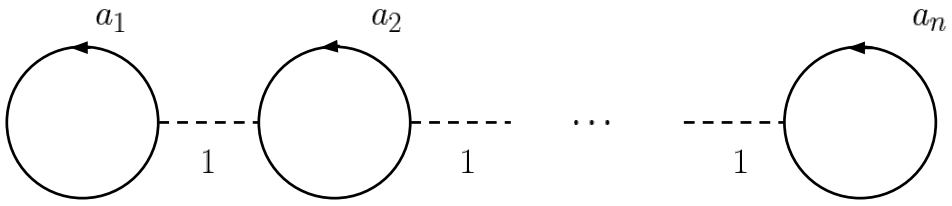

Figure 6.1:

The gate set will be formed by the image of the corresponding quantum representations of the mapping class group. We immediately note that this construction is a topological encoding.

Proposition 1 *The longitudinal encoding will necessarily have leakage out of the computational subspace unless*

$$[F_{\hat{b}}^{\hat{a}db}]_{1,(x,\mu,\nu)}\theta_x[F_a^{a\hat{b}b}]_{(x,\mu,\nu),(y,\alpha,\beta)} = 0$$

for all $y \neq 1$.

Proof: This follows immediately from the action formula computed in section 3.3 specialized to the basis vectors used in the longitudinal encoding. ■

We note that this is very dependent on taking the entirety of $\rho(\mathrm{MCG}(\Sigma_g))$ as the gate set. It is a very interesting question to determine if there is a better choice of gate set, meaning some subset of $\rho(\mathrm{MCG}(\Sigma_g))$ which avoids leakage. A quick example which avoids leakage

is to only take only the Dehn twists about longitudinal curves and meridinal curves. This recovers the quantum representation of $\mathrm{MCG}(\Sigma_1) = \mathrm{PSL}(2,\mathbb{Z})$ on each tensor factor, which is known to be finite in all cases due to Ng and Shauenburg [38]. This exhibits the true question here. Can we find a better gate set such that our encoding is invariant, but the gate set is universal.

6.5 Abelian Anyon Models

An abelian anyon model is one in which all quantum dimensions are 1, these correspond to pointed modular tensor categories. The fusion rules of an abelian anyon model form a finite abelian group, G. We list some of the relevant evaluation data [42]: Let $a, b, c \in G$

$$[F^{a,b,c}_{a+b+c}]_{a+b,b+c} = f(a,b,c) \in H^3(G, \mathbb{Q}/\mathbb{Z})$$

$$d_a = 1$$

$$\theta_a = e^{2\pi i q(a)}$$

Where q is a quadratic form on G.

$$S_{x,y} = \frac{1}{\sqrt{|G|}} e^{2\pi i b(x,y)}$$

where

$$b(x,y) = q(x+y) - q(x) - q(y)$$

is a bi-linear form associated to q.

6.5.1 Specializing to Abelian Anyon Models

With these computations in mind we look to ground ourselves with the concrete example discussed in the introduction. For the remainder of this section let our modular tensor category $\mathcal{C}$ have fusion rules forming a group $G = \mathbb{Z}/m_1\mathbb{Z} \times ... \times \mathbb{Z}/m_s\mathbb{Z}$ with $m_i|m_{i+1}$ and modular data determined by $\vec{k}$.

Hilbert Spaces of States

Let Σ_g be a closed surface of genus g. We look to describe $V(\Sigma_g)$ concretely. We note that abelian MTCs are multiplicity free, meaning

$$a \otimes b = a + b = \sum N_c^{ab} c$$

where $N_c^{ab} = \delta_{c,a+b}$, and in particular that the dimension of the Hom spaces are either 0 or 1, meaning we can ignore vertex labels. Now we also know $\hat{a} = -a$, so we have $a + \hat{a} = 0$ and $a + b = 0$ exactly when $b = \hat{a}$. Now we look at the following lemma.

Lemma 9 *When looking at the trivalent graph seen in Fig. 6.2 colored by a finite abelian group G. Then $a_i = 0$ for all i.*

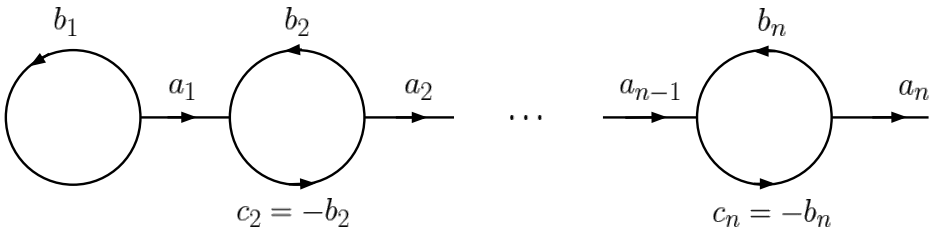

Figure 6.2:

Proof: This is a simple proof by induction. ■

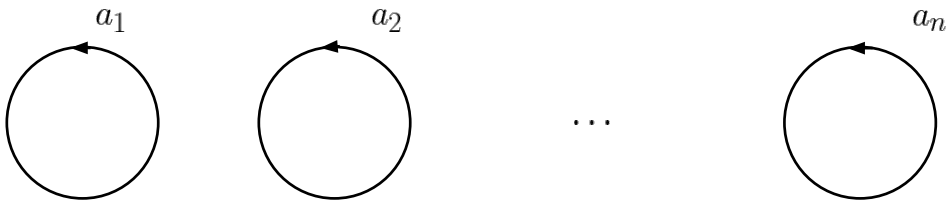

Figure 6.3: •

Applying this lemma we have:

Proposition 2 *We have* $V(\Sigma_g) \cong \mathcal{H}_G^{\otimes g}$*, where the basis is given in Fig. 6.3.*

Proof: This is an immediate application of the above lemma. ■

We will denote an element of the basis shown in Fig. 6.3 as $\vec{a} = (a_1, ..., a_g)$.

The MCG **Action**

T_0 **and** T_1

This computation is identical to that of the general setting. And so

$$T_0(\vec{a}) = \frac{p_-}{D}\theta_{a_2}\vec{a} = \frac{p_-}{D}\omega^{a_2^2}\vec{a}$$

and

$$T_1(\vec{a}) = \frac{p_-}{D}\theta_{a_1}\vec{a} = \frac{p_-}{D}\omega^{a_1^2}\vec{a}.$$

Now define

$$L : \mathcal{H}_G \to \mathcal{H}_G$$

defined by

$$L(|a\rangle) = \theta_a |a\rangle$$

Then we have

$$T_0 = L_2(\vec{a})$$

and

$$T_1 = L_1(\vec{a})$$

where

$$L_i = Id \otimes Id \otimes ... \otimes L \otimes Id \otimes ... \otimes Id$$

where L acts on the i^{th} component.

T_{2i+1} **for** $i = 1, ..., g-1$

This computation is also identical, but we are able to make use of the explicit F-moves. In particular we have

$$T_{2i+1}(\vec{a})$$

$$= \frac{p_-}{D} \sum_{f,h} [F_{-a_{i+1}}^{(-a_i)a_i(-a_{i+1})}]_{(0,f)} \theta_f [F_{a_i}^{a_i(-a_{i+1})a_{i+1}}]_{(f,h)} \vec{a}'_h,$$

but we have the only non-zero F-move is

$$[F_{a+b+c}^{a,b,c}]_{a+b,b+c} = f(a,b,c) \in H^3(G, U(1))$$

Now we also note that we elected to describe all F-moves as positive powers, but actually

$$[F_{a_i}^{a_i(-a_{i+1})a_{i+1}}] = [F_{-a_{i+1}}^{(-a_i)a_i(-a_{i+1})}]^{-1}$$

$$T_{2i+1}(\vec{a}) = f(a_i, -a_{i+1}, a_{i+1}) \theta_{a_i - a_{i+1}} \overline{f(a_i, -a_{i+1}, a_{i+1})} \vec{a} = \theta_{a_i - a_{i+1}} \vec{a}$$

Now define

$$M : \mathcal{H}_G \otimes \mathcal{H}_G \to \mathcal{H}_G \otimes \mathcal{H}_G,$$

defined by

$$M(|a\rangle \otimes |b\rangle) = \theta_{a-b}|a\rangle \otimes |b\rangle.$$

The crucial observation here is that M can also be described as follows:

$$M : \mathcal{H}_{G\oplus G} \to \mathcal{H}_{G\oplus G},$$

where

$$M(|a+b\rangle) = \theta_{a-b}|a+b\rangle$$

$$T_{2i+1}(\vec{a}) = M_{i,i+1}(\vec{a}).$$

T_{2i} **for** $i = 1, ..., g$

In Fig. 6.4 and Fig. 6.5 we provide an alternative version of this computation which utilizes many of the specific properties of the fusion rules for abelian MTCs which allow for the use of shortcuts.

1

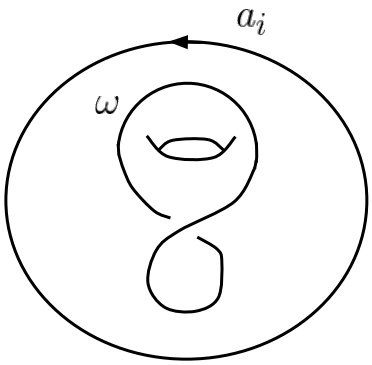

2

$=$

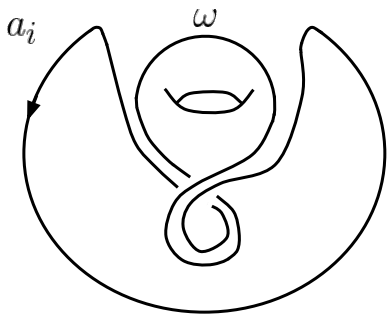

3

$= \theta_{a_i}^{-1}$

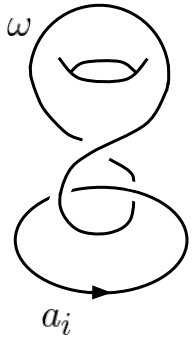

Figure 6.4: Steps $1, 2$, and 3

$$= \theta_{a_i}^{-1} \sum_{b \in L} \frac{d_b}{D} \qquad 4$$

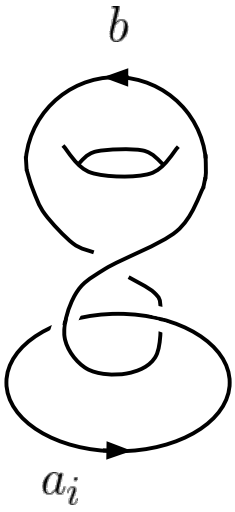

$$= \theta_{a_i}^{-1} \sum_{b \in L} S_{a_i b} \qquad 5$$

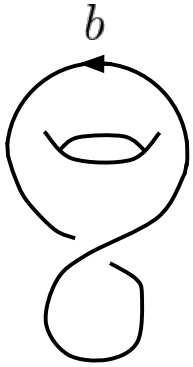

$$= \theta_{a_i}^{-1} \sum_{b \in L} S_{a_i b} \theta_b^{-1} \qquad 6$$

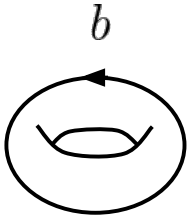

Figure 6.5: Steps 4, 5, and 6

Then we can see that

$$T_{2i}(\vec{a}) = \theta_{a_i}^{-1} \sum_{b \in G} S_{a_i b} \theta_b^{-1} \vec{a}'_b$$

Where $\vec{a}'_b = (a_1, .., a_{i-1}, b, a_{i+1}, .., a_g)$ is determined from $\vec{a}$ by replacing the $i^t h$ coordinate from a_i to b. Now define

$$O : \mathcal{H}_G \to \mathcal{H}_G$$

defined by

$$O(|a>) = \sum_{b \in G} \theta_a^{-1} S_{a,b} \theta_b^{-1} |b> .$$

Then we have that

$$T_{2i}(\vec{a}) = O_i(\vec{a}).$$

6.5.2 Clifford Operators

Theorem 15 *Let Σ_g be the closed surface of genus g and*

$$\rho_G : \mathrm{MCG}(\Sigma_g) \to PU(\mathcal{H}_{G^g})$$

ρ_G be the quantum representation coming from an abelian MTC with fusion rules determined by a finite abelian group G. Then

$$\rho_G(\mathrm{MCG}(\Sigma_g)) \leq C_{g,G},$$

meaning the image of the mapping class group under this representation lies entirely in the g^{th} Clifford group over G. Moreover, each Humphries generator is sent to a Normalizer circuit over $\bigoplus_{i=1}^{g} G$.

Corollary 4 *The computational framework using mapping class group representations*

arising from abelian anyon models can be classically efficiently simulated in at most polynomial time in the number of Dehn twists about Humphries generators of type γ_{2i} (longitudinal), the number of gates in the circuit, the number of cyclic factors of the groups, and the logarithm of the orders of the cyclic factors.

Proof: As only normalizer gates can be achieved this follows immediately from Van Den Nest's results on simulating normalizer circuits over finite abelian groups [15]. Note that longitudinal Dehn Twists implement quantum Fourier transforms. ■

Lemma 10 *$\sqrt{|G|}S_{x,y}$ is a bi-character, meaning*

$$|\sqrt{|G|}S_{x,y}| = 1$$

$$\sqrt{|G|}S_{x+y,g} = \sqrt{|G|}S_{x,g}\sqrt{|G|}S_{y,g}$$

$$\sqrt{|G|}S_{g,x+y} = \sqrt{|G|}S_{g,x}\sqrt{|G|}S_{g,y}$$

Proof: This follows immediately as

$$\sqrt{|G|}S_{x,y} = exp(2\pi i b(x,y))$$

where $b(x,y)$ is bilinear. ■

Now we return to the proof of our theorem. *Proof:*

We see that based on the structure computed above we need only show that L, M, and O lie $C_{1,N}$, $C_{2,N}$, and $C_{1,N}$ respectively as tensoring with the identity operator will preserve that result and the root of unity $\frac{p_-}{D}$ can be ignored as these operators are only considered projectively.

L

Recall

$$L(|x>) = \theta_x|x> .$$

We first look to show that L lies in $C_{1,G}$, and in particular that $L \in N_G$. In fact we will show that L is a quadratic phase gate, meaning θ_x is a quadratic phase. We first note that θ_x is a root of unity, thus we need only show that

$$\theta_{x+y} = \theta_x\theta_y B(x,y)$$

In fact we have

$$\frac{\theta_{x+y}}{\theta_x\theta_y} = \sqrt{|G|}S_{x,y}$$

which as we have seen in Lemma 4.3 is a bicharacter. Thus L is a quadratic phase gate and $L \in N_G$.

M

Recall

$$M(|x> \otimes |y>) = \theta_{x-y}|x> \otimes |y> .$$

We we look to show that $M \in C_{2,G}$. More so we will show that M is a normalizer circuit over $G \oplus G$. We have

$$M(|x+y\rangle) = \theta_{x-y}|x+y\rangle$$

The form of this operator should look very similar that of the previous section. As such the computation is very similar. We must show that

$$\theta_{(x+a)-(y+b)} = theta_{x-y}\theta_{a-b}B((x,y),(a,b)),$$

where $B((x,y),(a,b))$ is a bicharacter. We have

$$\theta_{(x+a)-(y+b)} = \theta_{(x-y)+(a-b)} = \theta_{x-y}\theta_{a-b}\sqrt{|G|}S_{x-y,a-b}.$$

Thus we need only show that $\sqrt{|G|}S_{x-y,a-b}$ is a bicharacter. We have

$$B((x+g,y+h),(a,b)) = \sqrt{|G|}S_{(x+g)-(y+h),a-b}$$

$$= \sqrt{|G|}S_{(x-y)+(g-h),a-b} = \sqrt{|G|}S_{x-y,a-b}\sqrt{|G|}S_{g-h,a-b}$$

$$= B((x,y),(a,b))B((g,h),(a,b)).$$

And similarly

$$B((x,y),(a+g,b+h)) = B((x,y),(a,b))B((x,y),(g,h)).$$

Thus we have $M \in C_{2,G}$ and in particular it is a normalizer gate over $G \oplus G$.

O

Recall

$$O(|x>) = \sum_{y\in G} \theta_x^{-1} S_{x,y} \theta_y^{-1} |y>$$

We look to show that $O \in C_{1,G}$ and in particular that $O \in N_G$. We quickly see that we are pre-composing and post-composing with θ_z^{-1}, which from above we have seen to a quadratic phase in N_G. Thus we need only show that

$$\sqrt{|G|}S : |x> \mapsto \sum_{y\in G} S_{x,y}|y>$$

is in N_G. Utilizing our lemma which proved that $S_{x,y}$ was a bicharacter we can in fact write

$$\sqrt{|G|}S_{x,y} = \chi_y(x)$$

where χ_y is a character. Then we have

$$S(|x>) = \frac{1}{|G|}\sum_{y\in g}\chi_y(x)|y>$$

which is exactly the global quantum Fourier transform. Thus we have $S \in N_G$ and so $O \in N_G$.

Thus we have completed our proof of Theorem 1. ■

6.6 General Anyons

Though the 1-qudit gates in our scheme always form a finite group, they are not always generalized Clifford gates as we show below for the Fibonacci anyon. For abelian anyon models, though all mapping class gates are generalized Clifford gates, we do not know if they can be efficiently simulated by classical computers.

6.6.1 Fib

The simple objects of Fib are 1 and τ. The only nontrivial fusion rule is

$$\tau \otimes \tau = 1 \oplus \tau.$$

Let $\phi = \frac{1+\sqrt{5}}{2}$ be the golden ratio. Then we can write the evaluation moves explicitly as [48]

$$d_1 = 1, \qquad d_\tau = \phi$$

$$T = \begin{pmatrix} 1 & 0 \\ 0 & e^{4\pi i/5} \end{pmatrix}$$

$$S = \frac{1}{\sqrt{2+\phi}} \begin{pmatrix} 1 & \phi \\ \phi & -1 \end{pmatrix}$$

$$R_1^{\tau\tau} = e^{\frac{-4\pi i}{5}} \qquad R_\tau^{\tau\tau} = e^{\frac{3\pi i}{5}}$$

$$F_\tau^{\tau\tau\tau} = \begin{pmatrix} \phi^{-1} & \phi^{-1/2} \\ \phi^{-1/2} & -\phi^{-1} \end{pmatrix}$$

This case differs greatly from the previous case. The most striking of these differences is the lack of a tensor product structure on $V_{Fib}(\Sigma)$. One potential way of introducing a tensor product structure into the picture is to embed $V(\Sigma)$ into $W^{\otimes m}$, where $W = \bigoplus_{a,b,c \in L} \mathrm{Hom}(a \otimes b, c)$ and m is taken to be the number of pairs of pants in a pants decomposition of Σ, meaning $m = 2g - 2$. Then we embed $V(\Sigma)$ into $W^{\otimes m}$ by sending a basis vector to the tensor product of the vertex vector for each vertex of the basis element. For Fib we see that $W \cong \mathbb{C}^5$ as their are 5 admissible triples:

$$(1,1,1), (\tau,\tau,0), (\tau,0,\tau), (0,\tau,\tau), (\tau,\tau,\tau).$$

Another possible thought would be to look at a computational subspace inside of $V(\Sigma)$. In particular the subspace $(\mathbb{C}^2)^{\otimes g}$ restricting all of the a_i labels to be 1. This leaves each genus to be encircled by either a 1 or a τ. This computational subspace is even invariant under T_0, T_1, and T_{2i} for $i = 1, ..., g$. Unfortunately this subspace is not invariant under T_{2i+1} for $i = 1, ..., g-1$. This lack of invariance does imply that this computational subspace will inherently lead to leakage, but that does not rule this out as a promosing model.

Theorem 16 *There does not exist a basis for $V(T^2)$ for which both S and T lie in the associated Clifford group on the single qubit.*

Proof: First we observe that $T^5 = Id$. Then as the order of the Clifford group is 24 we know that as 5 does not divide 24 the only possibility is that in our chosen basis T is the identity matrix. So in our new "normalized" basis we have

$$T = \begin{pmatrix} 1 & 0 \\ 0 & 1 \end{pmatrix}$$

and

$$S = \frac{1}{\sqrt{2+\phi}} \begin{pmatrix} 1 & e^{-4\pi i/5}\phi \\ \phi e^{4\pi i/5} & -1 \end{pmatrix}$$

By explicit computation we can show S is not a Clifford operator, even up to a global phase. We quickly see that S has order 2. Then we have 9 matrices to compare this to, up to global phase. Explicit computation (refer to Appendix A A.2) shows that of these 9 matrices, 4 have the property that their off diagonals are equal, 3 have the property that their off diagonals sum to zero, and the remaining two have at least one zero entry. All three of these properties are preserved under global phases, but our matrix S does not have these properties. Thus in this computational basis S is not a Clifford operator. Then as this is the only basis that allowed T to be a Clifford operator we have shown that it is not possible for both S and T to be Clifford operators in the same basis. ■

Appendix A

The Abstract Clifford Group

A.1 The Pauli Group on One Qubit

We start by looking at the Pauli Group on one qubit. This is a specialization of the definition given at the beginning of this paper. In particular we have

$$P_1 :=< X, Y, Z >= \{\pm Id, \pm iId, \pm X, \pm iX, \pm Y, \pm iY, \pm Z, \pm iZ\}$$

Abstractly this is a 16 element group. As we will only be working up to a global phase it is convenient for us to define

$$P := \{\pm Id, \pm X, \pm Y, \pm Z\}.$$

Once a computational basis for the underlying 2 dimensional Hilbert space is chosen, then we have a realization of this group as a matrix group. Here we have

$$X = \begin{pmatrix} 0 & 1 \\ 1 & 0 \end{pmatrix}$$

$$Y = \begin{pmatrix} 0 & -i \\ i & 0 \end{pmatrix}$$

$$Z = \begin{pmatrix} 1 & 0 \\ 0 & -1 \end{pmatrix}$$

A.2 The Clifford Group on One Qubit

Now the Clifford group on one qubit can be viewed as the normalizer of the Pauli group, up to overall global phases.

Definition A.2.1 *The Clifford group on one qubit is*

$$C_1 := \{U \in U(2) : UpU^* \in P - \{\pm Id\}, p \in P - \{\pm Id\}\}/U(1)$$

Proposition 3 *The Clifford group on one qubit has order* 24.

Proof: We first note that conjugation must preserve the group structure, and in particular here we mean the multiplication of the Pauli matrices. Thus as $Y = iXZ$, we will not need to specify the image of Y under the conjugation. Similarly $-X$ and $-Z$ will be determined by where X and Z are sent as well. Thus we will only need to specify where X and Z end up. We know that X and Z anti-commute and so UXU^* and UZU^* will also need to anti-commute. This tells us that X can be sent to any element of $P - \{\pm Id\}$, but Z can only be send to $P - \{\pm Id, UXU^*\}$. Thus there are 6 possibilities for X to be sent to and 4 possibilities for Z, and so C_1 has order $6 \cdot 4 = 24$. ■

Theorem 17 *[?] Similar to above, once a computational basis is chosen for the Hilbert space it is possible to describe C_1 explicitly. In fact*

$$C_1 =< H, Q >$$

where

$$H = \frac{1}{\sqrt{2}} \begin{pmatrix} 1 & 1 \\ 1 & -1 \end{pmatrix}$$

and

$$Q = \begin{pmatrix} 1 & 0 \\ 0 & i \end{pmatrix}$$

We note that our description of C_1 is as a 24 element group. The usually order given to the group generated by H and Q would be 192, but recall we have an equivalence up to global phase of the words in H and Q. In particular the factor of 8 results in an overcounting seen from $(PQ)^3 = e^{2\pi i/8} Id$ which for our purposes is the identity.

Corollary 5 *As* 24 *element groups*

$$C_1 \cong S_4.$$

As a note, S_4 *is the symmetry group of the cube.*

Proof: We see

$$S_4 =< (1,2), (1,2,3,4) > .$$

Then using the description afforded by Theorem 3 we are done. ■

We now provide a table of representatives of the elements of C_1 along with corresponding elements of S_4 coming from the isomorphism used in Corollary 1.

C_1	S_4	C_1	S_4
$\begin{pmatrix} 1 & 0 \\ 0 & 1 \end{pmatrix}$	(1)	$\frac{1}{\sqrt{2}}\begin{pmatrix} 1 & i \\ -1 & i \end{pmatrix}$	(132)
$\frac{1}{\sqrt{2}}\begin{pmatrix} 1 & 1 \\ 1 & -1 \end{pmatrix}$	(12)	$\frac{1}{\sqrt{2}}\begin{pmatrix} 1 & -1 \\ -1 & -1 \end{pmatrix}$	(34)
$\begin{pmatrix} 1 & 0 \\ 0 & i \end{pmatrix}$	(1234)	$\begin{pmatrix} 0 & 1 \\ -1 & 0 \end{pmatrix}$	(12)(34)
$\begin{pmatrix} 1 & 0 \\ 0 & -1 \end{pmatrix}$	(13)(24)	$\begin{pmatrix} 0 & 1 \\ i & 0 \end{pmatrix}$	(24)
$\begin{pmatrix} 1 & 0 \\ 0 & -i \end{pmatrix}$	(1432)	$\begin{pmatrix} 0 & 1 \\ 1 & 0 \end{pmatrix}$	(14)(23)
$\frac{1}{\sqrt{2}}\begin{pmatrix} 1 & 1 \\ i & -i \end{pmatrix}$	(134)	$\frac{1}{\sqrt{2}}\begin{pmatrix} 1 & i \\ -i & -1 \end{pmatrix}$	(14)
$\frac{1}{\sqrt{2}}\begin{pmatrix} 1 & 1 \\ -1 & 1 \end{pmatrix}$	(1423)	$\frac{1}{\sqrt{2}}\begin{pmatrix} 1 & -1 \\ -i & -i \end{pmatrix}$	(123)
$\frac{1}{\sqrt{2}}\begin{pmatrix} 1 & 1 \\ -i & i \end{pmatrix}$	(243)	$\frac{1}{\sqrt{2}}\begin{pmatrix} 1 & -i \\ -i & 1 \end{pmatrix}$	(1342)
$\frac{1}{\sqrt{2}}\begin{pmatrix} 1 & i \\ 1 & -i \end{pmatrix}$	(234)	$\frac{1}{\sqrt{2}}\begin{pmatrix} 1 & -i \\ -1 & -i \end{pmatrix}$	(124)
$\frac{1}{\sqrt{2}}\begin{pmatrix} 1 & -1 \\ 1 & 1 \end{pmatrix}$	(1324)	$\begin{pmatrix} 0 & 1 \\ -i & 0 \end{pmatrix}$	(24)
$\frac{1}{\sqrt{2}}\begin{pmatrix} 1 & -i \\ 1 & i \end{pmatrix}$	(143)	$\frac{1}{\sqrt{2}}\begin{pmatrix} 1 & -i \\ i & -1 \end{pmatrix}$	(23)
$\frac{1}{\sqrt{2}}\begin{pmatrix} 1 & i \\ i & 1 \end{pmatrix}$	(1243)	$\frac{1}{\sqrt{2}}\begin{pmatrix} 1 & -1 \\ i & i \end{pmatrix}$	(142)

Bibliography

[1] J. Andersen. Asymptotic faithfulness of the quantum $SU(n)$ representations of the mapping class group. *Ann. of Math.*, 2006.

[2] J. Andersen. The Nielsen-Thurston classification of mapping classes is determined by TQFT. *J. Math. Kyoto Univ.*, 2008.

[3] M. Atiyah. Topological quantum field theories. *Inst. Hautes Études Sci. Publ. Math.*, 1988.

[4] M. Atiyah. On framings of 3−manifolds. *Topology*, 1990.

[5] A. Beliakova and C. Blanchet. Modular categories of types B, C, and D. *Comment. Math. Helv.*, 2001.

[6] J. Bermejo-Vega. *Normalizer Circuits and Quantum Computation.* PhD thesis, Technische Universität München, 2016.

[7] C. Blanchet. Hecke algebras, modular categories, and 3−manifolds quantum invariants. *Topology*, 2000.

[8] C. Blanchet, N. Habegger, G. Masbaum, and P. Vogel. Topological quantum field theories derived from the Kauffman bracket. *Topology*, 1995.

[9] W. Bloomquist. Asymptotic faithfulness of quantum SP(4) mapping class group representations. *Submitted.*

[10] W. Bloomquist and A. Mejia. Admissibility and the C_2 spider. *Submitted.*

[11] W. Bloomquist and Z. Wang. Comparing skein and quantum group representations and their applications to asymptotic faithfulness. *Pure and Applied Mathematics Quarterly*, 2016.

[12] W. Bloomquist and Z. Wang. On topological quantum computing with mapping class group representations. *Journal of Physics A*, 2018.

[13] Parsa Hassan Bonderson. *Non-abelian anyons and interferometry.* PhD thesis, California Institute of Technology, 2007.

[14] S. Cautis, J. Kamnitzer, and S. Morrison. Webs and quantum skew Howe duality. *Math. Annalen*, 2014.

[15] M. Van den Nest. Efficient classical simulations of quantum Fourier transforms and normalizer circuits over abelian groups. *Quantum Info. Comput*, 2013.

[16] V. G. Drinfeld. Hopf algebras and the quantum Yang-Baxter equation. *Dokl. Akad. Nauk. SSSR*, 1985.

[17] P. Etingof, S. Gelaki, D. Nikshych, and V. Ostrik. *Tensor Categories.* American Mathematical Society, 2015.

[18] M. Freedman, C. Nayak, K. Walker, and Z. Wang. On picture $(2+1)-$TQFTs. In *Topology and Physics: Proceedings of the Nankai International Conference in Memory of Xiao-Song Lin.*

[19] M. Freedman, K. Walker, and Z. Wang. Quantum $SU(2)$ faithfully detects mapping class groups modulo center. *Geom. Topol.*, 2002.

[20] M. H. Freedman, M. Larsen, and Z. Wang. A modular functor which is universal for quantum computation. *Commun. Math. Phys.*, 2002.

[21] M. Jimbo. A $q-$difference analogue of $U(\mathfrak{g})$ and the Yang-Baxter equation. *Lett. Math. Phys.*, 1985.

[22] V. Jones. Braid groups, Hecke algebras and type II_1 factors. In *Geometric Methods In Operator Algebras (Kyoto, 1983).*

[23] V. Jones. Planar algebras, 1. Preprint: math.QA/9909027.

[24] V. Jones. A polynomial invariant for knots via von Neumann algebras. *Bull. Amer. Math. Soc.*, 1985.

[25] V. Jones. Hecke algebra representations of braid groups and link polynomials. *Ann. of Math.*, 1987.

[26] L. Kauffman. State models and the Jones polynomial. *Topology*, 1987.

[27] L. Kauffman and S. Lins. *Temperley-Lieb recoupling theory and invariants of* $3-$*manifolds.* Princeton University Press, 1994.

[28] D. Kim. Jones-wenzl idempotents for rank 2 simple Lie algebras. *Osaka J. Math.*, 2007.

[29] R. Kirby. A calculus for framed links in S^3. *Invent. Math.*, 1978.

[30] R. Kirby and P. Melvin. The 3−manifold invariants of Witten and Reshetikhin-Turaev for $\mathfrak{sl}(2,\mathbb{C})$. *Invent. Math.*, 1991.

[31] A. Yu. Kitaev. Fault-tolerant quantum computation by anyons. *Annals of Physics*, 2003.

[32] G. Kuperberg. The quantum G_2 link invariant. *Int. J. Math.*, 1994.

[33] G. Kuperberg. Spiders for rank 2 Lie algebras. *Comm. Math. Phys.*, 1996.

[34] S. MacLane. *Categories for the working mathematician*. Graduate texts in mathematics, 1998.

[35] G. Masbaum and J. Roberts. On central extensions of mapping class groups. *Math. Annalen.*, 1995.

[36] S. Morrison, E. Peters, and N. Snyder. Knot polynomial identities and quantum group coincidences. *Quantum Topol.*, 2011.

[37] S. Morrison, E. Peters, and N. Synder. Skein theory for the D_{2n} planar algebras. *J. Pure Appl. Algebra*, 2010.

[38] S.-H. Ng and P. Schaenburg. Congruence subgroups and generalized Frobenius-Schur indicators. *Commun. Math. Phys.*, 2010.

[39] N. Reshetikhin and V. G. Turaev. Ribbon graphs and their invariants derived from quantum groups. *Comm. Math. Phys.*, 1990.

[40] N. Reshetikhin and V. G. Turaev. Invariants of 3−manifolds via link polynomials and quantum groups. *Invent. Math.*, 1991.

[41] s. Cautist. Clasp technology to knot homology via the affine grassmannian. *Math. Ann.*, 2015.

[42] S. Stirling. *Abelian Chern-Simons with toral gauge group, modular tensor categories, and group categories*. PhD thesis, University of Texas at Austin, 2008.

[43] L. C. Suciu. *The $SU(3)$ wire model*. PhD thesis, Penn State University, 1997.

[44] W. Thurston. On the geometry and dynamics of diffeomorphisms of surfaces. *Bull. Amer. Math. Soc.*, 1988.

[45] V. G. Turaev. *Quantum Invariants of Knots and 3 Manifolds*. de Gruyter Studies in Mathematics, Berlin, second edition, 2010.

[46] V. G. Turaev and H. Wenzl. Quantum invariants of 3−manifolds associted with classical simple Lie algebras. *Int. J. of Math.*, 1993.

[47] V. G. Turaev and H. Wenzl. Semisimple and modular cateogires from link invariants. *Math. Ann.*, 1997.

[48] Z. Wang. *Topological Quantum Computation*. Amer. Math. Soc., 2010.

[49] H. Wenzl. On sequences of projections. *C. R. Math. Rep. Acad. Sci. Canada*, 1987.

[50] E. Witten. Quantum field theory and the Jones polynomial. *Comm. Math. Phys.*, 1989.